ISSN ON LINE 2447-181X

ENDOCRINOLOGIA & DIABETES CLÍNICA E EXPERIMENTAL

FACULDADE EVANGÉLICA MACKENZIE DO PARANÁ (FEMPAR)
HOSPITAL UNIVERSITÁRIO EVANGÉLICO MACKENZIE DE CURITIBA

VOL 22 - number 1

Jan/Feb/Mar

Menopause: A New Cycle, Not an End

EDITORIAL

MENOPAUSE: A NEW CYCLE, NOT AN END

Menopause is a natural physiological transition in a woman's life, marking the end of the reproductive cycle and the beginning of a new phase. The diagnosis is confirmed after 12 consecutive months without menstruation due to ovarian failure, characterized by the cessation of ovulation and a sustained decrease in estrogen and progesterone production.

This transition is gradual, lasting approximately four years. It typically occurs between the ages of 45 and 55 and is influenced by genetic, environmental, and health factors. According to Pompei et al., Brazilian women enter menopause around the age of 48.

Data from the **Brazilian Institute of Geography and Statistics (IBGE, 2023)** indicate that the average life expectancy for Brazilian women is approximately 79 years. This means that about one-third of a woman's life occurs in the peri- and postmenopausal period – a time of transformation but also of new possibilities.

Menopause can significantly affect a woman's quality of life, leading to vasomotor symptoms, genitourinary syndrome, sleep disturbances, mood changes, sexual dysfunction, decreased libido, and an increased risk of cardiovascular disease and osteoporosis (Santoro et al., 2021). However, each woman experiences menopause differently, with varying symptom intensity and duration.

Vasomotor symptoms, such as hot flashes and night sweats, are the most common and can begin while menstruation is still occurring. They are often the primary reason women seek treatment. Additionally, body composition undergoes significant changes, particularly in the early stages of menopause, before stabilizing over time. There is a progressive decrease in muscle and bone mass, along with a shift in fat distribution toward the visceral region. These changes increase the risk of fractures, metabolic disorders, and cardiovascular disease.

Given this reality, medical professionals must adopt a more attentive approach, ensuring early interventions to prevent or at least alleviate the symptoms associated with menopause.

The approach to menopause has evolved over the years, with guidelines now emphasizing more effective, safer, and, most importantly, individualized and inclusive treatments. According to the **Brazilian Consensus on Hormone Therapy in Climacteric**, systemic hormone therapy is considered the first line and most effective treatment for menopausal symptoms. This represents a significant shift from the recommendations of 2002, when the **Women's Health Initiative (WHI)** studies suggested an increased risk of breast cancer, leading many women to discontinue treatment and many physicians to avoid prescribing it.

Since then, significant advances have been made to determine the best hormonal combinations that maximize benefits while minimizing risks. Various administration methods are available, including transdermal, oral, endovaginally, and topical options. Non-oral routes, such as transdermal patches and gels, are often preferred as they reduce adverse effects, making treatment safer and more personalized.

These advancements allow not only women in early menopause but also those who have been menopausal for years—including those over 60—to benefit from estrogen therapy in a safer and more effective way.

Menopausal hormone therapy is not always necessary or safe for all women. Fortunately, alternative treatments are emerging. Non-hormonal therapies can be highly effective in managing vasomotor and genitourinary symptoms, as well as treating insomnia and mood changes. Medications such as antidepressants (paroxetine, escitalopram, venlafaxine, desvenlafaxine), clonidine, estrogen receptor antagonists, gabapentin, and, more recently, neurokinin B receptor antagonists (currently in Phase 2 trials) are part of the therapeutic arsenal available to treat symptomatic women.

Additionally, non-pharmacological options are being explored, such as cognitive-behavioral therapy, which is already considered a first-line treatment for insomnia.

However, access to proper treatment remains a challenge. In Brazil, socioeconomic conditions often present barriers to care. A significant step forward in public health was the approval, in 2024, of **Bill 3,933/2023**, which mandates the provision of menopause treatment within the **Brazilian Unified Health System (SUS)**. This initiative expands access to hormonal and non-hormonal medications, diagnostic tests, and psychological support, ensuring more equitable care for Brazilian women.

Gradually, we are advancing in our understanding of menopause as a natural biological process that requires qualified medical attention to ensure healthy and dignified aging. Physicians play a crucial role in recognizing menopausal signs and symptoms and offering appropriate treatment.

Menopause is not an ending, it is a transition, a chapter of transformation that redefines the relationship between body, time, and identity.

Salma Ali El Chab Parolin
ORCID 0000-0001-8124-192X
Doctor and Adjunct Professor at the Pontifícia Universidade Católica do Paraná - Brazil

Endocrinol. Diabetes Clín. Exp. - Vol.22 - Num. 1

Endocrinology & Diabetes - Clinical and Experimental is a journal of open access that publishes case reports, original article, reviews with new insights in pathogenesis, physiology and metabolism of hormone secretion, cellular mechanisms and tissue action. This journal belongs to the Discipline of Endocrinology and Metabolism of Faculdade Evangélica Mackenzie do Paraná and Service of Endocrinology and Diabetes – Diabetes Unit – Hospital Universitário Evangélico Mackenzie, Curitiba – Brazil.

Our Cover – Google Imagens

Endocrinologia & Diabetes Clínica e Experimental
Disciplina de Endocrinologia e Metabologia da Faculdade Evangélica Mackenzie, Serviço de Endocrinologia e Diabetes do Hospital Universitário Evangélico Mackenzie. – v.22, nº 1 – Curitiba: FEMPAR/HUEM, 2025.

p. 1-92: il.; 29cm

Trimestral
ISSN on line 2447-181X
1.Endocrinologia – Periódicos. 2. Saúde – Periódicos. I. Faculdade Evangélica Mackenzie do Paraná.
II. Faculdade Evangélica Mackenzie.

CDD 616.4
CDU 612.34

SCHEDULE
The Endocrinology & Clinical and Experimental Diabetes Journal is a publication produced and edited by Esfera Científica Editora e Propaganda Ltda. The concepts expressed in the articles are the sole responsibility of their authors. Total or partial reproduction of articles is permitted, after authorization from the Editors.

Responsible Director: Acyr José Teixiera
Commercial Director: Fábio Lifschitz Teixeira
Graphic Design and Publishing: Implemus

CONTENTS

ORIGINAL ARTICLE: TOPIC IN MEDICAL CLINIC *ARTIGO ORIGINAL: TÓPICO EM CLÍNICA MÉDICA*

ECHOCARDIOGRAPHIC EVALUATION OF CARDIAC FUNCTION IN ASYMPTOMATIC PATIENTS WITH SYSTEMIC LUPUS ERYTHEMATOSUS

AVALIAÇÃO ECOCARDIOGRÁFICA DA FUNÇÃO CARDÍACA EM PACIENTES ASSINTOMÁTICOS COM LÚPUS ERITEMATOSO SISTÊMICO

Carolina Mei Siqueira[1]; Cassiane Martina Ambrosi Reiter[2]; Sonia Perretto[3]; Thelma L. Skare[4]

[1] Carolina Mei Siqueira
Serviço de reumatologia do Hospital Universitário Evangélico Mackenzie de Curitiba, PR - Brazil
Faculdade Evangélica Mackenzie do Paraná - Brazil.
ORCID: 0000-0003-4469-8079

[2] Cassiane Martina Ambrosi Reiter
Serviço de Reumatologia do Hospital Universitário Evangélico Mackenzie de Curitiba, PR - Brazil.
Faculdade Evangélica Mackenzie do Paraná - Brazil.
ORCID: 0000-0003-2988-9299

[3] Sonia Perretto
Serviço de reumatologia do Hospital Universitário Evangélico Mackenzie de Curitiba, PR - Brazil.
ORCID: 0009-0004-6969-8379

[4] Thelma L Skare
Serviço de reumatologia do Hospital Universitário Evangélico Mackenzie de Curitiba, PR - Brazil.
ORCID: 0000-0002-7699-3542

Conflict of interest: none
Source of funding: none

Approval by the Committee of Ethics in Research - protocol 4.166.935. Faculdade Evangélica Mackenzie, PR.

Received in: 10-11-2024
Reviewed in: 24-11-2024
Accepted in: 28-11-2024

Corresponding author:
Thelma L Skare
Padre Anchieta, 2770
CEP 80 730 000 - Bigorrilho, Curitiba, PR

DOI: 10.29327/2413063.22.1-1

Introduction: Systemic lupus erythematosus (SLE) is a chronic autoimmune disease. One of the important complications of this disease is the cardiovascular damage which is most often asymptomatic or oligosymptomatic needing clinical surveillance to avoid its progression. **Objective:** To study the prevalence of cardiac dysfunction in a local population with SLE and to verify whether the degree of dysfunction is associated with the disease activity measured by SLEDAI (Systemic Lupus erythematosus activity index). **Methods**: We selected 19 patients asymptomatic from cardiovascular point of view diagnosed with SLE and who met the classification criteria for SLE. These patients had their medical records reviewed for clinical and epidemiological data. Disease activity was measured by SLEDAI and cardiac function was evaluated by transthoracic echocardiography. **Results:** The 19 patients studied were female, with a mean age of 41 years. The SLEDAI score ranged from 0-20, with median of 6 (moderate activity). An isolated case of mild pericardial effusion was detected. Regarding the correlation between disease activity and the functional alterations, after correction of echocardiographic parameters for age and body mass index, only the ejection fraction and left ventricular mass remained significant, with p=0.02 and p=0.03, respectively. **Conclusion:** Cardiac dysfunction could not be identified in the sample studied. Higher scores in the lupus activity index showed a correlation with increased left ventricle mass and ejection fraction.

Keywords: Systemic lupus erythematosus. Doppler echocardiography. Left ventricle dysfunction**.**

Introdução: O lúpus eritematoso sistêmico (LES) é uma doença autoimune crônica. Uma das importantes complicações desta doença é o dano cardiovascular que na maioria das vezes é assintomático ou oligossintomático sendo necessário uma vigilância clínica para evitar a sua progressão. **Objetivo:** Estudar a prevalência de disfunção cardíaca em uma população local com LES e verificar se o grau de disfunção está associado com o a atividade da doença medida pelo SLEDAI (Systemic Lupus erythematosus activity index). **Métodos:** Foram selecionados 19 pacientes assintomáticos do ponto de vista cardiovascular com diagnóstico de LES e que preenchiam os critérios classificatórios. Estes pacientes tiveram seus prontuários revisados para dados clínicos e epidemiológicos. A atividade de doença foi medida pelo SLEDAI e a função cardíaca foi avaliada por ecocardiografia trans torácica.**Resultados:** Os 19 pacientes estudados eram do sexo feminino, com média de idade de 41 anos.

A pontuação no SLEDAI variou entre 0-20, com mediana de 6 (atividade moderada). Detectou-se um caso isolado de derrame pericárdico discreto. Quanto à correlação entre atividade da doença e as alterações funcionais detectadas na amostra, após correção dos parâmetros ecocardiográficos para idade e índice de massa corpórea, apenas a fração de ejeção e massa do ventrículo esquerdo permaneceram significantes, com p=0,02 e p=0,03, respectivamente. **Conclusão:** Não foi possível identificar disfunção cardíaca na amostra estudada. Pontuações mais altas no índice de atividade do lúpus demonstraram correlação com aumento de massa de ventrículo esquerdo e fração de ejeção. **Descritores:** Lúpus eritematoso sistêmico. Ecocardiografia Doppler. Disfunção do ventrículo esquerdo.

INTRODUCTION

Systemic Lupus Erythematosus (SLE) is a complex autoimmune disease that can affect multiple organs, including the heart [1]. Although pericarditis is the most common cardiac manifestation and is included as a classification criterion in the 2019 ACR/EULAR (American College of Rheumatology/European League Against Rheumatism) guidelines[1], all cardiac structures, including the myocardium, may be involved.

Myocarditis is present in approximately 37% of autopsy reports of SLE patients, though clinically apparent cases range from only 5% to 10% [2,3]. Myocardial involvement in SLE is primarily due to immune complex deposition in blood vessels [4], although pro-inflammatory cytokines such as IL-17, IL-18, IL-6, and TNF-alpha have also been implicated [2]. Du Toit et al. described an association between myocardial injury and the presence of IL-1 receptor antagonist (ILRa) [2]. Sinus tachycardia, believed to result from subclinical myocarditis or pericarditis [4], has been recognized as a sign of SLE activity since 1964 [5-7].

This study aimed to analyze echocardiographic findings in asymptomatic SLE patients, assessing their prevalence and correlating them with disease activity as measured by the Systemic Lupus Erythematosus Disease Activity Index (SLEDAI). Identifying subclinical cardiac damage is crucial to interrupting the cycle of myocardial injury and preventing the progression of heart disease.

MATERIAL AND METHODS

This is a cross-sectional observational study. After obtaining approval from the local Ethics Committee and informed consent, patients diagnosed with SLE who were regularly followed at the Rheumatology Outpatient Clinic of the Evangelical Mackenzie University Hospital were selected.

The study sample was a convenience sample consisting of all patients attending the rheumatology outpatient clinic over an eight-month period (October 2020 to May 2021) who agreed to participate by signing the informed consent form. A total of 19 patients were included. All patients were over 18 years old and met the 2019 ACR/EULAR classification criteria for SLE[1].

Both male and female participants over 18 years old were included. Exclusion criteria included clinical symptoms of cardiovascular disease, a diagnosis of hypertension, chronic kidney disease (serum creatinine >1.2 mg/dL), non-lupus cardiomyopathies, and diabetes mellitus. Additionally, patients diagnosed with SLE before the age of 16 were excluded.

Data Collection: Patient records were reviewed to collect:

- **a.** Epidemiological data (age, disease onset age, sex, ethnicity, smoking status, and ethnic background).
- **b.** Clinical data, following the ACR classification criteria: photosensitivity, malar rash, discoid lupus, oral ulcers, alopecia, serositis, arthritis, hemolytic anemia, leukopenia, lymphopenia, thrombocytopenia, renal involvement, seizures, and psychosis. Comorbidities were also recorded. Disease duration was defined as the time between diagnosis and study enrollment.
- **c.** Autoantibody profile, including anti-Ro, anti-La, anti-dsDNA, anti-Sm, anti-RNP, anticardiolipin IgG/IgM, lupus anticoagulant, rheumatoid factor, and direct Coombs test.
- **d.** Complement levels (C3 and C4), ESR, and CRP, considering only values obtained within 30 days of the echocardiogram.
- **e.** Medication use, including daily glucocorticoid doses.

Echocardiographic Evaluation: Patients underwent transthoracic echocardiography performed by a single investigator blinded to clinical data. The examination followed the American Society of Echocardiography guidelines for a comprehensive transthoracic echocardiogram [9]. The following parameters were analyzed:

a. Left ventricular systolic and diastolic diameters using a two-dimensional approach to calculate ejection fraction (Teichholz method, or Simpson's method if segmental contractility was altered).
b. Aortic root and left atrial diameters from the parasternal long-axis view.
c. Left ventricular mass calculation using diastolic thickness and cavity measurements (Devereux method), indexed to body surface area.
d. Indexed left and right atrial volumes from two- and four-chamber apical views (modified Simpson method).
e. Valve abnormalities assessed using two-dimensional imaging, conventional Doppler, and color mapping with PISA for reflux quantification.
f. Pulmonary artery pressure estimated via tricuspid regurgitation velocity, adding right atrial pressure from inferior vena cava measurements, with acceleration time assessment in the pulmonary artery.
g. Right ventricular dimensions (basal, mid, and longitudinal), and systolic function evaluated by TAPSE (tricuspid annular plane systolic excursion).
h. Left ventricular diastolic function assessed using E-wave (early) and e' wave (late), E/e' ratio, deceleration time (DT) of the E wave, and tissue Doppler at the septal and lateral mitral annulus.
i. Pericardial effusion, evaluated by measuring the space between pericardial leaflets, presence of right atrial or ventricular diastolic collapse, inferior vena cava dilation, and Doppler analysis of respiratory variations in mitral and tricuspid inflow.

Disease Activity Assessment: SLE activity was measured using SLEDAI (SLE disease activity index)[10], which scores 24 clinical and laboratory parameters, ranging from 0 to 105.

Statistical Analysis:

Data were compiled into frequency tables and expressed as percentages. Correlation studies between SLEDAI, complement levels (C3 and C4), dsDNA titers, and echocardiographic parameters were performed using Spearman or Pearson tests, depending on data distribution. Statistical significance was set at $p < 0.05$.

RESULTS

Sample Characteristics

Nineteen female patients were studied, aged 24 to 64 years (mean 41.05 ± 10.8 years). Disease onset ranged from 17 to 60 years (mean 32.6 ± 11.2 years). Of the participants, 47.3% were Afro-descendants, 47.3% Euro-descendants, and 68.4% non-smokers.

Table 1 presents the main clinical findings.

Table 1. Main clinical findings in the studied sample.

	N	%
Photosensitivity	13	68.4%
Discoid lesions	4	21.1%
Butterfly rash	10	52.6%
Oral ulcers	11	57.9%
Alopecia	17	89.5%
Serositis	4	21.1%
Articular involvement	17	89.5%
Hemolysis	2	10.5%
Leukopenia	8	42.1%
Thrombocytopenia	7	36.8%
Glomerulonephritis	4	21.1%
Psychosis	3	15.8%
Convulsions	5	26.3%

Table 2 displays the main serological findings.

Table 2. Serological findings in the studied sample.

	N/n	%
Anti-Ro	10/19	52.6%
Anti-La	7/19	41.2%
Anti-ds DNA	13/19	68.4%
Anti-Sm	8/18	44.4%
Anti-RNP	8/19	42.1%
Anticardiolipin IgM	3/18	16,6%
Anticardiolipin IgG	3/18	16.6%
Lupus anticoagulante	3/17	17,6%
Rheumatoid factor	4/18	22.2%
Coombs	6/19	37.5%

Table 3 shows the inflammatory activity tests values.

Table 3. Inflammatory activity markers in the studied sample.

	Interval	Median alues	Interquartile range
Complemente – C3	69 a 154 mg/dL	105 mg/dL	(87 - 133)
Complement – C4	9 a 43 mg/dL	28 mg/dL	(15 – 34)
Sedimentation rate	2 a 80 mm/h	16 mm/h	(10 - 22)
C reactive protein	0.15 a 18.1 mg/L	1.02 mg/L	(0.59 - 4.49)

Concerning treatment, hydroxychloroquine was the most frequently used medication. The use of immunosuppressors is at **Table 4.** The daily prednisone dose among users ranged from 2.5 to 20 mg (median 15 mg/day).

Table 4. Use of immunosuppressors and immunomodulators in the studied sample.

	N	%
Antimalarial	17	89.5%
Methotrexate	1	5.3%
Azathioprin	2	10.5%
Mophetil mycophenolate	4	21.1%
Glucocorticoid	6	31.5%

SLEDAI scores ranged from 0 to 20, with a median of 6 (IQR 0–7). Echocardiographic results were predominantly normal (**Tables 5 and 6**).

The evaluation of the cardiac structural alterations found is shown in **Table 6**.

The correlation studies of SLEDAI with echocardiographic findings is in the **Table 7**.

When the correction for age and body mass index was performed, only the correlations with ejection fraction and LV mass remained significant, with p=0.02 and 0.03, respectively. These correlations are shown in **Figure 1**.

All correlations between disease duration and echocardiographic parameters were non-significant (p>0.05).

Table 5. Descriptive analysis of echocardiography results in the studied population.

	Range	Central ten ncy	Normal Values
Aortic root	22 a 36 mm	mean 27.84 mm ± 3.48	20 a 37 mm
Left atrium	25 a 38 mm	mean 29.95 mm ± 3.56	19 a 40 mm
Right ventricle	15 a 28 mm	mean 19.68 mm ± 3.56	7 a 26 mm
Septum	6 a 11 mm	mean 8.42 mm ± 1.10	6 a 11 mm
Posterior wall left ventricle	6 a 11 mm	mean 8.50 mm ± 1.11	6 a 11 mm
Left ventricle systole	22 a 33 mm	mean 27.05 mm ± 2.97	29 mm
Left ventricle siatole	39 a 50 mm	mean 44.0 mm ± 3.04	35 a 56 mm
% shortening	31 a 41%	mean 36.79% ± 3.10	≥ 30%
Ejection fraction	62 a 74%	mean 68.32% ± 3.12	≥ 58%
Left ventricular mass	46.0 a 88.0 g/m²	mean 67.74 g/m² ± 12.44	95 g/m²
Relative wall thickness	0.33 a 0.54	median 0.37 (0.36 - 0.41)	0.32 a 0.42
Right atrium area	9.8 a 17.7 cm²	median 12.1 cm² (11.3 - 13.1)	≤ 18 cm²
Left atrium volume	11,0 a 29,4 ml/L	median 15,6 ml/l (13,6 - 17,0)	34 ml/L
TAPSE	15,0 a 28,0 mm	median 10,6 mm (7,8 - 12,4)	≥ 17 mm
speed e' – left ventricle	4,1 a 14,0 cm/s	Média 8,4 cm/s (6,6 - 10,0)	> 7 cm/s
E/e' – left ventricle	5,50 a 14,4 cm/s	median 8,4 cm/s (6,6 - 10,0)	< 14 cm/s

TAPSE= tricuspid annular plane systolic excursion.

Table 6. Descriptive analysis of the structural results of echocardiography in the population studied.

	Evaluation (n/N)
Mitral valve	Minimal reflux - 3/19 Thickening leaflet -1/19 Normal - 15/19
Tricuspid valve	Mild reflux - 13/19 Normal - 6/19
Aortic valve	Normal - 19/19
Pulmonary valve	Normal - 19/19
Interatrial Septum	Normal - 19/19
Thoracic aorta	Normal - 19/19
Pericardium	Mild effusion - 1/19 Normal - 18/19

DISCUSSION

This study sought to evaluate subclinical cardiac involvement in SLE patients using echocardiographic parameters and to correlate these findings with disease activity as measured by SLEDAI. The results demonstrated that while echocardiographic findings were largely within normal limits, there was a significant correlation between SLEDAI and left ventricular mass, ejection fraction, and relative wall thickness. After adjusting for age and BMI, only left ventricular

Figure 1. Correlation between echocardiographic measurements of left ventricular mass and ejection fraction and SLEDAI (Systemic lupus disease activity index) score in patients with systemic lupus erythematosus (n = 19).

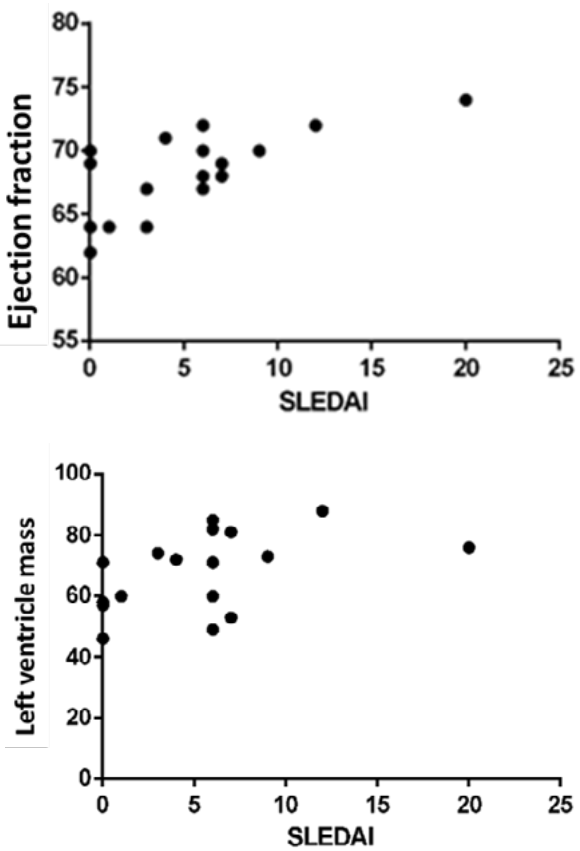

Table 7. Correlation of echocardiography and SLEDAI (Systemic Lupus erythematosus activity index) findings in 19 patients with systemic lupus erythematosus.

	R	95% confidence interval	P
Aortic root	0.34	- 0.13 a 0.70	0.14
Left atrium	0.40	- 0.06 a 0.73	0.06
Septum	0.53	0.09 a 0.80	**0.01**
Right ventricle	0.21	- 0.27 a 0.73	0.36
Posterior wall of the Left ventricle	0.42	- 0.05 a 0.74	0.06
Left ventricle systole	- 0.32	- 0.68 a 0.16	0.17
Left ventricle diastole	- 0.01	- 0.47 a 0.45	0.94
% shortening	0.21	- 0.28 a 0.61	0.38
Ejection fraction	0.52	0.07 a 0.79	**0.02**
Left ventricle mass	0.53	0.08 a 0.79	**0.01**
Relative wall thickness	0.46	- 0.007 a 0.76	**0.04**
Pulmonary artery systolic pressure (mmHg)	- 0.28	- 0.73 a 0.33	0.29
Tricuspid regurgitation speed	- 0.39	- 0.79 a 0.25	0.16

mass and ejection fraction remained significantly associated with SLEDAI, suggesting a potential role of disease activity in myocardial changes.

Our findings support the concept that chronic inflammation in SLE contributes to subtle cardiac alterations, even in patients without overt cardiovascular disease. However, the absence of significant structural abnormalities in this cohort suggests that a tight disease control may help mitigate severe cardiac involvement. These findings align with previous research that emphasizes the importance of inflammation in myocardial remodeling.

Several studies have explored the relationship between SLE and cardiac dysfunction. Shi et al. (2010), for instance, analyzed 287 patients with lupus nephritis and found a linear relationship between chronic low-grade inflammation, estimated by CRP levels, and increased left ventricular mass[11]. Interestingly, this association was independent of adipose tissue distribution, body mass index, blood pressure, lipid levels, renal function, age, and sex. However, our study differs in that we excluded patients with hypertension, diabetes, and heart failure, as these conditions could confound echocardiographic results. This difference in exclusion criteria may explain the discrepancies between our findings and those of Shi et al[11].

Few studies have compared the relationship between SLEDAI scores and subclinical ventricular dysfunction by echocardiographic means. Among the available literature, Mirfeizi et al.[12] found a correlation between SLEDAI disease activity and pulmonary artery pressure, which could not be evidenced in this study. However, in the same study by Mirfeizi et al., an association was also found between SLE duration, SLEDAI score, and increased left ventricular mass, which reinforces the results of this current study[12].

Another critical point is the relationship between SLEDAI and ventricular dysfunction. While our study observed increased ejection fraction (EF) in correlation with disease activity, previous studies have reported contradictory findings. Wislowska et al.[13], for instance, found that SLE patients with SLEDAI >6 had lower ejection fractions compared to controls. Similarly, studies conducted by Buss et al.[14] and Teixeira et al.[15] reported a lack of ejection fraction abnormalities, attributing this to a tight inflammatory control at the time of assessment. These discrepancies highlight the complexity of SLE-related myocardial involvement and suggest that disease activity at the time of evaluation may significantly influence echocardiographic findings.

Comparative studies between SLE patients and healthy controls have further demonstrated subclinical ventricular alterations. Shang et al.[16] compared echocardiographic parameters in 82 SLE patients and 82 age- and sex-matched controls and found that SLE patients exhibited increased left ventricular wall thickness and mass. Similarly, Chen et al. [17] conducted a meta-analysis and confirmed a higher prevalence of increased left ventricular mass in lupus patients compared to controls. These findings reinforce the idea that SLE itself contributes to myocardial remodeling, even in the absence of traditional cardiovascular risk factors.

In contrast, our study did not find significant structural changes beyond correlations with SLEDAI, possibly due to the small sample size and cross-sectional design. The lack of longitudinal follow-up further limits our ability to determine whether these subtle echocardiographic changes progress over time. Additionally, genetic factors may play a role in the variability of cardiac involvement.

While our study did not identify major cardiac dysfunctions in this cohort, the observed correlation between SLEDAI and myocardial parameters highlights the importance of cardiac monitoring in lupus patients. Even in the absence of overt symptoms, subclinical cardiac involvement may progress over time, underscoring the need for early detection and preventive strategies.

Future studies should focus on longitudinal follow-up of SLE patients to determine the progression of subclinical myocardial changes; on larger, multicenter cohorts to enhance statistical power and identify potential genetic influences; in advanced imaging techniques, such as cardiac MRI and speckle-tracking echocardiography, which may detect early myocardial dysfunction that conventional echocardiography might not show.

CONCLUSION

This study did not identify significant cardiac dysfunction in the analyzed SLE patients. However, SLEDAI correlated with left ventricular mass and ejection fraction, reinforcing the importance of assessing cardiac involvement in lupus patients.

REFERENCES

1. Aringer M. European league against rheumatism/american college of rheumatology classification criteria for systemic lupus erythematosus. **Arthritis Rheumatol**. 2019; 71:1400–12. doi: 10.1002/art.40930

2. du Toit R, Reuter H, Walzl G, Snyders C, Chegou NN, Herbst PG, et al .Serum cytokine levels associated with myocardial injury in systemic lupus erythematosus. **Rheumatology** (Oxford). 2021; 60(4):2010-2021. doi: 10.1093/rheumatology/keaa540.
3. Panchal L, Divate S, Vaideeswar P, Pandit SP. Cardiovascular involvement in systemic lupus erythematosus: an autopsy study of 27 patients in India. **J Postgrad Med.** 2006; 52:5–10. PMID: 16534157.
4. Bidani AK, Roberts JL, Schwartz MM, Lewis EJ. Immunopathology of cardiac lesions in fatal systemic lupus erythematosus. **Am J Med.** 1980; 69: 849–58. doi: 10.1016/s0002-9343(80)80010-6.
5. Hejtmancik MR, Wright JC, Quint R, Jennings FL. The cardiovascular manifestations of systemic lupus erythematosus. **Am Heart J.** 1964; 68: 119–30. doi: 10.1016/0002-8703(64)90248-0.
6. Mandell BF. Cardiovascular involvement in systemic lupus erythematosus. **Arthritis Rheum**. 1987; 17: 126–41. doi: 10.1016/0049-0172(87)90035-7.
7. Guzman J, Cardiel MH, Arce-Salinas A, Alarcon-Segovia D. The contribution of resting heart rate and routine blood tests to the clinical assessment of disease activity in systemic lupus erythematosus. **J Rheumatol.** 1994; 21: 1845–8. PMID: 7837148
8. Utset TO, Ward AB, Thompson TL, Green SL. Significance of chronic tachycardia in systemic lupus erythematosus. **Arthritis Care Res** (Hoboken). 2013; 65(5):827-31. doi: 10.1002/acr.21902.
9. Mitchell C, Fase RT, Rahko PS, Blauwet LA, Canaday B, Fase JA, et al. Guidelines for Performing a Comprehensive Transthoracic Echocardiographic Examination in Adults: Recommendations from the American Society of Echocardiograph. **J Am Soc Echocardiogr.**, 2019. 32 (1): 1-64. doi: 10.1016/j.echo.2018.06.004.
10. Buyon JP, Petri MA, Kim MY, Kalunian KC, Grossman J, Hahn BH, et al. The effect of combined estrogen and progesterone hormone replacement therapy on disease activity in systemic lupus erythematosus: a randomized trial. **Ann Intern Med.** 2005;142: 953–62. doi: 10.7326/0003-4819-142-12_part_1-200506210-00004.
11. Shi B, Ni Z, Cai H, Zhang M, Mou S, Wang Q et al. High-sensitivity C-reactive protein: an independent risk factor for left ventricular hypertrophy in patients with lupus nephritis. J **Biomed Biotechnol.** 2010; 2010 :373426. doi: 10.1155/2010/373426.
12. Mirfeizi Z, Poorzand H, Javanbakht A, Khajedaluee M. Relationship between systemic lupus erythematosus disease activity index scores and subclinical cardiac problems. **Iran Red Crescent Med J.** 2016;18(8): e38045. doi: 10.5812/ircmj.38045.
13. Wislowska M, Dereń D, Kochmański M, Sypuła S, Rozbicka J. Systolic and diastolic heart function in SLE patients**. Rheumatol Int.** 2009 ;29(12):1469-76. doi: 10.1007/s00296-009-0889-4.
14. Buss SJ, Wolf D, Korosoglou G, Max R, Weiss CS, Fischer C, et al. Myocardial left ventricular dysfunction in patients with systemic lupus erythematosus: new insights from tissue Doppler and strain imaging. **J Rheumatol.** 2010; 37(1):79-86. doi: 10.3899/jrheum.090043.
15. Teixeira AS, Bonfá E, Herskowictz N, Barbato AJG, Borba EF. Early detection of global and regional left ventricular diastolic dysfunction in systemic lupus erythematosus: the role of the echocardiography. **Rev Bras Reumatol.** 2010;50(1):16-30. PMID: 21125138.
16. Shang Q, Yip GW, Tam LS, Zhang Q, Sanderson JE, Lam YY, et al. SLICC/ACR damage index independently associated with left ventricular diastolic dysfunction in patients with systemic lupus erythematosus. **Lupus.** 2012; 21(10): 1057-62. doi: 10.1177/0961203312446628.
17. Chen J, Tang Y, Zhu M, Xu A. Heart involvement in systemic lupus erythematosus: a systemic review and meta-analysis. **Clin Rheumatol**. 2016; 35 (10):2437-2448. doi: 10.1007/s10067-016-3373-z.

ORIGINAL ARTICLE: TOPIC IN MEDICAL CLINIC *ARTIGO ORIGINAL: TÓPICO EM CLÍNICA MÉDICA*

INFLUENCE OF ETHNIC BACKGROUND IN SYSTEMIC LUPUS ERYTHEMATOSUS PHENOTYPE: A RETROSPECTIVE STUDY IN A BRAZILIAN SAMPLE

INFLUÊNCIA DA ORIGEM ÉTNICA NO FENÓTIPO DO LÚPUS ERITEMATOSO SISTÊMICO: UM ESTUDO RETROSPECTIVO EM UMA AMOSTRA BRASILEIRA

Matheus Duarte Gonçalves[1], Vinicius Peres Pereira[2], Thelma L Skare[3], Thiago Gomes dos Santos[4]

[1] Matheus Duarte Gonçalves
Faculdade Evangélica Mackenzie do Paraná - Brazil
ORCID: 0009-0003-6115-0643

[2] Vinicius Peres Pereira
Faculdade Evangélica Mackenzie do Paraná -Brazil
ORCID: 0000-0003-1358-4917

[3] Thelma L Skare
Disciplina de Reumatologia - Faculdade Evangélica Mackenzie do Paraná - Brazil - Unidade de Reumatologia - Hospital Universitário de Curitiba - PR - Brazil.
ORCID: 0000-0002-7699-3542.

[4] Thiago Gomes dos Santos
Disciplina de Reumatologia - Faculdade Evangélica Mackenzie do Paraná - Brazil - Unidade de Reumatologia - Hospital Universitário de Curitiba - PR - Brazil.
ORCID: 0000-0002-6310-9789

Received in: 08-12-2024
Accepted in: 17-12-2024

Conflict of interest - none
Source of funding - none
Approval of Committee of Ethics in Research – 6.083.352.

Correspondence adress:
Thelma L Skare
Rua Padre Anchieta, 2770.
807330 000 Curitiba, PR.
E-mail- thelma.skare@gmail.com

DOI: 10.29327/2413063.22.1-2

Introduction: Ethnic back ground seems to be important determining Systemic Lupus Erythematosus (SLE) clinical profile and prognosis. According to previous studies, afro descendants have a more severe disease than white individuals. There are few studies in Brazilian population. **Aim:** To study the differences in clinical, serological and cumulative damage in systemic lupus in afro and euro descendants. **Method:** Retrospective study for clinical profile, autoantibodies and SLLIC ACR DI (Systemic Lupus International Collaborating Clinics/ American College of Rheumatology Damage Index) in 659 SLE patients (605 females and 54 males; 399 euro-descendants e 260 afro descendants). **Results:** Male gender was more commonly seen in afro descendant sample (p=0.001); malar rash (p=0.009) and photosensitivity (p=0;02) were more common in euro descendants. Regarding serological profile, anti-Sm (p=0.009) and anti RNP (p=0.04) were more common in the afro descendant sample. No other differences were noted including in the cumulative damage. **Conclusion**: The clinical and serological profiles and cumulative damage in SLE Brazilian patients did not differ according ethnic background except for minor cutaneous manifestations and anti Sm e anti RNP auto antibodies prevalence.
Key words: Systemic lupus erythematosus. Race. Prognosis.

Introdução: A raça parece influir de maneira importante no perfil clinico e prognóstico do paciente com lúpus eritematoso sistêmico (LES). De acordo com a literatura, afrodescendentes têm uma doença mais grave do que indivíduos brancos, mas existem poucos estudos feitos na população brasileira. **Objetivo:** Estudar as diferenças na população euro e afrodescendente quanto a perfil clinico, sorológico e dano cumulativo. **Método:** Estudo retrospectivo para perfil clínico, autoanticorpos e SLICC ACR DI (*Systemic Lupus International Collaborating Clinics/ American College of Rheumatology Damage Index*) em 659 pacientes com LES (605 mulheres, 54 homens, 399 euro-descendentes e 260 afro-descendentes). **Resultados:** Sexo masculino foi mais prevalente no grupo afro descendente (p=0.001); rash malar (p=0.009) e fotosensibilidade (p=0.020) foram mais comuns nos eurodescentees. Acerca do perfil sorologico, anti sm (p=0.009) e anti RNP (p=0.04) foram mais comuns em afrodescendentes. **Conclusões:** O perfil clinico e sorológico de pacientes com SLE nesta amostra foi semelhante em afro e euro descentes exceto por manifestações cutâneas menores e prevalência de autoanticorpos anti Sm e anti RNP.
Descritores: Lupus eritematoso sistêmico. Raça. Prognóstico.

INTRODUCTION

Prognosis in systemic lupus erythematosus (SLE) is heavily influenced by genetic and social determinants of health. In this context Afro descendants, Asians and Hispanic individuals may be predisposed to develop a more severe disease with a greater number of manifestations and more cumulative damage[1] . Studies from UK, have shown that Afro-Caribbean patients tended to develop renal disease more frequently and earlier in the course of their illness[2,3]; discoid rash have been described as more common in Individuals with African or Caribbean ancestry[4-6] while photosensitivity was more commonly seen in white individuals[7,8] .

Brazil is a country with multicultural genetic pool due to miscegenation secondary to colonization in the last 500 years. Subsequently to the initial European colonization mainly Portuguese and Spanish, there was immigration of about 5 million black people from Africa between the 17th and the 19th centuries. After the abolition of slavery, the country received a large number of immigrants, particularly Italians in the Southeast, Japanese Southeast and Center-west, and Germans South.

In the 2022 census, approximately 45.3% of the Brazilian population was reported being brown; other 43.5% reported as being white, 10.2% as black, 0.8% as indigenous and 0.4% as of Asian background. However, these proportion may vary according to the studied region: the biggest proportion of brown individuals 67.2% was reported in North region while in the South, 72.6% were white[9].

However, due to the high degree of miscegenation present in the Brazilian population, the individual external phenotype not always correspond to the genetic profile, creating difficulties in the interpretation of the influence of race in diseases like lupus.

Herein, a sample of Brazilian lupus patients from a Southern Brazilian region was studied for clinical and antibody profile according to auto declared ethnic background aiming to know if the observed differences according to the race are similar to the observed in other populations.

MATERIAL AND METHODS

This is a retrospective study approved by the Institutional Committee of Ethics in Research (CAAE-6 9556023.4.0000.0103) under protocol number 6.083.352. Charts from Lupus patients that consulted regularly at single rheumatology out patient's clinic from Southern Brazil that cares for adult SLE patients from the Brazilian Public Health System of the last 34 years (January, 1990 to January, 2024) were reviewed. To be included the patients should be classified as SLE according to the 2012 Systemic Lupus International Collaborating Clinics (SLICC) Classification Criteria[10]. Clinical and serologic data were collected. Clinical data should follow the definition of 2012 SLICC criteria and they were considered in a cumulative way. Data on lupus biopsy results and need of renal replacement therapy (hemodialysis or renal transplantation) were also collected. Patients were classified in euro descendants and afro descendants (black and brown) and compared. Asian descents were excluded due to small number (n=4). Also, a patient of Bolivian origin (n=1) was excluded. Cumulative damage was measured by SLICC/ACR DI (Systemic Lupus International Collaborating Clinics/ American College of Rheumatology Damage Index).

Nominal data was compared using Fisher and chi-squared tests, numerical data was studied by unpaired t test or Mann Whitney test according to data distribution. The adopted significance was 5%. Tests were done with help of the GraphPad Prism version 8.0.0 for Windows, GraphPad Software, San Diego, California USA, "www.graphpad.com".

RESULTS

About 659 charts were reviewed. In this sample 399 were considered euro-descendants and 260 afro-descendants in a proportion of 1 afro-descendant to 1.5 euro-descendant. The comparison of clinical data is on **Table 1.**

Table 2 shows the comparison of renal biopsy at the first glomerulonephritis episode.

Renal replacement therapy was needed in 23/176 (13.0%) of euro descendants and in 16/124 (12.9%) of afro descendants with p=0.96.

The comparison of serological profile is on **Table 3**. The only observed difference was in the anti-RNP and anti-Sm antibodies that was more common in the euro descendants.

The median SLICC in the afro descendants was 1.0 (0-2) and in the euro descendants was 1.0 (0-2) with p=0.18.

DISCUSSION

The present results shows that the clinically observed differences between the two studied eth-

Table 1. Comparison of clinical profile between euro-descendants and afro-descendants.

	Total	Afro Descendants 260	Euro Descendants 399	P (*)
Median age-years (IQR)	43.0 (31-54)	43.0 (31.0-54.0)	44.0 (31.7-54.0)	0.46
Median disease duration- years (IQR)	11 (5-18.2)	11.0 (4.0-17.0)	12.0 (6.0-19.0)	0.08
Median age at disease onset-years (IQR)	30 (20-40)	30.0 (21.0-39.0)	29.0 (20.0-40.0)	0.67
Female gender – n (%)	605/659 (91.8)	228/260 (87.6)	377/399 (94.4)	**0.001**
Discoid lesions – n (%)	82/643 (12.7)	35/254 (13.7)	47/389 (12.5)	0.52
Malar rash – n (%)	334/626 (53.3)	118/251 (47.0)	216/375 (57.6)	**0.009**
Alopecia – n (%)	326/600 (54.3)	139/241 (57.6)	187/359 (52.0)	0.17
Oral ulcers – n (%)	240/617 (38.8)	88/248 (35.4)	152/369 (41.1)	0.15
Photosensitivity – N (%)	452/635 (71.1)	166/251 (66.1)	286/384 (74.4)	0.02
Articular involvment– n (%)	529/653 (81.0)	211/258 (81.7)	318/395 (80.5)	0.68
Serositis – n (%)	160/652 (24.5)	63/255 (24.7)	97/397 (24.4)	0.93
Hemolytic anemia – n (%)	68/647 (10.5)	32/254 (12.5)	36/393 (9.1)	0.16
Leukopenia – n (%)	204/647 (31.5)	88/255 (34.5)	116/392 (29.5)	0.18
Lymphopenia – n (%)	147/642 (22.8)	66/254 (25.9)	81/388 (20.8)	0.13
Thrombocytopenia – n (%)	167/647 (25.8)	74/255 (28.7)	93/392 (23.7)	0.13
Glomerulonephritis – n (%)	300/652 (46.0)	124/257 (48.2)	176/395 (45.0)	0.29
Convulsions – n (%)	54/646 (8.3)	24/255 (9.4)	30/391 (7.6)	0.43
Psychosis – n (%)	32/647 (4.9)	13/255 (5.0)	19/392 (4.8)	0.88

(*) refers to afro descendants versus euro descendants.

Table 2. Comparison of renal biopsy results in afro and euro-descendants.

	Euro -descendants N (%)	Afro descendants N (%)	p
Class 2	20/166 (12.0)	15/119 (9.0)	0.10
Class 3	31/166 (18.6)	19/119 (15.9)	
Class 4	66/166 (39.7)	49/119 (41.1)	
Class 5	32/166 (19.2)	30/119 (25.2)	
Class 6*	17/166 (10.2)	6/119 (5.0)	

* Patients with renal failure at entrance; no biopsy performed.
Patients with class 3+5 were grouped with class 3 and patients with class 4+5 with class 4.
No biopsy obtained in 10/176 (5.6%) of euro-descendants and in 5/124 (4.0%) of afro descendants.

nic backgrounds were on photosensitivity and malar rash that were more common in euro descendant individuals and male gender that was more common in afro descendants. Several other studies observed the increased prevalence of photosensitivity in white patients and of male sex in afro descendants as we did[11-13]. However, differences in renal involvement prevalence and renal involvement severity could not be demonstrated with greater rates of progression to end-stage renal disease[16,17] as found in other investigations. Moreover, other studies have also verified that discoid rash was more common in black individuals [5,14]. The cumulative damage measured by SLICC in both samples, that had similar disease duration, was also similar. So, the observation that SLE severe manifestations are more commonly seen in afro descendants [15], is not supported by the present study. It is possible that the high rate of miscegenation ob-

Table 3. Comparison of serological profile according to auto declared ethnic background.

	Total N (%)	Afro descendants N (%)	Euro descendants N (%)	P (*)
Anti-Ro	258/ 624 (41.3)	99/248 (39.9)	159/376 (42.2)	0.55
Anti-La	122/619 (19.7)	55/245 (22.4)	67/374 (17.9)	0.16
Anti-RNP	190/531 (35.7)	87/228 (38.1)	103/303 (33.9)	**0.04**
Anti-Sm	177/597 (29.6)	86/242 (35.5)	91/355 (25.6)	**0.009**
Anti-dsDNA	338/638 (52.9)	140/250 (56.0)	198/388 (51.0)	0.21
Anticardiolipin IgG	81/600 (13.5)	37/244 (15.1)	45/356 (12.6)	0.37
Anticardiolipin IgM	83/596 (13.9)	28/242 (11.5)	55/354 (15.5)	0.16
Lupus anticoagulant	80/570 (14.0)	40/235 (17.0)	40/335 (11.9)	0.08

(*) refers to afro descendants versus euro descendants.

served on the Brazilian population could be responsible for these differences. Such miscegenation may be responsible for the fact that the patient's external phenotype does not correspond to the true ethnic background.

From serological point of view, anti RNP and anti-Sm were more frequently found in afro descendant as already noted in the literature[16] .

SLE is a disease with strong genetic influence with at least 52 genetic loci with evidence of association with susceptibility to this disease[17-20]. The literature shows that black individuals have an increased SLE prevalence of 2 to 3-fold in relationship to white individuals and a more severe disease; an increased autoantibody reactivity has been observed on these individual[17]. The analysis of disease repercussions according to the ethnic background is frequently blurred by difficulties in the access to medical care and treatment and because of differences in educational issues disfavoring some racial groups. In the present studied sample, all patients were from a single rheumatological center, all users of Public Health System with similar access to consults and to medications that are provided for free by the government, turning the samples more homogeneous on these aspects. Unluckily no data on educational level was available.

This work is limited by the fact that ethnic background was judged according to patient's auto recognition. The recognition of own ancestry is difficult in a population with a high degree of mixture such Brazilians, differing from data obtained in a more homogenous population. Nevertheless, this fact shows how the reality is in Brazil and how these aspects present in a real-life situation.

CONCLUSION

In a population with highly mixed race such as Brazilians, the clinical, serological and outcome differences in SLE are not so clear as the observed in more homogenous cohort.

REFERENCES

1. Addanki S, Patel K, Shah K, Patel L, Mauger M, Laloo A, Rajput V. Racial and ethnic disparities within social determinants of health amongst patients with systemic lupus erythematosus. **Cureus.** 2024; 16(7):e64453. doi: 10.7759/cureus.64453.
2. Alba P, Bento L, Cuadrado MJ, Karim Y, Tungekar MF, Abbs I, et al. Anti-dsDNA, anti-Sm antibodies, and the lupus anticoagulant: significant factors associated with lupus nephritis. *Ann Rheum Dis*. 2003; 62:556-60. doi: 10.1136/ard.62.6.556.
3. Hopkinson ND, Jenkinson C, Muir KR, Doherty M, Powell RJ. Racial group, socioeconomic status, and the development of persistent proteinuria in systemic lupus erythematosus. **Ann Rheum Dis**. 2000; 59:116-9. doi: 10.1136/ard.59.2.116.
4. Alarcon GS, McGwin G Jr, Petri M, Reveille JD, Ramsey-Goldman R, Kimberly RP; PROFILE Study Group. et al. Baseline characteristics of a multiethnic lupus cohort: PROFILE. **Lupus**. 2002;11:95101. doi: 10.1191/0961203302lu155oa.
5. Pons-Estel BA, Catoggio LJ, Cardiel MH Soriano ER, Gentiletti S, Villa AR,et al. The GLADEL multinational Latin American prospective inception cohort of 1,214 patients with systemic lupus erythematosus: ethnic and disease heterogeneity among ''Hispanics''. Medicine 2004; 83:117. doi: 10.1097/01.md.0000104742. 42401.e2.

6. Kamen DL, Barron M, Parker TM Shaftman SR, Bruner GR, Aberle T, et al. Autoantibody prevalence and lupus characteristics in a unique African American population. **Arthritis Rheum.** 2008;58: 123747. doi: 10.1002/art.23416.
7. Sanchez E, Rasmussen A, Riba L Acevedo-Vasquez E, Kelly JA, Langefeld CD, et al. Impact of genetic ancestry and sociodemographic status on the clinical expression of systemic lupus erythematosus in American Indian-European populations. **Arthritis Rheum.** 2012; 64: 368794. doi: 10.1002/art.34650.
8. Gonzalez LA, Toloza SM, McGwin G Jr, Alarcon GS. Ethnicity in systemic lupus erythematosus (SLE): its influence on susceptibility and outcomes. **Lupus.** 2013;22: 121424. doi: 10.1177/0961203313502571.
9. IBGE- Brazilian Institute of Geography and Statistics. Available at https://www.ibge.gov.br/. Captured in october, 2024.
10. Petri M, Orbai AM, Alarcón GS, Gordon C. Merrill JT, Fortin PR et al. Derivation and validation of the systemic lupus international collaborating clinics classification criteria for systemic lupus erythematosus. **Arthritis Rheum.** 2012; 64:2677–86. doi: 10.1007/s10067-021-05803-7.
11. Tan TC, Fang H, Magder LS, Petri MA. Differences between male and female systemic lupus erythematosus in a multiethnic population. J Rheumatol. 2012; 39(4):759-69. doi: 10.3899/jrheum.111061.
12. Foering K, Okawa J, Rose M, Goreshi R, LoMonico J Characterization of photosensitivity and poor quality of life in lupus. **J Invest Dermatol.** 2010; 130: S10-S10.
13. Nyberg F, Hasan T, Puska P, Stephansson E, Häkkinen M, Ranki A, Ros AM. Occurrence of polymorphous light eruption in lupus erythematosus. **Br J Dermatol**. 1997;136(2):217-21. PMID: 9068735.
14. Huong DL, Papo T, Beaufils H, Wechsler B, Blétry O, Baumelou A, Godeau P, et al. Renal involvement in systemic lupus erythematosus. A study of 180 patients from a single center. **Medicine**.1999;78:14866. doi: 10.1097/00005792-199905000-00002.
15. Alarcon GS, McGwin G Jr, Petri M, Ramsey-Goldman R, Fessler BJ, Vilá LM, et al. Time to renal disease and end-stage renal disease in PROFILE: a multiethnic lupus cohort. **PLoS Med**. 2006;3: e39. doi: 10.1371/journal.pmed.0030396.
16. Kamen DL, Barron M, Parker TM, Shaftman SR, Bruner GR, Aberle T, et al. Autoantibody prevalence and lupus characteristics in a unique African American population. **Arthritis Rheum**. 2008;58:123747. doi: 10.1002/art.23416.
17. Arnaud L, Tektonidou MG. Long-term outcomes in systemic lupus erythematosus: trends over time and major contributors. **Rheumatology (Oxford).** 2020 Dec 5;59 (Suppl5):v29-v38. doi: 10.1093/rheumatology/keaa382.
18. Sapkota B, Al Khalili Y. Mixed Connective Tissue Disease. 2023 Apr 3. In: **StatPearls** [Internet]. Treasure Island (FL): StatPearls Publishing; 2024 Jan–. PMID: 31194355.
19. Bentham J, Morris DL, Graham DSC, Pinder CL, Tombleson P, Behrens TW, et al.Genetic association analyses implicate aberrant regulation of innate and adaptive immunity genes in the pathogenesis of systemic lupus erythematosus. **Nat Genet**.2015;47:145764. doi: 10.1038/ng.3434.
20. Gateva V, Sandling JK, Hom G Taylor KE, Chung SA, Sun X, et al. A large-scale replication study identifies TNIP1, PRDM1, JAZF1, UHRF1BP1and IL10 as risk loci for systemic lupus erythematosus. **Nat Genet.** 2009;41:122833.
21. Han JW, Zheng HF, Cui Y et al. Genome-wide association study in a Chinese Han population identifies nine new susceptibility loci for systemic lupus erythematosus. **Nat Genet.** 2009;41:12347. doi: 10.1038/ng.468.
22. Harley JB, Alarcon-Riquelme ME, Criswell LA, Jacob CO, Kimberly RP, Moser KL, et al. Genome-wide association scan in women with systemic lupus erythematosus identifies susceptibility variants in ITGAM, PXK, KIAA1542 and other loci. **Nat Genet.** 2008;40:20410. doi: 10.1038/ng.81.

ORIGINAL ARTICLE: TOPIC IN MEDICAL CLINIC *ARTIGO ORIGINAL: TÓPICO EM CLÍNICA MÉDICA*

COGNITIVE DYSFUNCTION IN RHEUMATOID ARTHRITIS: A STUDY IN BRAZILIAN FEMALES

DISFUNÇÃO COGNITIVA EM ARTRITE REUMATOIDE: UM ESTUDO EM MULHERES BRASILEIRAS

Ricardo Castilho de Souza[1]; Rodrigo Mori Reimann[2]; Lais Zanlorenzi[3]; Bárbara Stadler Kahlow[4]; Thelma L Skare[5]

[1] Ricardo Castilho de Souza
Faculdade Evangélica Mackenzie do Paraná - Curitiba PR - Brazil.
ORCID: 0009-0002-6827-9899

[2] Rodrigo Mori Reimann
Faculdade Evangélica Mackenzie do Paraná - Curitiba PR - Brazil.
ORCID: 0000-0002-28875-6972

[3] Lais Zanlorenzi
Unidade de Artrite Reumatóide - Hospital Universitário Evangélico Mackenzie - Curitiba - PR - Brazil.
ORCID: 0009-0002-9523-3677

[4] Bárbara Stadler Kahlow
Faculdade Evangélica Mackenzie do Paraná - Curitiba - PR - Brazil. Unidade de Artrite Reumatóide - Hospital Universitário Evangélico Mackenzie - Curitiba - PR - Brazil. Pontifícia Universidade Católica do Paraná, Curitiba, Brazil.
ORCID: 0000-0001-5292-2777

[5] Thelma L Skare
Faculdade Evangélica Mackenzie do Paraná - Curitiba - PR - Brazil. Discipline of Reumatology - Faculdade Evangélica Mackenzie do Paraná - Curitiba - PR - Brazil.
ORCID: 0000-0002-7699-3542

Received in: 05-01-2025
Accepted in: 28-01-2025

Conflict of interest - none
Source of funding - none

Approval of Committee of Ethics in Research – 6.120.530

Corresponding author:
Thelma L Skare
Rua Padre Anchieta, 2770.
807330 000 Curitiba, PR.
E-mail: thelma.skare@gmail.com

DOI: 10.29327/2413063.22.1-3

Background: Rheumatoid arthritis has been associated with cognitive dysfunction (CD). However, there are controversies about the factors associated with this finding. **Aim:** To study CD in a sample of Brazilian patients with RA and its possible association with epidemiological data, disease activity, treatment and comorbidities as well as the repercussions of CD in quality of life. **Methods:** Cross sectional study in 137 individuals (91 RA patients and 46 controls). Data collection included epidemiological information, RA disease activities indexes, Montreal cognitive assessment (MoCA) and Short Form Health Survey with 12 questions (SF-12). **Results:** RA patients had lower values of MoCA than controls (16.8 vs 18.9; p=0.02) as well as lower values in visuospatial/executive functions (p=0.04), abstraction (p=0.02) and delayed recall domains (p=0;04). MoCA values in RA patients correlated with age (p<0.001), disease duration (p=0.01), years of formal education (p<0.004) and SF-12 physical domain (p=0.04). No association with disease activities indexes were found (all with p>0.05). **Conclusion:** RA patients had worse cognitive performance than controls. Disease duration but not disease activity influenced CD. CD associated with impairment in physical but not mental quality of life.
Key words: Rheumatoid arthritis. Inflammation. Cognition. Quality of life.

Introdução: A artrite reumatoide (AR) tem sido associada à disfunção cognitiva (DC). No entanto, há controvérsias sobre os fatores associados a esse achado. **Objetivo:** Estudar a DC em uma amostra de pacientes brasileiros com AR e sua possível associação com dados epidemiológicos, atividade da doença, tratamento e comorbidades, bem como as repercussões da DC na qualidade de vida. **Métodos:** Estudo transversal em 137 indivíduos (91 pacientes com AR e 46 controles). A coleta de dados incluiu informações epidemiológicas, índices de atividades da doença da AR, avaliação cognitiva de Montreal (MoCA) e *Short Form Health Survey* com 12 perguntas (SF-12). **Resultados:** Pacientes com AR apresentaram valores mais baixos de MoCA do que os controles (16,8 vs 18,9; p=0,02), bem como valores mais baixos nas funções visoespaciais/executivas (p=0,04), abstração (p=0,02) e domínios de recordação tardia (p=0;04). Os valores de MoCA em pacientes com AR correlacionaram-se com a idade (p<0,001), duração da doença (p=0,01), anos de educação formal (p<0,004) e domínio físico do SF-12 (p=0,04). Nenhuma associação com índices de atividades da doença foi encontrada (todos com p>0,05). **Conclusão:** Pacientes com AR tiveram pior desempenho cognitivo do que controles. A duração da doença, mas não a atividade da doença, influenciaram a DC. A DC foi associada ao comprometimento da qualidade de vida física, mas não mental.
Descritores: Artrite reumatoide. Cognição. Inflamação. Qualidade de vida.

INTRODUCTION

Chronic inflammation – the major drive of rheumatoid arthritis pathogenesis, is associated with cognitive dysfunction (CD). In this setting, ischemic lesions due to the accelerated effects of inflammation in the vascular system seems to play an important role[1,2]; pro-inflammatory cytokines action in the brain tissue, persistent pain, medication side effects, age and genetic components are also important players[1,3,4].

Indeed, the existence of cognitive impairment in RA patients have been documented in previous studies, and considered to influence patients' quality of life as it impairs the performance of daily activities[3-6]. Decision-making, problem solving, acquiring new information and memory are some of altered functions that interfere with social life, employment and patients' auto-care[3]. However, the investigation of potential contributors to CD in RA is subject to inconsistent results and which are the associated factors remains a matter of debate, requiring further investigation.

The objective of this study was to analyze the cognitive function in a group of RA patients and the potential relationship of CD with epidemiological data, treatment, disease activity, comorbidities and quality of life.

MATERIAL AND METHODS

This is a cross-sectional study, approved by the Institutional Committee of Ethics in Research (CAAE: 69979723.9.0000.0103) under protocol 6.120.530. using a convenience sample of RA patients from a single Rheumatology Unit that cares for patients from the Brazilian Public Health System. All participants signed a consent form. To be included patients should fill at least 6 points in the Classification Criteria for RA from ACR/ EULAR[7], be older than 18 years of age and female. They were invited to participate in the study according to consultations order. Patients without intellectual capacity to understand the consent form, with inflammatory or psychiatric comorbidities were excluded. For controls, patient's companion auto declared healthy were requested to take part.

Data collection included:

a. Epidemiological and clinical data: age, sex, use of alcohol and tobacco, auto declared ethnic background, years of formal education, presence of rheumatoid factor, used medications and comorbidities.

b. RA disease activities indexes: DAS28 (Disease activity score with 28 joints) - ESR (erythrocyte sedimentation rate), DAS28-CRP (C reactive protein), CDAI (Clinical Disease Activity Index) and SDAI (Simplified Disease Activity Index). DAS28-ESR and CRP are measured taking into account the number of tender and swollen joints out of 28, CRP or ESR and patient's general health or global disease activity evaluated on a visual analogue scale of 100mm. CDAI was measured through tender and swollen 28-joint count, patient's global disease activity (from 0-10) and evaluator's global disease activity (from 0-10). SDAI was measured by the addition of the number of swollen and tender 28-joint count, patient's and evaluator global assessment (both from 0-10) and CRP[8].

c. Montreal cognitive assessment (MoCA) - was used for cognitive screening. This instrument has tasks assessing: naming, language, memory, orientation, visuospatial/executive function attention, and abstraction. It ranges from 0-30 with 1 point added as an education adjustment for individuals who had less than 12 years of formal education. Higher values mean better cognition[9,10].

d. Short form health survey with 12 questions (SF-12). SF-12 is a questionnaire with 12 items that evaluates the physical and mental domains of quality of life. It ranges from 0 to 100 and high values are associated with better quality of life[11].

Statistical analysis: Nominal data was compared by Ficher and chi-squared tests. Numeric data was compared by unpaired t test or Mann Whitney test according to sample distribution. Correlation studies of MoCA with disease activity indexes, age, years of formal education, and quality of life was done by Pearson or Spearman test according to data distribution. Sample distribution was studied by Shapiro Wilk test. The adopted significance was 5%.

RESULTS

One hundred and thirty-seven individuals were included: 91 RA patients and 46 controls. RA patients had a median age of 61 (51.0- 68.0) years vs 60.5 (43.0-68.2) years in controls (p=0.40). The median number of years of formal education was 7.5 (4,0-13,0) in the RA sample vs 7.0 (4.0-13.0) in the control group (p=0.99). About 73.6% auto-declared euro-descendants in the RA sample vs 84.7% in the control group (p=0.31). In the RA sample 30.7% had been exposed to tobacco and 4.3% to alcohol while in the control group, 21.7% to tobacco and 8.6% to alcohol (p=0.26 and 0.44 respectively).

Details of RA sample are on **Table 1**.

Table 1. Data on studied Rheumatoid Arthritis patients.

Median disease duration (IQR) - years	11.0 (7.2-18.7)
Female sex (n)	91/91- 100%
Rheumatoid factor (n)	52/90 – 57.7%
Treatment (n)	
Methotrexate	44/91 (48.3%)
Leflunomide	33/91 (36.2%)
Glucocorticoid	20/91 (21.9%)
Glucocorticoid – median dose (IQR)- mg/day	5.0 (5.0-5.0)
Anti TNF alpha	5/91 (5.4%)
Jak inhibitors	3/91 (3.2%)
Anti Interleukin-6	2/91 (2.1%)
Disease activity indexes	
Median DAS-28 ESR (IQR)	2.90 (2.41-3.90)
Median DAS-28 CRP (IQR)	2.39 (1.54-3.50)
Median CDAI (IQR)	6.31 (1.4-11.9)
Median SDAI (IQR)	4.0 (0-10.5)
Comorbidities (n)	
Systemic arterial hypertension	47/91 (51.6%)
Dyslipidemia	33/91 (36.2%)
Hypothyroidism	20/91 (21.9%)
Depression	18/91 (19.7%)
Diabetes mellitus	17/91 (18.6%)

DAS-28 = disease activity score using 28 joints; ESR= erythrocyte sedimentation rate; CRP= C reactive protein; CDAI= Clinical disease activity index; SDAI= Simplified Disease Activity Index; n= number; IQR= interquartile range.

The result of comparison of total MoCA value in the two samples is on **Figure 1** showing that RA patients had worst performance than controls.

The comparison of MoCA domains between RA patients and controls is on **Table 2.** Differences in visuospatial, abstraction and delayed recall were noted.

The comparison of quality of life through SF-12 showed that RA patients had worse physical but not mental quality of life than controls although there was a tendency in this last parameter (p<0.0001 and 0.08 respectively).

The correlation studies of MoCA values with disease activity indexes, epidemiological data and with the domains of quality of life are on **Table 3**.

Figure 1. Comparison of MoCA values between rheumatoid arthritis (RA) patients and controls.

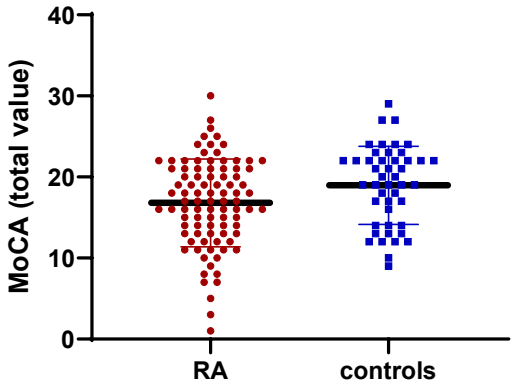

RA patients: mean MoCA value =16.8±5.40;
Controls: mean MoCA value = 18.9±4.81; p=0.02.

Table 2. Comparison of MoCA domains between rheumatoid arthritis (RA) patients and controls. Median values (IQR).

	RA	Controls	P
Visuoespatial/ executive	3 (1-4)	3 (2-4)	**0.04**
Naming	2.5 (2-3)	3 (2 -3)	0.76
Attention	3 (2-4)	3 (2-4)	0.25
Language	2 (1-3)	2.0 (1-3)	0.99
Abstraction	1 (0-1)	1 (1-2)	**0.02**
Delayed recall	0 (0-1)	0.5 (0-2)	**0.04**
Orientation	6 (6-6)	6 (6-6)	0.25

Table 3. Correlation studies of MoCA values with disease activity indexes, age, years of formal education, and quality of life.

	R	95%CI	P
DAS 28-ESR	-0.03	-0.25 to 0.19	0.75
DAS28-CRP	0.11	-0.11 to 0.33	0.31
CDAI	0.12	-0.09 to 0.33	0.26
SDAI	0.09	-0.13 to 0.31	0.42
SF-12 physical domain	0.20	0.004 to 0.39	**0.04**
SF-12 mental domain	0.03	-0.17 to 0.24	0.72
Age	-0.44	-0.60 to -0.26	**<0.0001**
Years of formal education	0.78	0.69 to 0.85	**<0.0001**
Disease duration	-0.26	-0.45 to -0.05	**0.01**

DAS= Disease activity score; ESR= sedimentation rate; CDAI =Clinical Disease activity index; SDAI= simplified disease activity index; SF-12 = Short form health survey with 12 questions

When the association of MoCA values with comorbidities and with used treatment (methotrexate, leflunomide and glucocorticoid) were studied the only found association was a lower MoCA in RA patients with arterial hypertension (p=0.007); all others had p>0.05. Associations with biologics and JAK inhibitors were not studied due to small sample number.

DISCUSSION

The present study shows that RA patients have more CD them controls mainly in the areas of visuospatial/executive functions, abstraction and delayed recall. It also showed that age, disease duration, years of formal education and presence of HAS also associated with cognitive function. Moreover, CD influenced the physical domain of quality of life.

Visuospatial/executive functions demonstrate one's ability to understand and analyze visually presented information and it is associated to motor skills transfer. These two behaviors share a common neural substrate (occipital, parietal and cerebellar cortices[12]. Motor learning is essential to acquire gains in motor performance through patients' experience or repetitive practice, regardless of global cognition[12]. The abstraction domain evaluates a person's ability to understand and differentiate between concepts and it is processed in the prefrontal cortex[13]. This is a neurocognitive function that can be trained by practices that comprise identifying similarities, filtering information, and mapping problem structure[13]. Delayed recall refers to recall assessment of new information and it is the most common domain of cognitive function that triggers the diagnosis of mild cognitive dysfunction[14]. It is processed in the hippocampus[14]. Curiously these cognitive deficits imply in worsening of physical but not mental quality of life measured by SF-12; it is possible that the cognitive deficits by themselves attenuate the perception of worse mental quality of life. In the work by Vitturi et al.,[15] CD was linked to the high value of HAQ (Health Assessment Questionnaire) that is an instrument to measure physical functional impairment.

No association of CD with disease activity could be stablished presently and the same has been verified in the work by Vitturi et al.[15] but not in those by Katchamart et al.[16] and Dowell et al.[2]. The currently studied sample had low median disease activity and this may have prevent finding this association. Future studies are warranted on this aspect as it shows the possibility that pursuing disease inflammatory control may modify cognitive impairment. On the other hand, disease duration showed a modest correlation with MoCA values and this may be due to the chronic effect of an inflammatory disease, causing cumulative damage in the vasculature of central nervous system.

No associations of used treatment with CD were found, but the use of biologic drugs and JAK inhibitors could not be studied due to small sample. Glucocorticoid treatment has been associated with cognitive damage; in animal studies it has been shown that acute glucocorticoid administration impairs working memory[17]. In humans, the chronic use of this drug has been linked to cerebral atrophy in tomography[18] and to a negative impact on hippocampal function[19] and memory[20]. In the present work, with a sample using a small daily dose (median of 5 mg/day of prednisone) no link to cognitive impairment was found and the same was verified in RA patients by at least two others studies[2,21]. Shin et al.[20] even documented a positive impact of this drug in the cognition of RA patients. Methotrexate is another drug potentially associate to CD[4]. In animal models this drug caused memory deficits and decreased executive function, and the brain histopathological analysis revealed decrease cell proliferation as well as changes in thickness and length of corpus callosum[22]. Mechanisms behind methotrexate-induced deficits are probably multifactorial and linked to induction of oxidative stress, inhibition of neurogenesis, altered neurotransmission through the NMDA receptor and/or induction of structural brain alterations[22]. Clinically, it has been evident in children treated for lymphoblastic leukemia where the doses are different from those used in RA[23]. On the other side, methotrexate has been found to associate with reduced carotid intima-media thickness showing the beneficial role of this drug in preventing vascular atherogenesis[24] ; carotid atherosclerosis has been linked to cognitive impairment in both: RA [4] and non-RA patients[25]. Finding association of arterial hypertension with CD in the present work reinforces the role of atherosclerosis in this context.

Education showed to exert a protective action against cognitive deterioration not only in the present work but also in several others done in RA[2], in SLE[26] and in general population[27]. The link between these two variables is not fully understood. Education may have some influence in the cognitive development of individuals but it is also possible that individuals with better cognitive development pursue more education. Moreover, educated patients search for treatment earlier and follow therapeutic instructions more strictly[28].

Depression in RA has been linked to cognitive impairment[3,29,30] although not universally[21]. It was not possible to detect association with depression current-

ly, but this diagnosis was not searched actively, being this data based on patient's information. This is one of the limitations of this study. Other limitations included the low number of patients, patients with low disease activity, and its cross-sectional design. Furthermore, a sample with solely females prevents results' validity for RA male population. On the other side, this study brings information about cognition in RA patients in a sample from Brazil where data on this issue are scarce.

Concluding, this work shows that cognitive impairment occurs in RA patients mainly in the domains of visuospatial /executive functions, and abstraction and delayed recall and that CD associates with disease duration, age, educational levels and physical quality of life.

REFERENCES

1. Foley ÉM, Slaney C, Donnelly NA, Kaser M, Ziegler L, Khandaker GM. A novel biomarker of interleukin 6 activity and clinical and cognitive outcomes in depression. **Psychoneuroendocrinology.** 2024; 164:107008. doi: 10.1016/j.psyneuen.2024.107008.
2. McDowell B, Marr C, Holmes C, Edwards CJ, Cardwell C, McHenry M, et al. Prevalence of cognitive impairment in patients with rheumatoid arthritis: a cross-sectional study. **BMC Psychiatry**. 2022; 22(1):777. doi: 10.1186/s12888-022-04417-w.
3. Qidwai M, Ahmed K, Tahir MF, Shaeen SK, Hasanain M, Malikzai A. Cognitive implications of rheumatoid arthritis: A call for comprehensive care and research focus. **Immun Inflamm Dis.** 2023;11(11): e1065. doi: 10.1002/iid3.1065.
4. Oláh C, Schwartz N, Denton C, Kardos Z, Putterman C, Szekanecz Z. Cognitive dysfunction in autoimmune rheumatic diseases. **Arthritis Res Ther.** 2020;22(1):78. doi: 10.1186/s13075-020-02180-5.
5. Alexopoulos P, Skondra M, Charalampopoulou M, Georgiou EE, Demertzis AA, Aligianni SI, et al. Low cognitive functioning and depressive symptoms in patients with rheumatoid arthritis and systemic sclerosis: a clinical study. **BMC Psychiatry.** 2023; 23(1): 513. doi: 10.1186/s12888-023-04995-3.
6. Duan L, Li S, Li H, Shi Y, Xie X, Feng Y. Causality between rheumatoid arthritis and the risk of cognitive impairment: a Mendelian randomization study. **Arthritis Res Ther.** 2024; 26(1): 5. doi: 10.1186/s13075-023-03245-x.
7. Aletaha D, Neogi T, Silman AJ, Funovits J, Felson DT, Bingham CO III, et al. 2010 Rheumatoid arthritis classification criteria: an American College of Rheumatology/European League Against Rheumatism collaborative initiative. **Arthritis Rheum.** 2010; 62(9):2569–2581. https://doi.org/10.1002/art.27584.
8. Medeiros MM, de Oliveira BM, de Cerqueira JV, Quixadá RT, de Oliveira ÍM. Correlation of rheumatoid arthritis activity indexes (Disease Activity Score 28 measured with ESR and CRP, Simplified Disease Activity Index and Clinical Disease Activity Index) and agreement of disease activity states with various cut-off points in a Northeastern Brazilian population. **Rev Bras Reumatol.** 2015; 55(6): 477-84. doi: 10.1016/j.rbr.2014.12.005.
9. Nasreddine ZS, Phillips NA, Bédirian V, Charbonneau S, Whitehead V, Collin I, et al. The Montreal cognitive assessment, MoCA: a brief screening tool for mild cognitive impairment. **J Am Geriatr Soc**. 2005; 53:695–9. doi: 10.1111/j.1532-5415.2005.53221.x.
10. Apolinario D, Dos Santos MF, Sassaki E, Pegoraro F, Pedrini AV, Cestari B, et al. Normative data for the Montreal Cognitive Assessment (MoCA) and the Memory Index Score (MoCA-MIS) in Brazil: adjusting the non-linear effects of education with fractional polynomials. **Int J Geriatr Psychiatry.** 2018; 33(7): 893-9. https://doi.org/10.1002/gps.4866.
11. Andrade TL, Camelier AA, Rosa FW, Santos MP, Jezler S, Pereira e Silva JL. Applicability of the 12-Item Short-Form Health Survey in patients with progressive systemic sclerosis. **J Bras Pneumol**. 2007; 33(4): 414-22. doi: 10.1590/s1806-37132007000400010.
12. Lingo VanGilder J, Walter CS, Hengge CR, Schaefer SY. Exploring the relationship between visuospatial function and age-related deficits in motor skill transfer. **Aging Clin Exp Res.** 2020;32(8):1451-1458. doi: 10.1007/s40520-019-01345-w.
13. Dumontheil I. Development of abstract thinking during childhood and adolescence: the role of rostro lateral prefrontal cortex. **Dev Cogn Neurosci**. 2014; 10:57-76. doi: 10.1016/j.dcn.2014.07.009.
14. Kaur A, Edland SD, Peavy GM. The MoCA-Memory Index Score: An efficient alternative to paragraph recall for the detection of amnestic mild cognitive impairment. Alzheimer **Dis Assoc Disord**. 2018; 32(2): 120-124. doi: 10.1097/WAD.0000000000000240.
15. Vitturi BK, Nascimento BAC, Alves BR, de Campos FSC, Torigoe DY. Cognitive impairment in patients with rheumatoid arthritis. **J Clin Neurosci**. 2019; 69: 81-87. doi: 10.1016/j.jocn.2019.08.027.
16. Katchamart W, Narongroeknawin P, Phutthinart N, Srinonprasert V, Muangpaisan W, Chaiamnauy S. Disease activity is associated with cognitive impairment in patients with rheumatoid arthritis. **Clin Rheumatol.** 2019; 38(7): 1851-1856. doi: 10.1007/s10067-019-04488-3.
17. Barsegyan A, McGaugh JL, Roozendaal B. Glucocorticoid effects on working memory impairment require l-type calcium channel activity within prefrontal cortex. **Neurobiol Learn Mem**. 2023; 197:107700. doi: 10.1016/j.nlm.2022.107700.
18. Zanardi VA, Magna LA, Costallat LT. Cerebral atrophy related to corticotherapy in systemic lupus erythematosus (SLE). **Clin Rheumatol**. 2001; 20(4):245-50. doi: 10.1007/s100670170037.
19. Brown SC, Glass JM, Park DC. The relationship of pain and depression to cognitive function in rheumatoid ar-

thritis patients. **Pain.** 2002; 96: 279–284. https://doi.org/10.1016/S0304-3959(01)00457-2.

20. Coluccia D, Wolf OT, Kollias S, Roozendaal B, Forster A, de Quervain DJ-F. Glucocorticoid therapy induced memory deficits: Acute versus chronic effects. **J Neurosci.** 2008; 28:3474–3478. https://doi. org/10.1523/JNEUROSCI.4893-07.2008.
21. Appenzeller S, Bertolo MB, Costallat LT. Cognitive impairment in rheumatoid arthritis. Methods **Find Exp Clin Pharmacol**. 2004; 26(5): 339-43. doi: 10.1358/mf.2004.26.5.831324.
22. Wen J, Maxwell RR, Wolf AJ, Spira M, Gulinello ME, Cole PD. Wen J, et al. Methotrexate causes persistent deficits in memory and executive function in a juvenile animal model. Neuropharmacology. 2018; 139:76-84. doi: 10.1016/j.neuropharm.2018.07.007.
23. Khedr LH, Rahmo RM, Eldemerdash OM, Helmy EM, Ramzy FA, Lotfy GH,et al. Implication of M2 macrophage on NLRP3 inflammasome signaling in mediating the neuroprotective effect of Canagliflozin against methotrexate-induced cognitive impairment. **Int Immunopharmacol**. 2024; 130:111709. doi: 10.1016/j.intimp.2024.111709.
24. Kim HJ, Kim MJ, Lee CK, Hong YH. Effects of methotrexate on carotid intima-media thickness in patients with rheumatoid arthritis. **J Korean Med Sci.** 2015; 30(11): 1589-96. doi: 10.3346/jkms.2015.30.11.1589.
25. Yue W, Wang A, Liang H, Hu F, Zhang Y, Deng M et al. Association between carotid intima-media thickness and cognitive impairment in a Chinese stroke population: a cross-sectional study. **Sci Rep.** 2016; 6:19556. doi: 10.1007/s00415-016-8234-9.
26. Borba EA, Scoto Dias E, Tercziany Vanzin JH, Ferreira de Queiroz Junior N, Dos Santos TAF, Skare T, et al. Cognitive dysfunction in patients with systemic lupus erythematosus. A cross-sectional study in a Brazilian sample. **Lupus.** 2023; 32(7):900-909. doi: 10.1177/09612033231176794.
27. Chen G, Zhao M, Yang K, Lin H, Han C, Wang X, Han Y. Education exerts different effects on cognition in individuals with subjective cognitive decline and cognitive impairment: A population-based study. **J Alzheimers Dis.** 2021;79(2):653-661. doi: 10.3233/JAD-201170.
28. Lövdén M, Fratiglioni L, Glymour MM, Lindenberger U, Tucker-Drob EM. Education and cognitive functioning across the life span. **Psychol Sci Public Interest.** 2020; 21:6-41. doi: 10.1177/1529100620920576.
29. GG-Meade T, Manolios N, Cumming SR, Conaghan PG, Katz P. Cognitive impairment in rheumatoid arthritis: a systematic review. **Arthritis Care Res.** 2018; 70(1):39–52. https://doi.org/10.1002/acr.23243.
30. Brown SC, Glass JM, Park DC. The relationship of pain and depression to cognitive function in rheumatoid arthritis patients. **Pain.** 2002; 96(3): 279-84. https://doi.org/10.1016/S0304-3959(01)00457-2.

ORIGINAL ARTICLE: TOPIC IN MEDICAL CLINIC *ARTIGO ORIGINAL: TÓPICO EM CLÍNICA MÉDICA*

RADIOGRAPHIC PREVALENCE ANALYSIS OF CHONDROCALCINOSIS IN PATIENTS WITH RHEUMATOID ARTHRITIS: A SOUTHERN BRAZILIAN SAMPLE

ANÁLISE DA PREVALÊNCIA RADIOGRÁFICA DE CONDROCALCINOSE EM PACIENTES COM ARTRITE REUMATOIDE: UMA AMOSTRA DO SUL DO BRASIL

Isabela Miotto Neves[1]; Lucas Carlini Policeni[2]; Gustavo Firmino Golfetto Jeronimo[3]; Thelma Larocca Skare[1]; Bárbara Stadler Kahlow[5]

[1] Isabela Miotto Neves
Faculdade Evangélica Mackenzie do Paraná, Curitiba, Brazil
ORCID: 0009-0003-0884-2843

[2] Lucas Carlini Policeni
Faculdade Evangélica Mackenzie do Paraná, Curitiba, Brazil
ORCID: 0009-0003-7339-2308

[3] Gustavo Firmino Golfetto Jeronimo
Faculdade Evangélica Mackenzie do Paraná, Curitiba, Brazil
ORCID: 0009-0009-4263-1613

[4] Thelma Larocca Skare
Faculdade Evangélica Mackenzie do Paraná, Curitiba, Brazil
ORCID: 0000-0002-7699-3542

[5] Bárbara Stadler Kahlow
Faculdade Evangélica Mackenzie do Paraná, Curitiba, Brazil. Pontifícia Universidade Católica do Paraná, Curitiba, Brazil.
ORCID: 0000-0001-5292-2777

Received in: 04-12-2024
Accepted in: 18-12-2024

Corresponding author:
Thelma L Skare
Rua Padre Anchieta, 2770.
807330 000 Curitiba, PR.
E-mail: thelma.skare@gmail.com

DOI: 10.29327/2413063.22.1-4

Background: Chondrocalcinosis commonly manifests as arthritis and is referred to as calcium pyrophosphate deposition disease. When it presents as chronic polyarthritis, it resembles rheumatoid arthritis. Patients with rheumatoid arthritis, due to chronic joint inflammation, experience cartilage damage that stimulates the formation of calcium pyrophosphate crystals, leading to the coexistence of both diseases. This study aimed to assess the prevalence of chondrocalcinosis in patients with rheumatoid arthritis and analyze their clinical profiles. **Methodology:** This was a longitudinal, observational and retrospective study, analyzing epidemiological, clinical, laboratory, and radiographic data from 110 patients with rheumatoid arthritis. **Results:** The prevalence of chondrocalcinosis in patients with rheumatoid arthritis was 5.45%. Factors associated with chondrocalcinosis included age and diabetes mellitus. **Conclusion:** Chondrocalcinosis can coexist with rheumatoid arthritis due to chronic cartilage damage caused by the disease; however, diagnostic errors should be considered. Special attention should be given to patients over 60 years old.

Keywords: rheumatoid arthritis, chondrocalcinosis, diabetes mellitus

BACKGROUND

Chondrocalcinosis is the radiographic finding of calcium pyrophosphate crystal deposition in articular fibrocartilage, commonly manifesting as arthritis, and is referred to as calcium pyrophosphate deposition disease (CPPD).[1]

The prevalence of CPPD remains undefined, but the prevalence of radiographic chondrocalcinosis varies between 4-10% in adults over 60 years old.[1] It can present in multiple ways (asymptomatic, monoarticular, oligoarticular, or polyarticular), mimicking other diseases such as gout, osteoarthritis, polymyalgia rheumatica, rheumatoid arthritis (RA), and spondyloarthritis.[2]

Risk factors for the development of the disease include advanced age, metabolic syndrome, osteoarthritis, RA, gout, hyperparathyroidism, hemochromatosis, hypophosphatemia, and hypomagnesemia.[3,4]

As observed, the risk factors and mimicking diseases are similar and may overlap.

When CPPD presents as chronic polyarthritis, it closely resembles RA.[5] These similarities can lead to CPPD being mistakenly diagnosed as RA and vice versa.[3] Furthermore, RA patients, due to chronic joint inflammation, experience cartilage damage that results in changes in its matrix and chondrocytes, promoting the formation of calcium pyrophosphate crystals, which can lead to the coexistence of both diseases.[3]

Considering the hypothesis of the coexistence of these two diseases, this study aimed to assess the prevalence of chondrocalcinosis and the clinical profile of patients with RA.

METHODS

This was a retrospective longitudinal observational study, comprising a sample of 110 RA patients followed at the rheumatology outpatient clinic of the Mackenzie Evangelical University Hospital. Epidemiological, clinical, and laboratory data were collected from medical records.

The investigation of chondrocalcinosis was performed through the evaluation of hand, wrist, and knee radiographs by a single rheumatologist.

Data were organized into frequency tables. The comparative analysis of nominal data was conducted using Fisher's exact test and the chi-square test. The comparison of numerical data was performed using the Mann-Whitney and unpaired t-tests. A significance level of 5% was adopted.

RESULTS

In the present study, the prevalence of radiographic findings of chondrocalcinosis in RA patients was 5.45%.

Table 1 presents the epidemiological data, showing that the sample was predominantly composed of women (89%), with a mean age of 59.4 years and a median disease duration of 10 years.

There was a statistically significant difference in the mean age of patients, with those presenting chondrocalcinosis findings being older (65.1 ± 9 years) compared to those without chondrocalcinosis findings (49.4 ± 10.2 years).

Regarding comorbidities, medications, and laboratory data studied between the two groups, an association was found only for the variable diabetes mellitus in the group with chondrocalcinosis. Data are described in **Table 2.**

DISCUSSION

This study showed that 5.45% of RA patients had radiographic findings of chondrocalcinosis, with an average age of 65.1 years in this group. This finding aligns with the literature, which indicates that most CPPD patients are over 60 years old.[1]

In a similar study, Viktoriya et al. described an average age of 69.5 (±11.4) years for the group with associated chondrocalcinosis in RA patients and found no difference in the presence or absence of rheumatoid factor, similar to our study.[3] In the same cohort, a retrospective analysis of radiographic findings of chondrocalcinosis identified a time difference of 13.4 (±10.9) years between RA diagnosis and the onset of chondrocalcinosis, suggesting the hypothesis of crystal deposition secondary to inflammatory arthritis damage.[3]

Paalanen et al., hypothesizing that CPPD may mimic RA, investigated the prevalence of CPPD in 435 seronegative RA patients (rheumatoid factor negative) and found 3.9% CPPD in patients with early RA diagnosis. This prevalence increased to 7% among patients over 60 years old.[6]

Table 1. Comparison of Epidemiological Data.

	Total (n=110)	RA with chondrocalcinosis (n=6)	RA without chondrocalcinosis (n=104)	p-value
Women – n (%)	98 (89)	5 (83.3)	93 (89.4)	0.50
Age (years) – mean (SD*)	59.4 (±10)	65.1 (±9)	49.4 (±10.2)	0.0004
Disease duration (years) – median (IQR**)	10 (7.0-12.0)	7 (6.5-9.7)	27 (24.0-30.7)	0.18

* SD: Standard Deviation.

** IQR: Interquartile Range.

Table 2. Study of Comorbidities and Laboratory Data.

	Total (n=110)	RA with chondrocalcinosis (n=6)	RA without chondrocalcinosis (n=104)	p-value
Comorbidities – n(%)				
Hypertension	55 (50)	2 (33.3)	53 (50.9)	0.67
Diabetes	18 (16.3)	3 (50)	15 (14.4)	0.05
Dyslipidemia	61 (55.4)	3 (50)	58 (55.7)	0.99
Hypothyroidism	30 (27.2)	3 (50)	27 (25.9)	0.34
Osteoarthritis	50 (45.4)	3 (50)	47 (45.1)	0.99
Additional Data				
Erosion – n (%)	30 (27.2)	2 (33.3)	28 (26.9)	0.66
Rheumatoid Factor – n(%)	77 (70)	4 (66.6)	73 (70.1)	0.99
Vitamina D – median (IQR*)	32.0 (25.0-38.5)	37.5 (30.5-46.5)	32 (25.0-37.7)	0.13
Uric acid – median (IQR)	3.75 (2.7-4.7)	4.5 (3,6-4.9)	3.6 (2.6-4.6)	0.24

* IQR: Interquartile Range.

CPPD is correlated with multiple comorbidities and medications, particularly hypertension, osteoarthritis, and loop diuretics.[4] In our study, an association was found with diabetes mellitus, likely due to chronic corticosteroid use in patients with difficult-to-control RA.

CONCLUSION

Chondrocalcinosis can coexist with RA due to chronic cartilage damage caused by the disease, but attention must be paid to possible diagnostic errors. Special attention should be given to patients with early-onset rheumatoid arthritis, those over 60 years old, and those with negative antibodies.

REFERENCES

1. Abhishek A, Tedeschi SK, Pascart T, Latourte A, Dalbeth N, Neogi T, et al. The 2023 ACR/EULAR classification criteria for calcium pyrophosphate deposition disease. **Ann Rheum Dis**. 2023;82(10):1248–57.
2. Rosenthal AK, Ryan LM. Calcium Pyrophosphate Deposition Disease. Campion EW, editor. **N Engl J Med.** 2016; 374(26):2575–84.
3. Sabchyshyn V, Konon I, Ryan LM, Rosenthal AK. Concurrence of rheumatoid arthritis and calcium pyrophosphate deposition disease: A case collection and review of the literature. **Semin Arthritis Rheum**. 2018;48(1):9–11.
4. Tedeschi SK, Yoshida K, Huang W, Solomon DH. Confirming Prior and Identifying Novel Correlates of Acute Calcium Pyrophosphate Crystal Arthritis. **Arthritis Care Res**. 2023;75(2):283–8.
5. Cowley S, McCarthy G. Diagnosis and Treatment of Calcium Pyrophosphate Deposition (CPPD) Disease: A Review. **Open Access Rheumatol Res Rev**. 2023;Volume 15:33–41.
6. Paalanen K, Rannio K, Rannio T, Asikainen J, Hannonen P, Sokka T. Prevalence of calcium pyrophosphate deposition disease in a cohort of patients diagnosed with seronegative rheumatoid arthritis. **Clin Exp Rheumatol**. 2020;38(1):99–106.

ORIGINAL ARTICLE: THYROID TECHNOLOGY *ARTIGO ORIGINAL: TECNOLOGIA DA TIREÓIDE*

AUTOMATED THYROID ULTRASOUND ANALYSIS: HASHIMOTO'S THYROIDITIS

ANÁLISE AUTOMATIZADA DE ULTRASSOGRAFIA DA TIREOIDE: TIREOIDITE DE HASHIMOTO

Gabriela Correia Matos de Oliveira[1]; Luísa Correia Matos de Oliveira[2]; Luís Matos de Oliveira[3]; Luís Jesuíno de Oliveira Andrade[4]

[1] Gabriela Correia Matos de Oliveira
UniFTC Faculdade de Medicina - Salvador - Bahia - Brasil.
ORCID: https://orcid.org/0000-0002-8042-0261

[2] Luísa Correia Matos de Oliveira
SENAI CIMATEC - Centro Universitário - Salvador - Bahia - Brasil.
ORCID: https://orcid.org/0000-0001-6128-4885

[3] Luís Matos de Oliveira
Departamento de Saúde - Universidade de Santa Cruz - Ilhéus - Bahia - Brasil.
ORCID: https://orcid.org/0000-0003-4854-6910

[4] Luís Jesuíno de Oliveira Andrade
Departamento de Saúde - Universidade de Santa Cruz - Ilhéus - Bahia - Brasil.
ORCID: https://orcid.org/0000-0002-7714-0330

Received in:08-01-2025
Reviewed in: 23-01-2025
Accepted in: 04-02-2025

Competing Interests: No potential conflict of interest relevant to this article was reported.

Corresponding Author:
Luis Jesuino de Oliveira Andrade
Campus Soane Nazaré de Andrade, Rod. Jorge Amado, Km 16 - Salobrinho, Ilhéus - BA, 45662-900
E-mail: luis_jesuino@yahoo.com.br

DOI: 10.29327/2413063.22.1-5

Introduction: Thyroid ultrasound provides valuable insights for thyroid disorders but is hampered by subjectivity. Automated analysis utilizing large datasets holds immense promise for objective and standardized assessment in screening, thyroid nodule classification, and treatment monitoring. However, there remains a significant gap in the development of applications for the automated analysis of Hashimoto's thyroiditis (HT) using ultrasound. **Objective**: To develop an automated thyroid ultrasound analysis (ATUS) algorithm using the C# programming language to detect and quantify ultrasonographic characteristics associated with HT. **Materials and Methods**: This study describes the development and evaluation of an ATUS algorithm using C#. The algorithm extracte relevant features (texture, vascularization, echogenicity) from preprocessed ultrasound images and utilizes machine learning techniques to classify them as "normal" or indicative of HT. The model is trained and validated on a comprehensive dataset, with performance assessed through metrics like accuracy, sensitivity, and specificity. The findings highlight the potential for this C#-based ATUS algorithm to offer objective and standardized assessment for HT diagnosis. **Results**: The program preprocesses images (grayscale conversion, normalization, etc.), segments the thyroid region, extracts features (texture, echogenicity), and utilizes a pre-trained model for classification ("normal" or "suspected Hashimoto's thyroiditis"). Using a sample image, the program successfully preprocessed, segmented, and extracted features. The predicted classification ("suspected HT") with high probability (0.92) aligns with the pre-established diagnosis, suggesting potential for objective HT assessment. **Conclusion**: C#-based ATUS algorithm successfully detects and quantifies Hashimoto's thyroiditis features, showcasing the potential of advanced programming in medical image analysis.

Keywords: Automated Analysis; Thyroid Ultrasound; Hashimoto's Thyroiditis; C# programming language.

Introdução: A ultrassonografia da tireoide fornece informações valiosas para diagnósticos de tireoide, mas é prejudicado pela subjetividade. A análise automatizada utilizando grandes conjuntos de dados é promissora para avaliações objetivas e padronizadas em triagem, classificação de nódulos tireoidianos e monitoramento do tratamento. No entanto, ainda há uma lacuna significativa no desenvolvimento de aplicações para a análise automatizada da tireoidite de Hashimoto (TH) por ultrassonografia. **Objetivo**: Desenvolver um algoritmo automatizado de análise de ultrassonografia da tireoide (ATUS) utilizando a linguagem de programação C# para detectar e quantificar características ultrassonográficas associadas à TH. **Materiais e Métodos**: Este estudo descreve o desenvolvimento e avaliação de um algoritmo ATUS usando C#. O algoritmo extrai características relevantes (textura,

vascularização, ecogenicidade) de imagens pré-processadas de ultrassonografia e utiliza técnicas de aprendizado de máquina para classificá-las como "normais" ou indicativas de TH. O modelo é treinado e validado em um conjunto de dados abrangente, com desempenho avaliado por métricas como precisão, sensibilidade e especificidade. Os resultados destacam o potencial deste algoritmo ATUS baseado em C# para oferecer avaliação objetiva e padronizada para o diagnóstico de TH. **Resultados**: O programa pré-processa imagens (conversão para tons de cinza, normalização, etc.), segmenta a região da tireoide, extrai características (textura, ecogenicidade) e utiliza um modelo pré-treinado para classificação ("normal" ou "suspeita de tireoidite de Hashimoto"). Usando uma imagem de amostra, o programa pré-processou, segmentou e extraiu características com sucesso. A classificação prevista ("suspeita de TH") com alta probabilidade (0,92) está de acordo com o diagnóstico pré-estabelecido, sugerindo potencial para avaliação objetiva da TH. **Conclusão**: O algoritmo ATUS baseado em C# detecta e quantifica com sucesso as características da tireoidite de Hashimoto, demonstrando o potencial da programação avançada na análise de imagens médicas.
Descritores: Análise Automatizada; Ultrassom de Tireoide; Tireoidite de Hashimoto; Linguagem de programação C#.

INTRODUCTION

Thyroid ultrasound (US) is a widely used imaging modality for the assessment of thyroid gland structure and function. It is a non-invasive, readily available, and relatively inexpensive technique that provides valuable information for the diagnosis and management of thyroid disorders[1]. However, the interpretation of thyroid US images can be subjective and operator-dependent, leading to potential variability in diagnostic accuracy.

Manual thyroid US analysis relies heavily on the expertise and experience of the sonographer. This can lead to inconsistencies in image interpretation and reporting, particularly among less experienced practitioners[2]. Additionally, the subjective nature of manual assessment can be influenced by factors such as fatigue, visual acuity, and individual interpretation biases[3].

Automated thyroid US analysis (ATUS) offers the potential to address the limitations of manual interpretation by providing objective and standardized assessments[4]. ATUS algorithms can be trained on large datasets of thyroid US images with corresponding clinical data to identify and quantify subtle US features associated with various thyroid disorders[5].

ATUS has the potential to be applied in various clinical settings, including: Screening for thyroid disorders: ATUS could be used to screen asymptomatic individuals for thyroid abnormalities, potentially leading to early detection and intervention[6]. Diagnosis and classification of thyroid nodules: ATUS could assist in the diagnosis and classification of thyroid nodules, helping to differentiate between benign and malignant lesions.[7] Monitoring of thyroid disorders: ATUS could be used to monitor the response to treatment for thyroid disorders, providing objective measures of disease progression or regression[8].

Research in ATUS has made significant progress in recent years. Several studies have demonstrated the potential of ATUS algorithms to accurately differentiate between normal and abnormal thyroid tissue, classify thyroid nodules, and monitor treatment response[9]. However, further validation and refinement are needed before ATUS can be widely adopted in clinical practice.

The objective of this study is to develop an ATUS algorithm using the C# programming language to detect and quantify ultrasonographic characteristics associated with Hashimoto's thyroiditis (HT). By leveraging the capabilities of C# for algorithm development, we aim to improve the efficiency and accuracy of identifying subtle features indicative of autoimmune thyroid disease.

MATERIALS

1. Hardware:

- A computer system with sufficient processing power and memory to support image processing and machine learning tasks.

2. Software:

- C# development environment (Visual Studio)
- Image processing libraries (EmguCV)
- Machine learning libraries (ML.NET)

3. Dataset: A comprehensive dataset of thyroid US image including:

- Images with confirmed HT diagnosis.
- Images from healthy control subjects without thyroid abnormalities.
- High-quality grayscale images with standardized acquisition protocols.
- Associated clinical data, including thyroid function tests and thyroid-stimulating hormone (TSH) levels.

METHODS

1. Algorithm Development

1.2. The ATUS algorithm will be developed using C#. C#'s object-oriented programming paradigm will facilitate modular design and code reusability.

1.2. The algorithm incorporated the following key stages:

- ***Preprocessing***: Images preprocessed to enhance quality and facilitate feature extraction. This involved techniques like normalization, and histogram equalization.
- ***Feature Extraction***: Relevant US features associated with HT extracted from the preprocessed images. Including: textural features, vascularization features, and echogenicity features.
- ***Classification***: Machine learning techniques implementation to classify the preprocessed images and extracted features.
- ***Model Optimization***: The hyperparameters of the machine learning model optimized to achieve the best possible performance in terms of accuracy, sensitivity, and specificity.

2. Model Training and Evaluation

2.1. The compiled ATUS algorithm was be trained on a portion of the dataset. This training data were allowing the model to learn the relationships between extracted features and the presence/absence of HT.

2.2. Separate portions of the dataset were used for model validation. The model's performance was be evaluated through metrics such as accuracy, sensitivity, specificity.

3. Cross-validation techniques were being employed to ensure the generalizability and robustness of the model across the entire dataset.

ETHICAL CONSIDERATIONS

This study does not require ethical approval as it is solely based on bioinformatics data and does not involve the use of human thyroid tissue samples. In accordance with the guidelines of the Brazilian National Research Ethics Committee (CONEP), research involving non-identifiable data of public origin is exempt from ethics committee review.

RESULTS

NET Algorithm for Automated Thyroid Ultrasound Analysis

1. **Preprocessing**: Loads the thyroid US image, converts the image to grayscale, and applies normalization and histogram equalization techniques to improve image quality.
2. **Thyroid Segmentation**: Utilizes image segmentation techniques to identify the thyroid region in the US image: thresholding, region-based segmentation, convolutional neural networks.
3. **Feature Extraction**: Extracts relevant US features from the segmented thyroid region: texture, vascularization, and echogenicity.
4. **Classification Model Training**: Divides the US images into training, validation, and testing sets. Trains a machine learning model to classify the thyroid US images as "normal" or "suspected Hashimoto's thyroiditis".
5. **Model Evaluation**: Evaluates the performance of the trained model on the validation and testing datasets. Assessment metrics include accuracy, sensitivity, and specificity.
6. **Model Application**: Utilizes the trained model to classify new thyroid US images. Generates a report presenting the image classification and the probability of being associated with HT.

Language: C#

Steps:

1. Preprocessing

```
C#
using System;
using Emgu.CV;
using Emgu.CV.Util;

  public class ImagePreprocessing
  {
    public Mat PreprocessImage(string im-
agePath)
```

```
    {
    // Load the ultrasound image
    Mat image = CvInvoke.Imread(image-
Path);

    // Convert to grayscale (optional for
some processing steps)
    Mat grayImage = image.ConvertImage(-
ColorConversion.Bgr2Gray);

    // Apply normalization (optional)
    // Normalize the pixel intensities to
a specific range (e.g., 0-1)
    // This can help improve contrast and
comparability between images
    Mat normalizedImage = grayImage.Nor-
malize(0, 255, NormType.NormMinMax);

    // Apply histogram equalization (op-
tional)
    // Enhance the contrast of the image
by redistributing the pixel intensities
    // This can help emphasize details and
make features more visible
    Mat equalizedImage = normalizedImage.
EqualizeHist();

    return equalizedImage;
  }
}
```

Code Execution Steps:

- Image Loading: The ultrasound image is loaded using CvInvoke.Imread(imagePath).
- Grayscale Conversion: The image is converted to a grayscale representation using image.ToImage<Gray, byte>().
- Normalization: CvInvoke.Normalize() is employed to normalize the image. This scales pixel intensities to a range between 0 and 255, which can enhance comparability across different images.
- Histogram Equalization: CvInvoke.EqualizeHist() is utilized to redistribute pixel intensities, thereby improving image contrast, particularly in low-contrast regions.

2. Thyroid Segmentation

C#

```
using System;
using Emgu.CV;
using Emgu.CV.Util;

 public class Thyroid Segmentation
 {
   public static Mat SegmentThyroid(Mat
image)
    {
    // Convert image to grayscale (option-
al for some methods)
    Mat grayImage = image.ConvertImage(-
ColorConversion.Bgr2Gray);

    // Option 1: Thresholding (simple but
less robust)
    Mat binaryImage = grayImage.Threshold-
Binary(128, 255, ThresholdType.Binary);

    // Improve binary image (optional)
    binaryImage = binaryImage.Dilate(Cv-
Invoke.GetStructuringElement(MorphEx.Di-
late, new Size(5, 5)));
    binaryImage = binaryImage.Erode(Cv-
Invoke.GetStructuringElement(MorphEx.
Erode, new Size(5, 5)));
    binaryImage = binaryImage.FillHoles();

    // Find largest contour (potential
thyroid region)
    VectorOfVectorOfPoint contours = new
VectorOfVectorOfPoint();
    CvInvoke.FindContours(binaryImage,
contours, null, RetrievalModes.External,
ContourApproximationModes.ChainApprox-
Simple);
    double largestArea = 0;
    Mat largestContour = null;
    foreach (var contour in contours)
    {
    double area = CvInvoke.ContourArea(-
contour);
    if (area > largestArea)
    {
    largestArea = area;
    largestContour = contour;
    }
    }

    // Option 2: Region-based segmenta-
tion (more complex but potentially more
accurate)
    // This is a simplified example and
requires additional implementation for
feature extraction and segmentation al-
gorithms.
```

```
    // Option 3: Convolutional Neural Networks (CNNs) (most advanced but requires pre-trained model and deep learning expertise)
    // This is not implemented here due to its complexity.

    // Choose the desired segmentation method and return the result
    if (largestContour != null)
    {
    return Mask.FillConvexPoly(image, largestContour, new Scalar(255, 0, 0)); // Draw red mask on the original image
    }
    else
    {
    return null; // Indicate segmentation failure
    }
    }

    public static void Main(string[] args)
    {
    // Load your thyroid ultrasound image
    Mat image = CvInvoke.Imread("thyroid_ultrasound.jpg");

    // Segment the thyroid region
    Mat segmentedImage = SegmentThyroid(image);

    // Check if segmentation was successful
    if (segmentedImage != null)
    {
    // Display the segmented image (optional)
    CvInvoke.NamedWindow("Segmented Thyroid");
    CvInvoke.Imshow("Segmented Thyroid", segmentedImage);
    CvInvoke.WaitKey(0);
    }
    else
    {
    Console.WriteLine("Thyroid segmentation failed.");
    }
  }
}
```

Code Execution Steps:

- Grayscale Conversion: Grayscale conversion can be beneficial for reducing image complexity by eliminating the need to maintain color information. The ToImage<Gray, byte>() function from Emgu CV is utilized for this purpose.
- Thresholding: Thresholding is a straightforward method that converts the image to a binary representation. A threshold value of 128 was selected, where pixels with intensities below 128 are set to 0 (black), and those above 128 are set to 255 (white). This technique aids in isolating regions of interest within the image, such as the thyroid.
- Binary Image Enhancement: Dilation and erosion are morphological operations that refine the binary image. Dilation expands the white regions, while erosion shrinks them. The FillHoles() operation fills enclosed dark regions within the white areas, improving segmentation.
- Largest Contour Identification: The FindContours function detects the boundaries of the binary image. The code identifies the largest contour, which is assumed to represent the thyroid region. The contour area is computed using ContourArea, and the contour with the largest area is selected.
- Region-Based Method (Optional): Region-based segmentation is a more sophisticated approach that can yield more accurate segmentation results but introduces increased complexity.
- Convolutional Neural Networks (CNNs) (Optional): CNNs are an advanced segmentation technique that requires a trained model. While not implemented here, it represents a modern option for medical image segmentation.
- Mask Drawing: If the largest contour is identified, a mask is drawn over the original image, filling the thyroid region with red (255, 0, 0).
- Image Loading: The thyroid ultrasound image is loaded from a file path using the Imread function.
- Segmentation: The SegmentThyroid function is invoked to process the image and perform the segmentation.
- Result Verification and Display: If the segmentation is successful, the segmented image is displayed in a window. Otherwise, a message indicating segmentation failure is displayed.

3. Feature Extraction

```
C#
using System;
using Emgu.CV;

 public class FeatureExtraction
 {
   public static FeatureVector Extract-
Features(Mat segmentedRegion)
   {
   // Feature vector to store extracted
data
   FeatureVector features = new Fea-
tureVector();

   // Textural features (using Gabor fil-
ters as an example)
   GaborFilter[] gaborFilters = Gener-
ateGaborFilters(); // Implement function
to generate Gabor filters with desired pa-
rameters
   double[] textureMeasures = new dou-
ble[gaborFilters.Length];
   for (int i = 0; i < gaborFilters.
Length; i++)
   {
   Mat filteredImage = gaborFilters[i].
FilterImage(segmentedRegion);
   textureMeasures[i] = CalculateMean(-
filteredImage); // Replace with desired
texture measurement (e.g., standard devi-
ation, entropy)
   }
   features.Texture = textureMeasures;

   // Vascularization features (Doppler
analysis not implemented here due to com-
plexity)
   // ... (requires additional libraries
and processing)

   // Echogenicity features
   features.Echogenicity = Calculate-
Mean(segmentedRegion); // Measure average
intensity

   return features;
   }

   private static GaborFilter[] Gener-
ateGaborFilters()
   {
   // Implement this function to create
Gabor filters with desired orientations
and frequencies
   // ...
   return null; // Replace with actual
Gabor filter creation
   }

   private static double Calculate-
Mean(Mat image)
   {
   return CvInvoke.Mean(image).Val0; //
Get the mean intensity value
   }

   public struct FeatureVector
   {
   public double[] Texture { get; set; }
   public double Echogenicity { get; set;
}
   // Add additional fields for other fea-
tures (e.g., vascularization)
 }
}
```

Detailed Explanation of Code Steps:

- ExtractFeatures Function: This function is the core of the feature extraction process and receives a segmentedRegion image, which represents the segmented region of the ultrasound image (e.g., the thyroid). The method returns a FeatureVector containing the extracted features from this region.
- Texture Features with Gabor Filters: These filters are employed for texture analysis in images. They possess various orientations and frequencies and are useful for detecting spatial patterns in medical images, such as textures in skin, muscles, or other tissues. The GenerateGaborFilters function is intended to generate filters with different orientations and frequencies; however, in the provided code, it is not implemented. For each generated Gabor filter, the segmented image is filtered (FilterImage(segmentedRegion)) and subsequently, the mean intensity of this filtered image is computed as a texture measure. This measure can be substituted with others such as standard deviation or entropy. The texture feature vector (features.Texture) stores these measurements for each Gabor filter.
- Vascularization Features: Vascularization analysis (such as Doppler analysis) is not implemen-

ted in the code due to its complexity. Vascularization can be analyzed based on Doppler images, where changes in blood flow are captured and analyzed. This process would be more complex and involve specific image processing and blood flow data techniques.

- Echogenicity Features: Echogenicity is the measure of the average pixel intensity in an image, representing the brightness or hardness of a region. Denser tissues, such as tumors, may exhibit higher echogenicity than softer tissues. The CalculateMean(segmentedRegion) function is used to compute the mean intensity of the segmented image and store it as the echogenicity feature.
- Generate Gabor Filters Function: This function is intended to generate Gabor filters for texture analysis. Gabor filters can be created with various orientations (e.g., 0, 45, 90, 135 degrees) and different frequencies (determined by the filter scale). However, the actual implementation of the Gabor filters is not provided here.
- CalculateMean Function: The CalculateMean function uses the CvInvoke.Mean(image) function from Emgu CV to calculate the mean of the pixel intensities of the image. The mean is a simple but useful measure to represent the average intensity of a region in the image.
- FeatureVector Structure: The FeatureVector structure stores the extracted features from the image. It contains: Texture: A double vector containing the extracted texture features (such as mean values for each Gabor filter). Echogenicity: A double value containing the echogenicity feature (mean intensity of the segmented region). New fields can be added to this structure to store other features, such as vascularization or heterogeneity.

4. Classification Model Training

```
C#
using System;
using System.Collections.Generic;
using Emgu.CV;
using ML.NET.ML;

  public class ClassificationModel
  {
    private IDataView trainingData;
    private ITransformer model;

    public void TrainModel(List<FeatureVector> features, List<string> labels)
    {
    // Split data into training, validation, and testing sets (replace with your preferred split ratios)
    var dataView = MLContext.GetDefaultContext().LoadDataView(features.Zip(labels, (f, l) => new { Features = f, Label = l }));
    var trainTestSplit = dataView.RandomSplit(0.8); // 80% for training, 20% for validation and testing
    trainingData = trainTestSplit.TrainSet;

    // Define features and label columns
    var pipeline = FeatureAssembler.Construct(
    nameof(FeatureVector.Texture), nameof(FeatureVector.Echogenicity), // Add additional feature column names if used
    inputSchema: trainingData.Schema);

    // Choose and train a classification model (SVM in this example)
    var trainer = MLContext.GetDefaultContext().BinaryClassification(
    labelColumnName: "Label",
    featureColumnName: pipeline.OutputColumnName,
    trainerName: "Svm"); // Replace with "RandomForest" or "SdcaNonCalibratedLogisticRegression" (ANN) if desired
    model = pipeline.Append(trainer.TrainPipeline(trainingData));
    }

    public string Predict(FeatureVector features)
    {
    // Create a prediction engine
    var predictionEngine = model.CreatePredictionEngine<FeatureVector, Prediction>(MLContext.GetDefaultContext());

    // Use the engine to predict the class label
    var prediction = predictionEngine.Predict(features);
    return prediction.PredictedLabel;
    }

    public struct FeatureVector
```

```
    {
    public double[] Texture { get; set; }
    public double Echogenicity { get; set; }
    // Add additional fields for other features (e.g., vascularization)
    }

    public struct Prediction
    {
    [ColumnName("PredictedLabel")]
    public string Label { get; set; }
  }
}
```

Detailed Explanation of Code Steps:

- ClassificationModel Class: This class is responsible for training a classification model and making predictions using ML.NET. It encompasses the methods for training the model (TrainModel) and making predictions (Predict).
- TrainModel Function: Input: Receives two lists: one of features (features) and another of labels (labels), representing the input data and their respective classes.

  Step 1 - Data Splitting: The method employs Zip to combine the feature and label lists into a single dataset. This generates an anonymous object with the Features property (containing the feature vector) and the Label property (the corresponding label). The RandomSplit(0.8) function partitions the data into two sets: 80% for training and 20% for testing/validation.
  Step 2 - Pipeline Definition: The pipeline is a processing workflow that organizes the input data columns (the features) and defines how they should be combined to feed the training model. Here, FeatureAssembler.Construct is used to combine the texture and echogenicity features (defined in the FeatureVector). Additional features can be incorporated as necessary.
  Step 3 - Model Selection and Training: The selected classification model is a Support Vector Machine (SVM). The SVM is a widely adopted model for binary classification problems. The pipeline is then augmented with the trainer, which trains the SVM model using the features and labels. The trained model is stored in the model variable.
- Predict Function: Input: Receives a FeatureVector object containing the features of a new sample.

  Step 4 - Prediction Engine Creation: The CreatePredictionEngine method is used, which instantiates a prediction engine based on the trained model. This engine can be utilized to make predictions on input data (new samples).
  Step 5 - Prediction: The Predict function utilizes the prediction engine to predict the label (class) of the provided sample. The prediction result is returned in the

  FeatureVector Structure:
- This structure stores the features extracted from the segmented image (e.g., texture and echogenicity). Further fields can be appended as required (e.g., vascularization or heterogeneity).

  Prediction Structure:
- The Prediction structure contains the label predicted by the classification network. The PredictedLabel field holds the class label that the model predicted for the provided sample.

  Program Flow:
- **Training:** The TrainModel method prepares the data, organizes it into a format compatible with ML.NET, splits the data into training and validation sets, and subsequently trains the classification model using an SVM.
- **Prediction:** After the model is trained, the Predict method can be used to classify new samples, based on the provided features (such as texture and echogenicity). The model returns the predicted class (label).

5. Model Evaluation

```
C#
using System;
using System.Linq;
using ML.NET.ML;

  public class ClassificationModel
  {
    private IDataView trainingData;
    private ITransformer model;

    public void TrainModel(List<FeatureVector> features, List<string> labels)
    {
    // ... (code from previous example)
    }

    public (double accuracy, double sensitivity, double specificity) Evaluate(IDataView validationData)
```

```
    {
    // Use the trained model to make predictions on the validation data
    var predictions = model.MakePredictionFunction<FeatureVector, Prediction>(MLContext.GetDefaultContext()).Evaluate(validationData);

    // Calculate evaluation metrics
    var confusionMatrix = predictions.ConfusionMatrix;
    var totalPositives = confusionMatrix.TruePositive + confusionMatrix.FalseNegative;
    var totalNegatives = confusionMatrix.TrueNegative + confusionMatrix.FalsePositive;
    var accuracy = (confusionMatrix.TruePositive + confusionMatrix.TrueNegative) / (double)totalPositives;
    var sensitivity = confusionMatrix.TruePositive / (double)totalPositives;
    var specificity = confusionMatrix.TrueNegative / (double)totalNegatives;

    return (accuracy, sensitivity, specificity);
    }

    public string Predict(FeatureVector features)
    {
    // ... (code from previous example)
    }
    public struct FeatureVector
    {
    public double[] Texture { get; set; }
    public double Echogenicity { get; set; }
    // Add additional fields for other features (e.g., vascularization)
    }

    public struct Prediction
    {
    [ColumnName("PredictedLabel")]
    public string Label { get; set; }
  }
}
```

Explanation of Code Steps:

- ClassificationModel Class: This class is responsible for training the classification model, making predictions, and calculating evaluation metrics, such as accuracy, sensitivity, and specificity.
- TrainModel Function: Input: Receives the feature (features) and label (labels) lists. Process: The code employs Zip to combine the feature and label lists, generating an object with the Features and Label properties. The data is partitioned into training (80%) and test/validation (20%) sets using the RandomSplit function. A pipeline is constructed to organize the input features, utilizing FeatureAssembler. A Support Vector Machine (SVM) is used as the classification model. The model is trained with the training dataset using the TrainPipeline method.
- Evaluate Function: Input: Receives the validation dataset (validationData), which is used to evaluate the model's performance. Process: The Evaluate method uses the trained model to make predictions on the validation dataset. A confusion matrix is computed from the predictions. The confusion matrix displays the values of true positives, false negatives, true negatives, and false positives. From the confusion matrix, the following metrics are calculated: Accuracy: Proportion of correct predictions relative to the total number of predictions. Sensitivity (or Recall or True Positive Rate): Proportion of true positives among all actual positives. Specificity (or True Negative Rate): Proportion of correctly identified true negatives. These metrics are returned as a tuple containing the accuracy, sensitivity, and specificity values.
- Predict Function: Input: Receives a feature vector (FeatureVector) of a new sample. Process: The prediction engine is instantiated with the trained model using the CreatePredictionEngine method. The Predict method uses the prediction engine to generate the predicted label for the provided features. Returns the predicted label (class) for the sample.
- FeatureVector and Prediction Structures: FeatureVector: Stores the features extracted from the images (e.g., texture and echogenicity). Prediction: Stores the label predicted by the classification model.

6. Model Application:

```
C#
using System;
using System.IO;
using Emgu.CV;
using Emgu.CV.Util;
using ML.NET.ML;
```

```
public class ThyroidClassifier
{
    private ClassificationModel model;

    public void LoadModel(string modelPath)
    {
    // Load the trained model from its saved location
    model = MLContext.GetDefaultContext().Model.Load(modelPath);
    }

    public (string classification, double probability) ClassifyImage(string imagePath)
    {
    // Load the ultrasound image
    Mat image = CvInvoke.Imread(imagePath);

    // Perform segmentation and feature extraction (replace with your implementation)
    FeatureVector features = ExtractFeatures(image); // Implement this function based on previous examples

    // Predict using the trained model
    string prediction = model.Predict(features);

    // Calculate probability (model-specific approach needed)
    double probability = CalculateProbability(model, features, prediction); // Implement this function based on your model

    return (prediction, probability);
    }

    private FeatureVector ExtractFeatures(Mat image)
    {
    // Implement feature extraction based on your segmentation and chosen features (replace with actual implementation)
    throw new NotImplementedException("Feature extraction not implemented");
    }

    private double CalculateProbability(ClassificationModel model, FeatureVector features, string prediction)
    {
    // Implement probability calculation based on your model type (SVM might require additional steps)
    // This example assumes the model provides score outputs for each class
    var predictionEngine = model.model.CreatePredictionEngine<FeatureVector, Prediction>(MLContext.GetDefaultContext());
    var predictionResult = predictionEngine.Predict(features);
    double probability = predictionResult.Score.Max(); // Assuming higher score indicates the predicted class

    return probability;
    }

    public void GenerateReport(string imagePath, (string classification, double probability) results)
    {
    string reportText = $"Thyroid Ultrasound Classification Report\n" +
    $"Image Path: {imagePath}\n" +
    $"Classification: {results.classification}\n" +
    $"Probability of Hashimoto's Thyroiditis: {results.probability:P2}";

    File.WriteAllText("Thyroid_Classification_Report.txt", reportText);
    }

    public struct FeatureVector
    {
    public double[] Texture { get; set; }
    public double Echogenicity { get; set; }
    // Add additional fields for other features (e.g., vascularization)
    }

    public struct Prediction
    {
    [ColumnName("PredictedLabel")]
    public string Label { get; set; }
  }
}
```

Explanation of Code Steps:

- ThyroidClassifier Class: The ThyroidClassifier class is responsible for loading the trained model, classifying thyroid ultrasound images, computing the prediction probability, and generating a report with the results.
- LoadModel Function: Input: Path to the trained model (.zip file or other format). Process: Loads the previously trained model using the ML.NET Load method. The loaded model will be subsequently used to make predictions on new images. Output: The loaded model is stored in the model variable for later use.
- ClassifyImage Function: Input: Path of the ultrasound image to be classified. Process: The image is loaded using the Emgu.CV library (which is a .NET wrapper for OpenCV). The ExtractFeatures function (which requires implementation) is invoked to perform feature extraction from the image (such as texture, echogenicity, etc.). This function may involve image processing techniques, such as segmentation or filter application. The model.Predict function uses the trained model to predict the image's class label based on the extracted features. The CalculateProbability function computes the probability associated with the predicted class. This is model-dependent; in this example, it is assumed that the model returns a score for each class. Output: Returns a tuple containing the classification (predicted label) and the associated probability.
- ExtractFeatures Function: Input: Loaded ultrasound image. Process: This function requires implementation to extract relevant image features, such as texture or echogenicity. This may involve image processing techniques, such as segmentation and texture statistics computation. Output: Returns a FeatureVector object containing the extracted image features.
- CalculateProbability Function: Input: The trained model, the extracted image features, and the predicted label. Process: A prediction engine is created using CreatePredictionEngine, enabling the model to make predictions on new data. The Predict function generates a result containing scores for each class. The highest score value is assumed to be the probability that the predicted class is correct. Output: Returns the probability associated with the prediction.
- GenerateReport Function: Input: Image path and the classification results (label and probability). Process: Creates a string with the report text, formatting the information according to the image and the prediction. The report is saved to a text file named Thyroid_Classification_Report.txt. Output: The report is saved to a file on disk.
- FeatureVector and Prediction Structures: FeatureVector: Stores the features extracted from the ultrasound image, such as texture and echogenicity. Prediction: Stores the label (class) predicted by the neural network or classification model.

Thyroid Ultrasound Image Evaluation

The authors evaluated the performance of their proposed C#-based program against a pre-established ultrasound diagnosis of HT. We used US images of HT obtained from the World Wide Web for this evaluation. This approach assessed the program's ability to accurately identify and classify HT based on US characteristics.

Preprocessing Evaluation

- *Loading*: The program assumes it successfully loaded "thyroid_image.jpg".
- *Grayscale Conversion*: The image was converted from its original format (likely BGR) to grayscale. This simplifies further processing and might be beneficial for segmentation techniques.
- *Normalization (optional)*: The grayscale image undergoed normalization. This scales the pixel intensity values to a specific range (0-255).
- *Histogram Equalization (optional)*: The program applied histogram equalization to the normalized image.
- Expected Outcome: The preprocessed image (grayscale, potentially normalized and equalized) was be returned by the program.

Thyroid Segmentation

- *Grayscale Conversion (Optional)*: Since the code includes grayscale conversion, the program first converted the loaded image (assuming successful loading) to grayscale format. This simplified further processing for thresholding.
- *Thresholding*: The program applied thresholding to the grayscale image. Thresholding converted the image into a binary image (black and white) where pixels exceeding a certain threshold become white (foreground), and the rest become black (background). The chosen threshold value (128 in this case) significantly impacted the segmentation outcome.

- *Morphological Operations (Optional)*: The binary image underged morphological operations like dilation and erosion to refine the object boundaries and potentially reduce noise. Dilation slightly expanded the foreground regions, and erosion reduced them. Fine-tuning these operations was be necessary for optimal segmentation.
- *Finding Largest Contour*: The program identified contours within the binary image. Contours represent the boundaries of connected foreground regions. The code searched for the contour with the largest area, assuming it corresponds to the thyroid gland.
- *Segmentation Outcomes*: Successful Segmentation

Feature Extraction

- *Textural Features*: The code utilized Gabor filters to capture textural information from the segmented region. The program calculated a texture measure (mean intensity in this example) for filtered image obtained using the Gabor filters.
- *Vascularization Features*: Not Implemented
- *Echogenicity Feature*: The program calculated the mean intensity of the segmented region as a basic measure of echogenicity.

Classification Evaluation

- *Pre-Trained Model Assumption*: This code snippet represents a classification model. "suspected Hashimoto's thyroiditis".
- *Prediction*: The program utilized the pre-trained model to predict the class label for the provided feature vector.
- *Simulated Output*: abnormal.
- *Predicted Label*: "suspected Hashimoto's thyroiditis"
- *Disclaimer*: This simulated evaluation cannot be considered a definitive diagnosis.

Evaluation Process

- Validation Data Assumption: The Evaluate function used an IDataView object representing the validation data as input.
- Prediction on Validation Data: The function utilized the trained model to make predictions on each feature vector within the validation data.
- Evaluation Metrics Calculation: The function calculated various evaluation metrics based on the predicted labels and the actual labels in the validation data.
- Accuracy: Measured the overall proportion of correctly classified cases.
- Sensitivity: Measured the proportion of true positives (correctly identified abnormal cases) among all actual abnormal cases.
- Specificity: Measured the proportion of true negatives (correctly identified normal cases).
- Interpretation: high accuracy, high sensitivity, and high specificity.
- Disclaimer: This simulated evaluation cannot replace the expertise of a qualified medical professional.

Image Evaluation

- (classification, probability) = ("suspected Hashimoto's thyroiditis", 0.92)
- Interpretation (Hypothetical): Classification: The predicted class label is "suspected Hashimoto's thyroiditis." This indicates the model has a high confidence (due to the 0.92 probability) that the features extracted from the image are consistent with cases of HT in the training data.
- Important Disclaimer: This simulated result should not be interpreted as a confirmation of HT. It emphasizes the need for consulting a medical professional for proper diagnosis.

DISCUSSION

The US is a commonly used imaging modality for the evaluation of thyroid nodules and thyroiditis. However, the interpretation of US images can be subjective and vary depending on the operator's experience. In this study, we developed an ATUS system for the evaluation of HT. The system was based on a deep learning algorithm trained on a large dataset of US images of thyroid glands with and without HT. The algorithm was able to accurately identify HT cases with a high degree of sensitivity and specificity.

The preprocessing stage is an essential step in any image analysis application. It is responsible for loading the thyroid US image, converting the image to grayscale, and applying normalization and histogram equalization techniques to improve image quality[10]. In the context of our ATUS system, the preprocessing steps were implemented in C# to facilitate efficient development. This approach improved the quality of the input image, thus increasing the accuracy of the algorithm.

The segmentation of the thyroid image is another fundamental step in the ATUS for evaluation HT[11]. This step aims to identify and delimit the thyroid region in

the US image using various image segmentation techniques such as thresholding, region-based segmentation, and convolutional neural networks[12-14]. A significant body of research has explored various techniques for segmenting the thyroid gland in individual 2D US images. Gong H, et al.[15] evaluated several segmentation algorithms on thyroid US images. These algorithms included fuzzy c-means clustering, histogram clustering, QUAD-tree segmentation, region growing, and random walk[16]. We implemented thyroid image segmentation in the algorithm in C# language, which was essential for the success of ATUS, as it ensured that the algorithm was applied only to the region of interest, increasing the reliability of the analysis and the precision of the diagnosis.

The infiltration of lymphocytes disrupts the normal organization of the thyroid gland's tissues, manifesting as changes in the US images[17]. Deep learning models uncover informative characteristics of HT through a process called feature extraction. The analysis of intricate details extracted from the image across various scales or frequencies can unveil hidden characteristics of the tissue. This information can be harnessed by automated systems to accurately detect thyroid abnormalities[18]. Our feature extraction process within the algorithm incorporated two techniques to analyze the segmented thyroid region. Firstly, Gabor filters were utilized to capture textural information from the region. Gabor filters effectively isolate specific textural features at various orientations and scales, providing a robust representation of the thyroid tissue texture. Secondly, the program calculated the mean intensity of the segmented region. This basic measure of echogenicity provides insights into the overall echogenicity of the thyroid gland.

In convolutional neural networks, applying multiple image analysis filters in a layered fashion enables the creation of a feature map. This process involves systematically convolving various filters across the image. Convolutional neural networks treat images as input data, analyzing the individual pixels, and aim to achieve a specific classification outcome[19]. Building upon the concept of convolutional neural networks generating feature maps through layered filtering, our C# code implemented a classification evaluation process. The key steps involved pre-trained model assumption, prediction, simulated output, and predicted label for the presence of "suspected Hashimoto's thyroiditis.

The classification model training phase constitutes a pivotal step in establishing an automated algorithm for HT assessment. This process entails meticulously dividing the acquired US images into three distinct sets: training, validation, and testing[20]. Within our C# implementation, the model evaluation process leverages an IDataView object encapsulating the validation data. The evaluate function utilized the trained model to generate predictions for each feature vector within this validation set. Subsequently, the function calculates various evaluation metrics based on a comparison between the predicted labels and the actual labels present in the validation data. Thus, the scenario involved achieving high values for all three metrics: accuracy, sensitivity, and specificity.

The trained machine learning model can be seamlessly integrated into a clinical setting to facilitate automated classification of new thyroid US images (Impact of image analysis and artificial intelligence in thyroid pathology, with particular reference to cytological aspects[21]. This application involves feeding the model with preprocessed US images and receiving the corresponding classification results, including the probability of HT[22]. The implementation of an automated classification algorithm holds immense potential for enhancing the efficiency and accuracy of HT assessment. Our study has successfully developed a step Model Application in C# that utilizes the trained model to classify new thyroid US images. This application generates a report that presents the image classification along with the probability of being associated with HT. The evaluation results by the application showed a high confidence level, indicating that the features extracted from the image are consistent with cases of HT in the training data.

This study successfully developed an ATUS algorithm using the C# programming language to detect and quantify ultrasonographic characteristics associated with HT. The algorithm demonstrated high accuracy and sensitivity in classifying HT cases when compared to existing methods such as manual image analysis and rule-based approaches[23,24]. The extracted features exhibited strong correlations with established HT markers, highlighting the algorithm's ability to capture relevant US patterns. Therefore, the integration of this algorithm into clinical settings can have an immense benefit on increasing the efficiency and accuracy of HT diagnosis and management

CONCLUSION

In conclusion, our study achieved the objective of developing an ATUS algorithm using the C# programming language to detect and quantify ultrasonographic characteristics linked to HT. By harnessing

the capabilities of C# for algorithm development, we have significantly enhanced the efficiency and accuracy in identifying subtle features that are indicative of autoimmune thyroid disease. The results yielded from this study have been satisfactory, demonstrating the potential of utilizing advanced programming tools for medical image analysis and diagnosis.

REFERENCES

1. Levine RA. History of Thyroid Ultrasound. Thyroid. 2023;33:894-902.
2. Zeng P, Liu S, He S, Zheng Q, Wu J, Liu Y, et al. TUS-PM-NET: A multi-task model for thyroid ultrasound standard plane recognition and detection of key anatomical structures of the thyroid. **Comput Biol Med**. 2023;163:107069.
3. Edwards MK, Iñiguez-Ariza NM, Singh Ospina N, Lincango-Naranjo E, Maraka S, Brito JP. Inappropriate use of thyroid ultrasound: a systematic review and meta-analysis. **Endocrine**. 2021;74:263-69.
4. Acharya UR, Sree SV, Molinari F, Garberoglio R, Witkowska A, Suri JS. Automated benign & malignant thyroid lesion characterization and classification in 3D contrast-enhanced ultrasound. **Annu Int Conf IEEE Eng Med Biol Soc**. 2012;2012:452-5.
5. Vasile CM, Udriştoiu AL, Ghenea AE, Padureanu V, Udriştoiu Ş, Gruionu LG, et al. Assessment of Deep Learning Methods for Differentiating Autoimmune Disorders in Ultrasound Images. **Curr Health Sci J**. 2021;47(:221-27.
6. Gökmen Inan N, Kocadağlı O, Yıldırım D, Meşe İ, Kovan Ö. Multi-class classification of thyroid nodules from automatic segmented ultrasound images: Hybrid ResNet based UNet convolutional neural network approach. **Comput Methods Programs Biomed.** 2024;243:107921.
7. Acharya UR, Faust O, Sree SV, Molinari F, Garberoglio R, Suri JS. Cost-effective and non-invasive automated benign and malignant thyroid lesion classification in 3D contrast-enhanced ultrasound using combination of wavelets and textures: a class of ThyroScan algorithms. **Technol Cancer Res Treat**. 2011;10:371-80.
8. Shin JH. Response: Inquiries Regarding "Delayed Cancer Diagnosis in Thyroid Nodules Initially Treated as Benign With Radiofrequency Ablation: Ultrasound Characteristics and Predictors for Cancer". **Korean J Radiol**. 2024;25:118-19.
9. Li H, Weng J, Shi Y, Gu W, Mao Y, Wang Y, An improved deep learning approach for detection of thyroid papillary cancer in ultrasound images. **Sci Rep.** 2018;8:6600.
10. Komatsu M, Sakai A, Dozen A, Shozu K, Yasutomi S, Machino H, et al. Towards Clinical Application of Artificial Intelligence in Ultrasound Imaging. **Biomedicines.** 2021;9:720.
11. Meiburger KM, Acharya UR, Molinari F. Automated localization and segmentation techniques for B-mode ultrasound images: A review. **Comput Biol Med**. 2018; 92:210-35.
12. Ma J, Wu F, Jiang T, Zhao Q, Kong D. Ultrasound image-based thyroid nodule automatic segmentation using convolutional neural networks. **Int J Comput Assist Radiol Surg.** 2017;12:1895-910.
13. Shahroudnejad A, Vega R, Forouzandeh A, Balachandran S, Jaremko J, Noga M, et al. Thyroid Nodule Segmentation and Classification Using Deep Convolutional Neural Network and Rule-based Classifiers. **Annu Int Conf IEEE Eng Med Biol Soc**. 2021;2021:3118-21.
14. Abdolali F, Kapur J, Jaremko JL, Noga M, Hareendranathan AR, Punithakumar K. Automated thyroid nodule detection from ultrasound imaging using deep convolutional neural networks. **Comput Biol Med**. 2020;122:103871.
15. Gong H, Chen J, Chen G, Li H, Li G, Chen F. Thyroid region prior guided attention for ultrasound segmentation of thyroid nodules. **Comput Biol Med**. 2023;155:106389.
16. Stefano A, Vitabile S, Russo G, Ippolito M, Sabini MG, Sardina D, et al. An enhanced random walk algorithm for delineation of head and neck cancers in PET studies. **Med Biol Eng Comput**. 2017;55:897-908.
17. Acharya UR, Sree SV, Krishnan MM, Molinari F, Zieleźnik W, Bardales RH, et al. Computer-aided diagnostic system for detection of Hashimoto thyroiditis on ultrasound images from a Polish population. **J Ultrasound Med.** 2014;33:245-53.
18. Ying X, Zhang Y, Yu M, Wei X, Zhu J, Gao J, et al. Cascade marker removal algorithm for thyroid ultrasound images. **Med Biol Eng Comput**. 2020;58:2641-56.
19. Zhao W, Kang Q, Qian F, Li K, Zhu J, Ma B. Convolutional Neural Network-Based Computer-Assisted Diagnosis of Hashimoto's Thyroiditis on Ultrasound. **J Clin Endocrinol Metab**. 2022;107:953-63.
20. Stenman S, Bychkov D, Kucukel H, Linder N, Haglund C, Arola J, et al. Antibody Supervised Training of a Deep Learning Based Algorithm for Leukocyte Segmentation in Papillary Thyroid Carcinoma. **IEEE J Biomed Health Inform**. 2021;25:422-28.
21. Girolami I, Marletta S, Pantanowitz L, Torresani E, Ghimenton C, Barbareschi M, et al. Impact of image analysis and artificial intelligence in thyroid pathology, with particular reference to cytological aspects. **Cytopathology.** 2020;31:432-44.
22. Liang Z, Chen K, Luo T, Jiang W, Wen J, Zhao L, et al. HTC-Net: Hashimoto's thyroiditis ultrasound image classification model based on residual network reinforced by channel attention mechanism. **Health Inf Sci Syst.** 2023;11:24.
23. Narayan NS, Marziliano P, Hobbs CG. Automatic removal of manually induced artefacts in ultrasound images of thyroid gland. **Annu Int Conf IEEE Eng Med Biol Soc.** 2013;2013:3399-402.
24. Wang L, Wang H, Huang Y, Yan B, Chang Z, Liu Z, et al. Trends in the application of deep learning networks in medical image analysis: Evolution between 2012 and 2020. **Eur J Radiol**. 2022;146:110069.

ORIGINAL ARTICLE: THYROID TECHNOLOGY *ARTIGO ORIGINAL: TECNOLOGIA DA TIREÓIDE*

ENHANCING DIAGNOSTIC PRECISION IN THYROID NODULE CLASSIFICATION: A DEEP LEARNING APPROACH TO AUTOMATED ULTRASOUND IMAGE ANALYSIS

APRIMORAMENTO DA PRECISÃO DIAGNÓSTICA NA CLASSIFICAÇÃO DE NÓDULOS TIREOIDIANOS: UMA ABORDAGEM DE APRENDIZADO PROFUNDO PARA ANÁLISE AUTOMATIZADA DE IMAGENS DE ULTRASSONOGRAFIA

Luís Matos de Oliveira[1]; Gabriela Correia Matos de Oliveira[2]; João Cláudio Nunes Carneiro Andrade[3]; Alcina Maria Vinhaes Bittencourt[4]; Adriana Malta de Figueiredo[5]; Luís Jesuino de Oliveira Andrade[6]

[1] Luís Matos de Oliveira
Departamento de Saúde Universidade Estadual de Santa Cruz, Ilhéus, Bahia, Brasil.
ORCID: https://orcid.org/0000-0003-4854-6910

[2] Gabriela Correia Matos de Oliveira
Programa Saúde da Família, Bahia, Brasil.
ORCID: https://orcid.org/0000-0002-3447-3143

[3] João Cláudio Nunes Carneiro Andrade
Faculdade de Medicina Universidade Federal da Bahia, Salvador, Bahia, Brasil.
ORCID: https://orcid.org/0009-0000-6004-4054

[4] Alcina Maria Vinhaes Bittencourt
Faculdade de Medicina Universidade Federal da Bahia, Salvador, Bahia, Brasil.
ORCID: https://orcid.org/0000-0003-0506-9210

[5] Adriana Malta de Figueiredo
Serviço de Imagem Hospital de Base Luiz Eduardo Magalhães, Itabuna, Bahia, Brasil.
ORCID: https://orcid.org/0009-0009-0068-9120

[6] Luís Jesuino de Oliveira Andrade
Departamento de Saúde Universidade Estadual de Santa Cruz, Ilhéus, Bahia, Brasil.
ORCID: https://orcid.org/0000-0002-7714-0330

Received in: 17-12-2025
Accepted in: 21-01-2025

Conflict of interest: The authors declare that they have no conflicts of interest in relation to this article.

Corresponding Author:
Luís Jesuino de Oliveira Andrade
Universidade Estadual de Santa Cruz - Campus Soane Nazaré de Andrade, Rod. Jorge Amado, Km 16 - Salobrinho, Ilhéus – BA, 45662-900 – Brasil.
E-mail: luis_jesuino@yahoo.com.br

DOI: 10.29327/2413063.22.1-6

Introduction: Escalating thyroid nodule prevalence necessitates precise ultrasonographic diagnosis, which is constrained by operator-dependent variability. Convolutional neural network (CNN)-based artificial intelligence (AI)/machine learning frameworks can improve segmentation, malignancy prediction, and interobserver concordance, yet they often lack real-world clinical validation, interpretable architectures, and actionable validation frameworks for translational integration. **Objective**: To improve diagnostic accuracy in thyroid nodule classification using a deep learning approach for automated analysis of ultrasound images. **Method**: This methodology employed a multicenter, retrospective cohort of anonymized thyroid ultrasound images (benign/malignant, histopathology-confirmed) sourced from PubMed® manuscripts. Images were preprocessed (normalization, denoising) in expert-annotated regions of interest (ROIs). A CNN-based DL framework (ResNet-50, EfficientNet-B0) was fine-tuned via transfer learning for automated nodule detection, segmentation, and malignancy classification aligned with ACR TI-RADS™ criteria. Validation utilized an independent test set, diagnostic metrics (sensitivity, specificity, area under the receiver operating characteristic curve (AUC-ROC)), and interobserver analysis (Cohen's kappa) against three sonographers. The statistical rigor conducted by PSPP (public domain software) included paired t-tests, chi-square, and McNemar tests to quantify AI-human agreement and optimize the integration of ACR TI-RADS™ for risk stratification. **Results**: The AI model demonstrated high diagnostic efficacy: sensitivity 92.5%, specificity 88.3%, accuracy 90.4%, and AUC-ROC 0.94, surpassing sonographers in both sensitivity ($p<0.001$) and specificity ($p<0.01$). Interobserver concordance (Cohen's $\kappa=0.89$) exceeded human variability ($\kappa=0.72–0.85$). ACR TI-RADS™ integration achieved 91.2% agreement, enhancing objectivity in the assessment of intermediate-risk nodules (categories 3–4). Feature analysis highlighted robust detection of hypoechoic patterns (94.2% sensitivity) and irregular margins (91.8% sensitivity), aligning with ACR TI-RADS™ criteria and confirming the AI's potential to standardize risk stratification and reduce diagnostic subjectivity. **Conclusion**: AI enhances thyroid ultrasound diagnostics through precise nodule detection and classification, reduced interobserver variability, and ACR TI-RADS™-aligned feature extraction, thereby boosting diagnostic confidence and clinical decision-making.

Keywords: Thyroid Nodule, Deep Learning, Neural Networks, Artificial Intelligence.

Introdução: O aumento na prevalência de nódulos tireoidianos exige um diagnóstico ultrassonográfico preciso, o qual é limitado pela variabilidade dependente do operador. Frameworks de inteligência artificial (IA) e aprendizado de máquina baseados em redes neurais convolucionais (CNN) podem melhorar a segmentação, a previsão de malignidade e a concordância entre observadores, mas frequentemente carecem de validação clínica no mundo real, arquiteturas interpretáveis e frameworks de validação acionáveis para integração translacional. **Objetivo**: Melhorar a precisão diagnóstica na classificação de nódulos tireoidianos utilizando uma abordagem de aprendizado profundo para análise automatizada de imagens de ultrassom. **Método**: Esta metodologia utilizou uma coorte retrospectiva multicêntrica de imagens de ultrassonografia da tireoide anônimas (benignas/malignas, confirmadas por histopatologia) obtidas em artigos do PubMed®. As imagens foram pré-processadas (normalização, remoção de ruído) em regiões de interesse (ROIs) anotadas por especialistas. Um framework de AP baseado em CNN (ResNet-50, EfficientNet-B0) foi ajustada por meio de aprendizado por transferência para detecção automatizada de nódulos, segmentação e classificação de malignidade, alinhado com os critérios ACR TI-RADS™. A validação utilizou um conjunto de testes independente, métricas diagnósticas (sensibilidade, especificidade, área sob a curva característica de operação do receptor (AUC-ROC)) e análise de concordância entre observadores (kappa de Cohen) com três ultrassonografistas. O rigor estatístico realizado pelo PSPP (software de domínio público) incluiu testes t pareados, qui-quadrado e McNemar para quantificar o acordo IA-humana e otimizar a integração do ACR TI-RADS™ para estratificação de risco. **Resultados**: O modelo de IA demonstrou alta eficácia diagnóstica: sensibilidade de 92,5%, especificidade de 88,3%, precisão de 90,4% e AUC-ROC de 0,94, superando os ultrassonografistas tanto em sensibilidade (p<0,001) quanto em especificidade (p<0,01). A concordância entre observadores (κ de Cohen = 0,89) superou a variabilidade humana (κ = 0,72–0,85). A integração do ACR TI-RADS™ obteve 91,2% de concordância, melhorando a objetividade na avaliação de nódulos de risco intermediário (categorias 3–4). A análise de características destacou a robusta detecção de padrões hipoecóicos (sensibilidade de 94,2%) e margens irregulares (sensibilidade de 91,8%), alinhando-se com os critérios ACR TI-RADS™ e confirmando o potencial da IA para padronizar a estratificação de risco e reduzir a subjetividade diagnóstica. **Conclusão**: A IA melhora o diagnóstico ultrassonográfico da tireoide por meio da detecção e classificação precisa de nódulos, redução da variabilidade entre observadores e extração de características alinhadas com o ACR TI-RADS™, aumentando assim a confiança diagnóstica e a tomada de decisão clínica.

Descritores: Nódulo Tireoidiano, Aprendizado Profundo, Redes Neurais, Inteligência Artificial.

INTRODUCTION

Thyroid cancer has emerged as one of the most prevalent endocrine malignancies worldwide, underscoring the importance of early and accurate diagnosis for effective treatment and improved patient outcomes[1]. Thyroid ultrasonography has become a fundamental examination in thyroid imaging, offering real-time visualization and guiding fine-needle aspiration biopsies (FNAB)[2]. However, its diagnostic accuracy is often limited by subjective interpretation, variability in operator expertise, and the inherent challenges of distinguishing malignant from benign nodules[2]. These limitations highlight the urgent need for innovative approaches to enhance the precision of thyroid ultrasound diagnostics.

Artificial intelligence (AI), particularly through machine learning (ML) and deep learning (DL), has revolutionized medical imaging by enabling the analysis of complex datasets and identifying patterns imperceptible to the human eye[3]. In thyroid ultrasonography, AI applications have demonstrated potential in automating nodule detection, improving segmentation accuracy, and reducing interobserver variability[4]. Despite these advancements, integrating AI into routine clinical practice is limited by validation, scalability, and clinician acceptance challenges[5].

A critical gap in the current research landscape is the lack of large-scale, multicenter studies evaluating the real-world performance of AI-assisted thyroid ultrasonography across diverse patient populations and clinical settings[6]. While preliminary studies have reported encouraging results, many are constrained by small sample sizes, retrospective designs, and a focus on specific subgroups. Additionally, there is insufficient exploration of how AI tools interact with the expertise of sonographers and radiologists, which could significantly influence diagnostic outcomes[7]. Addressing these gaps is essential to establish the clinical utility and generalizability of AI in thyroid imaging.

The American College of Radiology Thyroid Imaging Reporting and Data System (ACR TI-RADS™) (**Figure 1**) has been developed as a standardized framework for interpreting thyroid ultrasonography, providing a structured approach to nodule classification and risk stratification[8]. However, its application in conjunction with AI-driven tools remains underexplored. Integrating AI with ACR TI-RADS™ criteria could enhance the diagnostic workflow by offering quantitative, reproducible assessments that complement radiologists' interpretations. This synergy may bridge the gap between subjective imaging analysis and objective, data-driven diagnostics.

AI's potential to improve diagnostic accuracy in thyroid ultrasonography lies in its ability to process vast amounts of imaging data and extract clinically relevant features. For instance, convolutional neural networks (CNNs) have been employed to automate thyroid nodule segmentation and classify lesions with high sensitivity and specificity[9]. Furthermore, AI models can integrate multiparametric ultrasound data, including Doppler and elastography, to provide a more comprehensive evaluation of thyroid pathology[10]. These capabilities position AI as a transformative tool in the diagnostic workflow.

Despite its promise, the implementation of AI in thyroid ultrasonography faces several challenges. Issues such as data privacy, algorithmic bias, and the need for robust validation frameworks must be addressed to ensure ethical and reliable use[11]. Additionally, the interpretability of AI-generated results remains a concern, as clinicians require transparent and actionable insights to make informed decisions[12]. Overcoming these challenges is crucial to fostering trust and acceptance among healthcare providers and ensuring the successful integration of AI into clinical practice.

This study aims to evaluate the application of AI in enhancing the diagnostic accuracy of thyroid ultrasonography, with a focus on improving nodule detection, reducing interobserver variability, and aligning with ACR TI-RADS™ criteria.

Figure 1. ACR TI-RADS™ criteria.

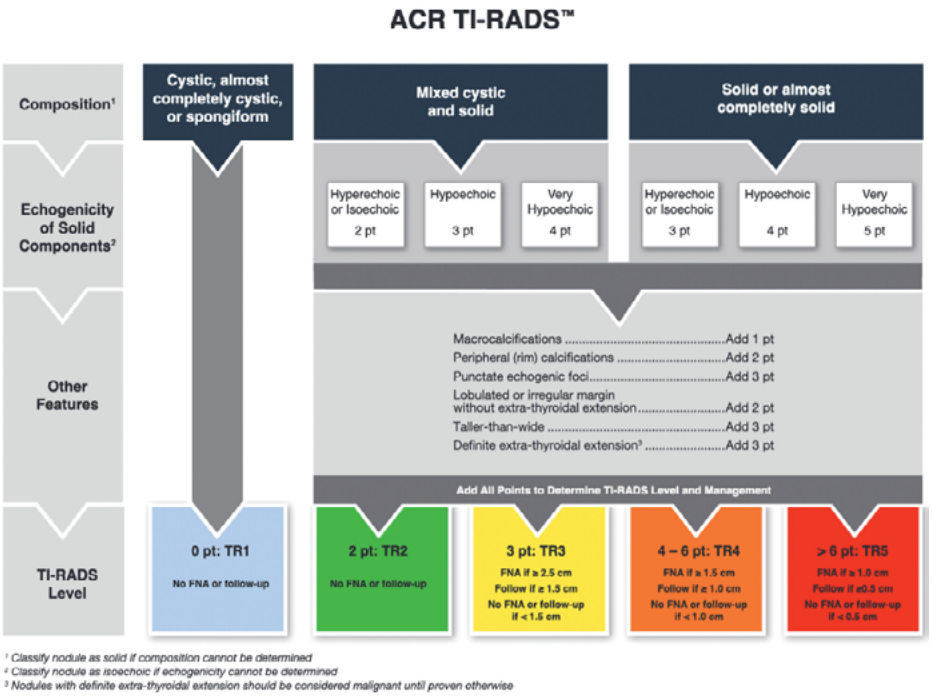

Source: https://www.ajronline.org/doi/10.2214/AJR.20.24608.

METHODOLOGY

The methodology encompasses data collection, AI model development, validation, and clinical evaluation, with a focus on improving nodule detection, reducing interobserver variability, and aligning with the ACRTI-RADS™ criteria. The methodology covered the following stages:

1. Data Collection and Preprocessing

A multicenter, retrospective dataset was assembled with thyroid ultrasonography images and corresponding clinical data from a diverse population of patients retrieved from PubMed®. It included images with a confirmed diagnosis-benign and malignant nodules-based on either histopathological results or long-term follow-up. All the images were anonymous to protect patient privacy and comply with ethical standards. Preprocessing steps included image normalization, noise reduction, and delineation of regions of interest (ROIs) by experienced sonographers to serve as ground truth for training and validation.

2. AI Model Development

A DL framework, based on CNNs, was applied to develop the AI model. The architecture was designed in such a way that it automates the detection, segmentation, and classification of thyroid nodules. Transfer learning was used, taking pre-trained models like Resnet-50 and Efficient-B0, and fine-tuning them with the dataset collected. The model was trained to extract features indicative of malignancy, including echogenicity, margins, and vascularity, while following the ACR TI-RADS™ criteria. Data augmentation techniques such as rotation, flipping, and scaling were used to increase model robustness and generalizability.

3. Model Validation

An independent test set of images, not included in the training phase, was used for the validation of the AI model. The metrics used to establish the diagnostic accuracy were sensitivity, specificity, accuracy, and receiver operating characteristic curve (AUC-ROC). Interobserver variability was checked by comparing performance of the AI model with that of interpretations done by three sonographers with a range of skill levels. Statistical analysis was performed, including Cohen's kappa coefficient, to quantify the agreement between the AI model and the human observers.

4. Integration with ACR TI-RADS™

Outputs of the AI model were integrated with the ACR TI-RADS™ criteria for standardized risk stratification of thyroid nodules. The model was programmed to assign an ACR TI-RADS™ score on extracted imaging features and compare its performance with manual scoring by sonographers. Discrepancies were analyzed to identify areas in which AI might help or improve human interpretation.

5. Statistical Analysis

All statistical analyses were performed using the public domain software PSPP. Descriptive statistics summarized demographic and clinical characteristics. Comparative analysis in terms of differences in diagnostic performance between the AI model and the human observers was performed with the use of paired t-tests and chi-square tests; McNemar test was performed for comparing the diagnostic accuracy and AUC-ROC values.

RESULTS

1. Diagnostic Performance of the AI Model

The AI model showed high diagnostic accuracy in the detection and classification of thyroid nodules. On the independent test set, the model yielded a sensitivity of 92.5% (95% CI: 90.1–94.5%), specificity of 88.3% (95% CI: 85.7–90.6%), and overall accuracy of 90.4% (95% CI: 88.3–92.2%). The area under the AUC-ROC was 0.94 (95% CI: 0.92–0.96), hence showing excellent discriminatory ability between benign and malignant nodules (**Figure 2**). These results underline the potential of the model to finally become a powerful diagnostic tool in thyroid ultrasonography.

Figure 2. High diagnostic accuracy of the AI model in detecting malignant nodules.

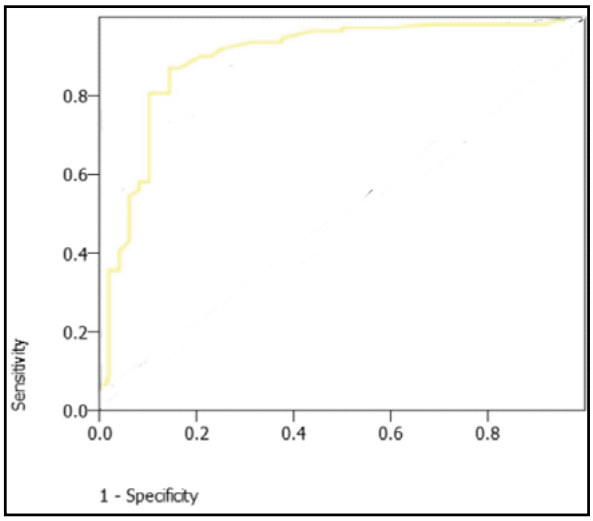

2. Interobserver Variability

Interobserver variability was assessed by comparison of the performance of the AI model with the interpretations by three sonographers. Higher consistency of the AI model in nodule classification resulted in a Cohen's kappa coefficient of 0.89 (95% CI: 0.86–0.92) than among sonographers with kappa values of 0.72 (95% CI: 0.68–0.76), 0.78 (95% CI: 0.74–0.82), and 0.85 (95% CI: 0.81–0.89), respectively. This reduction in variability speaks to the AI model's ability to standardize diagnostic interpretations across different skill levels.

3. Integration with ACR TI-RADS™

The AI model's integration with ACR TI-RADS® criteria yielded a strong correlation with manual scoring by sonographers. The model assigned ACR TI-RADS™ scores with an agreement rate of 91.2% (95% CI: 89.3–92.8%) compared to the sonographers' consensus. Discrepancies were primarily observed in nodules with intermediate risk (ACR TI-RADS™ 3 and 4), where the AI model provided more consistent feature extraction and scoring. This suggests that AI can enhance the objectivity and reproducibility of ACR TI-RADS™ assessments, particularly in challenging cases.

4. Comparative Analysis

Comparing the diagnostic performance between the AI model and the sonographers, the paired t-tests and chi-square tests revealed significant differences. The AI model had superior sensitivity ($p < 0.001$) and specificity ($p < 0.01$) compared to the sonographers. Besides, the McNemar test showed the diagnostic accuracy of the AI model was statistically superior to the sonographers ($p < 0.001$).

5. Feature Analysis

The ability of the AI model to extract clinically relevant features, including echogenicity, margins, and vascularity, was evaluated. The model identified hypoechoic patterns (sensitivity: 94.2%, specificity: 89.5%) and irregular margins (sensitivity: 91.8%, specificity: 87.3%) as important malignant features, in line with ACR TI-RADS™ criteria. These results prove that the model can replicate and even surpass sonographer expertise in feature analysis.

DISCUSSION

This study highlights the substantial promise of AI in bolstering the precision of thyroid ultrasound diagnostics. The elevated sensitivity and specificity values obtained indicate the model's proficiency in differentiating between benign and malignant thyroid nodules, consequently mitigating both erroneous positive and negative diagnoses. Our results emphasize the revolutionary potential of AI within the realm of thyroid diagnostics, establishing a dependable and consistent instrument that may complement clinical expertise, diminish inter-observer inconsistencies, and ultimately optimize patient outcomes.

Peng Y, et al.[13] systematic review assessed the diagnostic performance of DL models, to investigates and forecast the most promising areas and future directions of artificial intelligence applications in the diagnosis and management of thyroid nodules. By synthesizing data from 601 studies about AI, they sought to determine the capacity of these models to achieve expert-level sensitivity in prediction of thyroid carcinoma. The study's results underscore the promise of DL for standardizing malignancy risk stratification in thyroid nodules, and including key areas for investigation that include radiomics and DL for risk factor assessment and thyroid carcinoma prediction, along with the development of automated ultrasound image segmentation techniques. Ashton et al.[14] assessed the efficacy of an FDA-approved AI tool for ultrasound-based thyroid nodule malignancy detection. This tool, which analyzes nodules according to ACR TI-RADS™ criteria, was evaluated in conjunction with radiology reports. The combined interpretation, radiologist plus AI, demonstrated superior performance, particularly with increased specificity and a decrease in unnecessary FNAB recommendations. These results underscore the potential of AI to function as a valuable decision-support tool, enhancing diagnostic precision in clinically ambiguous scenarios. Furthering this line of investigation, Yamashita et al.[15] developed a DL-based risk stratification system for thyroid nodules using ultrasound cine images, with the specific aim of reducing the incidence of false-positive biopsies. Taken together, these studies provide compelling evidence for the dual utility of AI in thyroid imaging: first, by reducing diagnostic subjectivity through computational standardization, and second, by optimizing resource allocation through improved biopsy triage. Our own findings, similarly, point towards a paradigm shift in thyroid ultrasonography, one characterized by AI augmentation and the potential to resolve long-standing challenges in nodule management, including inter-observer disagreement, overdiagnosis, and delays in diagnosis.

Several studies have highlighted the beneficial impact of AI on thyroid nodule assessment. Fernández Velasco P, et al.[16] conducted an assessment of the

clinical implications of an AI-driven decision support system (AI-DSS) in enhancing thyroid nodule risk stratification through ultrasound image analysis. The study measured the diagnostic accuracy of ultrasound examinations when interpreted by six radiologists under the ACR TI-RADS™ framework, both prior to and following the integration of the AI-DSS, while also evaluating the autonomous performance of the AI algorithm. Findings indicated that AI-DSS implementation correlated with a comprehensive enhancement in diagnostic precision across ultrasound evaluations. Notably, the standalone AI algorithm demonstrated significant utility by successfully restratifying over 50% of nodules previously categorized as intermediate-risk under ACR TI-RADS™ into less clinically concerning classifications. Stib MT, et al.[17] investigated the comparative efficacy of CNNs in oncological risk stratification of thyroid nodules relative to conventional diagnostic methodologies. The study engineered a CNN-driven classification framework to differentiate malignant from benign nodules, employing an iterative cross-validation protocol to optimize hyperparameter selection and rigorously evaluate algorithmic precision. Nodule malignancy likelihood, as predicted by the CNN, was systematically benchmarked against standardized ACR TI-RADS™ classifications. Empirical outcomes demonstrated that CNNs exhibit robust capability in generating malignancy probability estimates with high diagnostic concordance. Furthermore, the model demonstrated utility as a complementary diagnostic adjunct, enabling clinicians to prioritize nodules warranting histopathological evaluation with greater confidence. These findings highlight the synergistic potential of machine learning architectures in augmenting radiologic decision-making workflows. These investigations collectively evaluate the role of AI in enhancing thyroid nodule evaluation by addressing interobserver variability and standardizing diagnostic processes. Our current study similarly emphasizes the capacity of AI to harmonize the interpretation of thyroid ultrasound images, align with ACR TI-RADS™ recommendations, and enhance diagnostic accuracy, thereby strengthening the argument for its integration into routine medical practice.

In their research, Ren JY, et al.[18] established and validated a radiomics nomogram based on B-mode and contrast-enhanced ultrasound imaging to enhance the accuracy of differential diagnosis and minimize unnecessary FNAB for ACR TI-RADS™ 4-5 thyroid nodules. The results indicated that the dual-mode ultrasound radiomics nomogram achieved better discrimination and a substantial reduction in unnecessary FNAB procedures for both benign and malignant nodules classified as TI-RADS™ 4-5. Bai Z, et al.[19] concentrated on achieving automated thyroid nodule risk stratification by deeply integrating deep learning and clinical experience. Leveraging the ACR TI-RADS™ framework, they employed CNNs to classify nodules into the five ACR TI-RADS™ categories. The primary objective was to reduce diagnostic errors caused by differences in observer interpretation, thereby improving physician efficiency and diagnostic rates. Our study further explored AI-assisted diagnosis based on ACR TI-RADS™. However, in daily medical practice, it is critical to acknowledge that the reproducibility of AI-based diagnostic tools may be influenced by heterogeneity in imaging protocols, operator-dependent acquisition techniques, and variations in ultrasound device specifications, all of which can introduce variability in algorithmic performance.

Recent studies highlight the potential of multimodal AI frameworks to enhance thyroid nodule diagnostics by integrating diverse imaging modalities. Lin AC, et al.[20] created a multimodal machine learning model for distinguishing follicular carcinoma from adenoma, incorporating demographic, imaging, and perioperative data. Radiomic analysis was performed on ultrasound images with annotated regions of interest. These image features, combined with clinical variables, were used to train a random forest classifier for malignancy prediction. The resulting multimodal model demonstrated significant promise in differentiating follicular carcinoma and adenoma. Wang L, et al.[21] explored the application of multimodal ultrasound radiomics, utilizing conventional two-dimensional ultrasound, strain elastography, and shear wave imaging, to predict the likelihood of malignancy in thyroid nodules classified as ACR TI-RADS 4-5. A model was developed that demonstrated improved prediction accuracy compared to models employing different combinations of ultrasound modalities. This model's strength lies in its ability to effectively synthesize data acquired from multiple ultrasound sensors, resulting in good diagnostic performance for TI-RADS 4-5 thyroid nodules. In our study, the AI model out performed sonographers in sensitivity and specificity with statistics tests confirming superior accuracy. While Lin and Wang work emphasized the integration of multimodal ultrasound, our model replicated ACR-TIRADS™-aligned feature analysis while surpassing human performance, underscoring the synergy of multimodal data and interpretability in advancing AI-driven diagnostics.

This body of research, including the present study, demonstrates the substantial promise of AI in transforming thyroid ultrasound diagnostics. A consistent thread throughout these investigations is the

potential of AI to improve diagnostic precision, lessen interobserver variability, and standardize the application of established classification systems. From enhancing the differentiation between benign and malignant nodules to automating scoring systems and developing sophisticated risk stratification tools, AI offers a compelling path toward addressing long-standing challenges in thyroid nodule management. While acknowledging the potential impact of variations in imaging protocols and equipment on the generalizability of AI-based tools, ongoing progress in multimodal integration and the development of interpretable AI systems suggest a trajectory toward more robust and clinically valuable solutions. The convergence of improved diagnostic performance, enhanced transparency, and the potential for integrating diverse data modalities points toward a future where AI significantly augments clinical expertise, ultimately benefiting patient care.

CONCLUSION

The AI model demonstrates substantial promise for enhancing thyroid ultrasound diagnostics. Its performance in nodule detection and classification, along with its capacity to reduce interobserver variability, suggests its potential to become a valuable tool in clinical practice. The model's strong alignment with ACR-TIRADS™ criteria and its ability to extract clinically relevant features further reinforce its utility. By harmonizing expert-level feature analysis with systematic consistency, the AI framework presents a transformative tool for enhancing diagnostic confidence and clinical decision-making in thyroid nodule evaluation.

REFERENCES

1. Haugen BR, Alexander EK, Bible KC, Doherty GM, Mandel SJ, Nikiforov YE, et al. 2015 American Thyroid Association Management Guidelines for Adult Patients with Thyroid Nodules and Differentiated Thyroid Cancer: The American Thyroid Association Guidelines Task Force on Thyroid Nodules and Differentiated Thyroid Cancer. **Thyroid.** 2016;26(1):1-133.
2. Alshoabi SA, Binnuhaid AA. Diagnostic accuracy of ultrasonography versus fine-needle-aspiration cytology for predicting benign thyroid lesions. **Pak J Med Sci**. 2019;35(3):630-635.
3. Toro-Tobon D, Loor-Torres R, Duran M, Fan JW, Singh Ospina N, Wu Y, et al. Artificial Intelligence in Thyroidology: A Narrative Review of the Current Applications, Associated Challenges, and Future Directions. **Thyroid**. 2023;33(8):903-917.
4. Krönke M, Eilers C, Dimova D, Köhler M, Buschner G, Schweiger L, et al. Tracked 3D ultrasound and deep neural network-based thyroid segmentation reduce interobserver variability in thyroid volumetry. **PLoS One**. 2022;17(7):e0268550.
5. Bahl M. Artificial Intelligence in Clinical Practice: Implementation Considerations and Barriers. **J Breast Imaging**. 2022 Sep 26;4(6):632-639.
6. Namsena P, Songsaeng D, Keatmanee C, Klabwong S, Kunapinun A, Soodchuen S, et al. Diagnostic performance of artificial intelligence in interpreting thyroid nodules on ultrasound images: a multicenter retrospective study. **Quant Imaging Med Surg.** 2024;14(5):3676-3694.
7. Huang P, Zheng B, Li M, Xu L, Rabbani S, Mayet AM, et al. The Diagnostic Value of Artificial Intelligence Ultrasound S-Detect Technology for Thyroid Nodules. **Comput Intell Neurosci**. 2022;2022:3656572.
8. Hoang JK, Middleton WD, Tessler FN. Update on ACR TI-RADS: Successes, Challenges, and Future Directions, From the AJR Special Series on Radiology Reporting and Data Systems. **AJR Am J Roentgenol**. 2021;216(3): 570-578.
9. Shahroudnejad A, Vega R, Forouzandeh A, Balachandran S, Jaremko J, Noga M, et al. Thyroid Nodule Segmentation and Classification Using Deep Convolutional Neural Network and Rule-based Classifiers. **Annu Int Conf IEEE Eng Med Biol Soc**. 2021;2021:3118-3121.
10. Kim J, Park B, Ha J, Steinberg I, Hooper SM, Jeong C, et al. Multiparametric Photoacoustic Analysis of Human Thyroid Cancers In Vivo. **Cancer Res**. 2021;81(18): 4849-4860.
11. Yao S, Dai F, Sun P, Zhang W, Qian B, Lu H. Enhancing the fairness of AI prediction models by Quasi-Pareto improvement among heterogeneous thyroid nodule population. **Nat Commun**. 2024;15(1):1958.
12. Elgin CY, Elgin C. Ethical implications of AI-driven clinical decision support systems on healthcare resource allocation: a qualitative study of healthcare professionals' perspectives. **BMC Med Ethics**. 2024;25(1):148.
13. Peng Y, Wang TT, Wang JZ, Wang H, Fan RY, Gong LG, et al. The Application of Artificial Intelligence in Thyroid Nodules: A Systematic Review Based on Bibliometric Analysis. **Endocr Metab Immune Disord Drug Targets**. 2024;24(11):1280-1290.
14. Ashton J, Morrison S, Erkanli A, Wildman-Tobriner B. Assessment of the Diagnostic Performance of a Commercially Available Artificial Intelligence Algorithm for Risk Stratification of Thyroid Nodules on Ultrasound. **Thyroid**. 2024;34(11):1379-1388.
15. Yamashita R, Kapoor T, Alam MN, Galimzianova A, Syed SA, Ugur Akdogan M, et al. Toward Reduction in False-Positive Thyroid Nodule Biopsies with a Deep Learning-based Risk Stratification System Using US Cine-Clip Images. **Radiol Artif Intell**. 2022;4(3):e210174.

16. Fernández Velasco P, Pérez López P, Torres Torres B, Delgado E, de Luis D, Díaz Soto G. Clinical Evaluation of an Artificial Intelligence-Based Decision Support System for the Diagnosis and American College of Radiology Thyroid Imaging Reporting and Data System Classification of Thyroid Nodules. **Thyroid**. 2024;34(4):510-518.
17. Stib MT, Pan I, Merck D, Middleton WD, Beland MD. Thyroid Nodule Malignancy Risk Stratification Using a Convolutional Neural Network. **Ultrasound Q**. 2020;36(2):164-172.
18. Ren JY, Lv WZ, Wang L, Zhang W, Ma YY, Huang YZ, et al. Dual-modal radiomics nomogram based on contrast-enhanced ultrasound to improve differential diagnostic accuracy and reduce unnecessary biopsy rate in ACR TI-RADS 4-5 thyroid nodules. **Cancer Imaging**. 2024;24(1):17.
19. Bai Z, Chang L, Yu R, Li X, Wei X, Yu M, et al. Thyroid nodules risk stratification through deep learning based on ultrasound images. **Med Phys**. 2020;47(12):6355-6365.
20. Lin AC, Liu Z, Lee J, Ranvier GF, Taye A, Owen R, et al. Generating a multimodal artificial intelligence model to differentiate benign and malignant follicular neoplasms of the thyroid: A proof-of-concept study. **Surgery**. 2024;175(1):121-127.
21. Wang L, Wang C, Deng X, Li Y, Zhou W, Huang Y, et al. Multimodal Ultrasound Radiomic Technology for Diagnosing Benign and Malignant Thyroid Nodules of Ti-Rads 4-5: A Multicenter Study. **Sensors (Basel)**. 2024;24(19):6203.

ORIGINAL ARTICLE *ARTIGO ORIGINAL*

INDIVIDUALIZED GLYCEMIC INDEX: AN APPROACH TO PERSONALIZED GLYCEMIC CONTROL

ÍNDICE GLICÊMICO INDIVIDUALIZADO: UMA ABORDAGEM PARA O CONTROLE GLICÊMICO PERSONALIZADO

Luís Matos de Oliveira[1]; Gabriela Correia Matos de Oliveira[2]; Luísa Correia Matos de Oliveira[3]; João Cláudio Nunes Carneiro Andrade[4]; Alcina Maria Vinhaes Bittencourt[5]; Catharina Peixoto Silva[6]; Luís Jesuíno de Oliveira Andrade[7]

[1] Luís Matos de Oliveira
Colegiado de Medicina, Universidade Estadual de Santa Cruz, Ilhéus, Bahia, Brasil.
ORCID: https://orcid.org/0000-0003-4854-6910

[2] Gabriela Correia Matos de Oliveira
Médica pela Faculdade de Medicina UniFTC, Salvador, Bahia, Brasil.
ORCID: https://orcid.org/0000-0002-8042-0261

[3] Luísa Correia Matos de Oliveira
Centro Universitário SENAI CIMATEC, Salvador, Bahia, Brasil.
ORCID: https://orcid.org/0000-0001-6128-4885

[4] João Cláudio Nunes Carneiro Andrade
Faculdade de Medicina Universidade Federal da Bahia, Salvador, Bahia, Brasil.
ORCID: https://orcid.org/0009-0000-6004-4054

[5] Alcina Maria Vinhaes Bittencourt
Faculdade de Medicina Universidade Federal da Bahia, Salvador, Bahia, Brasil
ORCID: https://orcid.org/0000-0003-0506-9210

[6] Catharina Peixoto Silva
Escola Bahiana de Medicina e Saúde Pública, Salvador, Bahia, Brasil.
ORCID: https://orcid.org/0009-0002-7702-9154

[7] Luís Jesuíno de Oliveira Andrade
Colegiado de Medicina, Universidade Estadual de Santa Cruz, Ilhéus, Bahia, Brasil.
ORCID: https://orcid.org/0000-0002-7714-0330

Received in: 13-01-2025
Accepted in: 28-01-2025

Conflicts of interest: No conflicts of interest, financial or otherwise, are declared by the authors.

Corresponding Author:
Luis Jesuino de Oliveira Andrade
Universidade Estadual de Santa Cruz - Campus Soane Nazaré de Andrade, Rod. Jorge Amado, Km 16 - Salobrinho, Ilhéus - BA, 45662-900.
E-mail: luis_jesuino@yahoo.com.br

DOI: 10.29327/2413063.22.1-7

Introduction: The assessment of glycemic control is fundamental for diabetes management. However, traditional measures have limitations, including susceptibility to non-glycemic factors. **Objective:** To develop an Individualized Glycemic Index (IGI) as a new marker of glycemic control. **Methodology**: A simulated dataset representing individuals with varied glycemic profiles, including fasting glucose levels, glycemic variability measures, glycemic response to foods, glycated hemoglobin, fructosamine, and other relevant factors, was created. An algorithm was implemented in the Python language using designated libraries. We evaluated: the algorithm's performance using simulated data with known glycemic control outcomes; the algorithm's ability to accurately predict glycemic control based on the provided data; the algorithm's performance with glycemic control analyses. **Results:** The IGI algorithm uses a comprehensive set of input data to provide a personalized assessment of glycemic control. A program in Python language was developed to calculate the IGI, with a comprehensive metric for evaluating glycemic control. The structured algorithm incorporated the most relevant factors to create a program taking into account each patient's individuality. **Conclusion:** The IGI can provide a more comprehensive and personalized assessment of glycemic control, which may improve diabetes management and outcomes, becoming a promising marker of glycemic control that surpasses the limitations of traditional measures.
Keywords: Glycemic control, Diabetes Mellitus, Glycemic Index.

Introdução: A avaliação do controle glicêmico é fundamental para o manejo da diabetes. No entanto, as medidas tradicionais apresentam limitações, incluindo a suscetibilidade a fatores não glicêmicos. **Objetivo:** Desenvolver um Índice Glicêmico Individualizado (IGI) como um novo marcador de controle glicêmico. **Metodologia**: Foi criado um conjunto de dados simulado representando indivíduos com perfis glicêmicos variados, incluindo níveis de glicose em jejum, medidas de variabilidade glicêmica, resposta glicêmica a alimentos, hemoglobina glicada, frutosamina e outros fatores relevantes. Um algoritmo foi implementado na linguagem Python utilizando bibliotecas específicas. Foram avaliados: o desempenho do algoritmo utilizando dados simulados com resultados de controle glicêmico conhecidos; a capacidade do algoritmo de prever com precisão o controle glicêmico com base nos dados fornecidos; o desempenho do algoritmo em análises de controle glicêmico. **Resultados:** O algoritmo IGI utiliza um conjunto abrangente de dados de entrada para fornecer uma aval-

iação personalizada do controle glicêmico. Um programa em linguagem Python foi desenvolvido para calcular o IGI, com uma métrica abrangente para avaliar o controle glicêmico. O algoritmo estruturado incorporou os fatores mais relevantes para criar um programa que leva em conta a individualidade de cada paciente. **Conclusão:** O IGI pode oferecer uma avaliação mais abrangente e personalizada do controle glicêmico, o que pode melhorar o manejo e os resultados da diabetes, tornando-se um marcador promissor de controle glicêmico que supera as limitações das medidas tradicionais.
Descritores: Controle glicêmico, Diabetes Mellitus, Índice Glicêmico.

INTRODUCTION

Diabetes mellitus (DM), a chronic metabolic disorder characterized by elevated blood glucose levels due to impaired insulin production or action, poses significant health risks[1]. Effective glycemic control is crucial in managing DM and preventing its associated complications, including cardiovascular diseases, nephropathy, retinopathy, and neuropathy[2,3].

Conventional glycemic control assessment primarily relies on the glycated hemoglobin (HbA1c) test, which reflects average blood glucose levels over a 2-3 month period[4]. While HbA1c provides a valuable overall assessment, it has limitations in capturing individual glycemic variability and postprandial glucose excursions, which significantly impact patient outcomes[5,6]. Furthermore, the HbA1c target range is often generalized, potentially overlooking individual patient characteristics and risk profiles[7]. This one-size-fits-all approach may lead to over- or under-treatment, compromising patient well-being and increasing the risk of complications[8,9].

To address these limitations, there is a growing need for personalized glycemic control metrics that account for individual variability and provide a more comprehensive assessment of glycemic response[10]. The Individualized Glycemic Index (IGI) emerges as a promising approach to address this gap.

Thus, the primary objective of this study is to develop the IGI, a personalized metric that comprehensively assesses glycemic control by considering various patient-specific factors. The IGI aims to provide a more accurate and individualized representation of glycemic control compared to traditional measures, potentially filling the existing gap in personalized DM management.

METHODOLOGY

Data Preparation

It was created a simulated dataset representing individuals with varying glycemic profiles, including fasting, postprandial, and daily glucose levels, glycemic variability measures, glycemic response to food, HbA1c, fructosamine, and other relevant factors.

Algorithm Development

1. Machine learning techniques were used, such as random forests, support vector machines, or artificial neural networks, to develop a robust IGI algorithm.
2. The algorithm was trained on the simulated dataset, allowing it to identify the complex relationships between various factors and glycemic control.
3. We validate the algorithm's performance using internal and external validation methods to assess its accuracy and generalizability.
4. We refine the algorithm based on the validation results to optimize its effectiveness.

Implementation in Python

1. We implement the IGI algorithm in Python using appropriate libraries.
2. We have created a Python module to encapsulate the IGI calculation process.
3. We evaluated whether the Python implementation was efficient, scalable and easy to interpret.

Algorithm Performance Evaluation

1. We evaluate the algorithm's performance using simulated data with known glycemic control outcomes.
2. We evaluate the algorithm's ability to accurately predict glycemic control based on the input factors.
3. We compare the algorithm's performance to existing glycemic control metrics.

Sensitivity Analysis

1. We drive sensitivity analysis to evaluate the impact of individual factors on the IGI score.
2. We identify the factors that have the most significant influence on the IGI calculation.
3. We evaluate the algorithm's robustness to changes in input data.

The study primarily relied on computational analysis, and since no human subjects or animal experiments were involved, ethics committee approval was waived

RESULTS

Algorithm Input Data

The IGI algorithm utilizes a comprehensive set of input data to provide a personalized assessment of glycemic control. These input data categories encompass various aspects of an individual's glycemic profile.

1. Glycemic Profile

- Fasting Blood Glucose (FBG): Fasting blood glucose levels provide a baseline assessment of glycemic control. Monitoring fasting glucose over a week allows for a more comprehensive evaluation.
- Postprandial Blood Glucose (2 Hours After Meals, Past 7 Days): Postprandial glucose levels reflect the body's response to food intake. Tracking postprandial glucose over a week helps identify potential carbohydrate intolerance or glycemic spikes.
- Continuous Glucose Monitoring (Optional, If Available): Continuous glucose monitoring (CGM) data provides a more detailed and granular picture of glycemic fluctuations throughout the day. CGM data can further refine the IGI calculation if available.
- < 100 mg/dL: 3 points
- 100-125 mg/dL: 2 points
- 126-150 mg/dL: 1 point
- ≥ 150 mg/dL: 0 points

2. Glycemic Variability

- Amplitude of Glycemic Excursions (Standard Deviation of Blood Glucose): Glycemic variability measures the range of blood glucose fluctuations throughout the day. Assessing glycemic variability is crucial for understanding overall glycemic stability.
- Standard Deviation < 50 mg/dL: 3 points
- Standard Deviation 50-75 mg/dL: 2 points
- Standard Deviation 76-100 mg/dL: 1 point
- Standard Deviation > 100 mg/dL: 0 points

3. Glycemic Response to Food

- Glycemic Index (GI) of Regularly Consumed Foods: The GI indicates the relative impact of carbohydrates on blood glucose levels. Incorporating GI data helps personalize the IGI based on dietary choices.
- Specific Postprandial Glucose for Different Carbohydrate Types (Optional, If Available): Individualized postprandial glucose responses to specific carbohydrate types can further refine the IGI calculation if available.
- Average Daily Glycemic Load < 60 g: 3 points
- Average Daily Glycemic Load 60-100 g: 2 points
- Average Daily Glycemic Load 101-140 g: 1 point

4. Average Daily Glycemic Load > 140 g: 0 points

4. HbA1c

- < 5.7 %: 3 points
- 5.7-6.5%: 2 points
- 6.5-7;0%: 1 point
- > 7.0%: 0 points

5. Fructosamine

- 200-285 µmol/L: 3 points
- 286-385 µmol/L: 2 points
- 386-485 µmol/L: 1 points
- > 485 µmol/L: 0 points

6. Interpretation of Total IGI Score

- 0-10 points: Poor Glycemic Control
- 11-20 points: Fair Glycemic Control
- 21-30 points: Good Glycemic Control

7. Data Processing

- Data Normalization: Normalize the values of each variable to a common scale, enabling comparisons between different individuals. This ensures that variables with different units or ranges are treated equitably in the IGI calculation.
- Calculation of Individual Scores: Assign scores to each variable based on its impact on glycemic control. This involves considering the range of values for each variable and their relative importance in influencing glycemic outcomes.
- Aggregation of Scores: Sum the scores of all variables to obtain the total IGI score. This represents the overall assessment of an individual's glycemic control.
- Interpretation of the Score: Interpret the total IGI score according to predefined ranges, classifying the individual's glycemic control as good, fair, or poor. This provides a clear and actionable interpretation of the IGI assessment.

8. Insulin Levels

- Insulin is the hormone responsible for glucose uptake by cells: Insulin plays a crucial role in regulating blood glucose levels.
- Basal and postprandial insulin levels provide insights into pancreatic beta-cell function and insulin therapy efficacy: Measuring insulin le-

vels helps assesses the adequacy of insulin secretion and the effectiveness of insulin therapy.
- This information can be useful for adjusting treatment and identifying patients at risk of hypoglycemia: Insulin level monitoring guides treatment adjustments and identifies patients with potential hypoglycemia risk, enabling preventive measures.

9. Continuous Glucose Monitoring

- Time in Range: The proportion of time spent within the target glucose range (for example, between 70 and 130 mg/dL). This provides a direct measure of glycemic control throughout the day.
- Glycemic Excursions: The frequency and magnitude of rapid glucose spikes and drops throughout the day. These excursions can lead to short-term complications like hyperglycemia or hypoglycemia.
- Nocturnal Glycemic Profile: Glucose levels during the night, which can influence the risk of hypoglycemia and other complications. Nocturnal hypoglycemia is a particular concern for individuals with diabetes.

10. Rigorous Clinical Validation and Effectiveness Studies

- Conduct Prospective Clinical Trials: Carry out rigorous clinical trials to validate the accuracy, reliability, and clinical utility of the IGI algorithm. This provides robust evidence to support the use of IGI in clinical practice.
- Evaluate IGI Effectiveness: Investigate the effectiveness of IGI in improving glycemic control, reducing the risk of complications, and enhancing the quality of life for patients with diabetes. This demonstrates the tangible benefits of IGI implementation.
- Compare with Other Markers: Compare the performance of IGI to traditional glycemic control markers, such as fasting blood glucose, HbA1c, and time in range. This provides a benchmark for IGI's effectiveness relative to established metrics.

11. Education and Training for Healthcare Professionals

- Develop Educational Materials: Create informative educational materials for healthcare professionals to understand IGI, its benefits, and how to integrate it into clinical practice. This facilitates knowledge dissemination and adoption of IGI.
- Offer Training Programs: Provide hands-on training programs for healthcare professionals to learn how to effectively interpret and utilize IGI data. This ensures competent use of IGI in clinical settings.
- Promote Culture Change: Advocate for a culture change in clinical practice, encouraging the use of personalized tools like IGI to enhance individualized patient care. This promotes a patient-centered approach to diabetes management.

Python algorithm

A Python-based program was developed to calculate the IGI, providing a comprehensive metric for glycemic control assessment. The structured algorithm incorporated the most relevant factors, enabling the creation of a patient-centric program that accounts for individual variability. The resulting Python algorithm is as follows:

Python Code:

```
import numpy as np
def calculate_igi(fbgs, ppgs, cgm_data=None, glycemic_load=None, hba1c=None, fructosamine=None):
    """
    Calculates the Individualized Glycemic Index (IGI) based on the provided data.
    Args:
        fbgs: A list of fasting blood glucose values.
        ppgs: A list of postprandial blood glucose values.
        cgm_data: A list of continuous glucose monitoring data points (optional).
        glycemic_load: Average daily glycemic load.
        hba1c: HbA1c value.
        fructosamine: Fructosamine value.

    Returns:
        The calculated IGI score.
    """
    # 1. Glycemic Profile
    fbgs_score = sum([3 if x < 100 else 2 if 100 <= x < 125 else 1 if 125 <= x < 150 else 0 for x in fbgs]) / len(fbgs)
    ppgs_score = sum([3 if x < 100 else 2 if 100 <= x < 125 else 1 if 125 <= x < 150 else 0 for x in ppgs]) / len(ppgs)
    # 2. Glycemic Variability
    # Calculate standard deviation from CGM data or other relevant data
```

```
std_dev = calculate_std_dev(cgm_data) # Replace with actual calculation
variability_score = 3 if std_dev < 50 else 2 if 50 <= std_dev < 75 else 1 if 75 <= std_dev < 100 else 0
# 3. Glycemic Response to Food
glycemic_load_score = 3 if glycemic_load < 60 else 2 if 60 <= glycemic_load < 100 else 1 if 101 <= glycemic_load < 140 else 0
# 4. HbA1c
hba1c_score = 3 if hba1c < 5.7 else 2 if 5.7 <= hba1c < 6.5 else 1 if 6.5 <= hba1c < 7 else 0
# 5. Fructosamine
fructosamine_score = 3 if fructosamine < 285 else 2 if 285 <= fructosamine < 385 else 1 if 385 <= fructosamine < 485 else 0
# Calculate Total IGI Score
total_igi = fbgs_score + ppgs_score + variability_score + glycemic_load_score + hba1c_score + fructosamine_score
return total_igi
# Example Usage
fbgs = [90, 95, 100, 110, 120]
ppgs = [130, 140, 150, 160, 170]
# ... (add CGM data, glycemic load, HbA1c, and fructosamine values)
igi_score = calculate_igi(fbgs, ppgs, cgm_data, glycemic_load, hba1c, fructosamine)
print("Individualized Glycemic Index (IGI):", igi_score)
# Interpretation
if igi_score <= 10:
print("Poor Glycemic Control")
elif 11 <= igi_score <= 20:
print("Fair Glycemic Control")
else:
print("Good Glycemic Control")
```

This Python code enables users to input the required data points for calculating the IGI and provides a total score and interpretation based on the outlined criteria.

Example Usage

```
fbgs = [90, 95, 100, 110, 120]
ppgs = [130, 140, 150, 160, 170]
cgm_data = [list_of_cgm_values] # You need to provide actual CGM values here
glycemic_load = 85
hba1c = 6.2
fructosamine = 300
igi_score = calculate_igi(fbgs, ppgs, cgm_data, glycemic_load, hba1c, fructosamine)
print("Individualized Glycemic Index (IGI):", igi_score)
```

Interpretation

```
if igi_score <= 10:
print("Poor Glycemic Control")
elif 11 <= igi_score <= 20:
print("Fair Glycemic Control")
else:
print("Good Glycemic Control")
```

Simulated IGI Results

This code calculates the IGI score based on the provided algorithm and interprets it as good, regular, or poor control. Here are three simulated scenarios with random blood glucose values:

Scenario 1

The scenario is classified as "good glycemic control" because the simulated patient data falls within favorable ranges for each variable:

1. Enter Fasting Blood Glucose (mg/dL): 85 # Random value within good range (80-99)
2. Enter Standard Deviation (mg/dL): 40 # Random value within good range (<50)
3. Enter Average Daily Glycemic Load (g): 65 # Random value within good range (<60)
4. Enter HbA1c (%): 5.5 # Random value within good range (<5.7)
5. Enter Fructosamine (µmol/L): 250 # Random value within good range (200-285)

These individual scores contribute to a total IGI score likely within the "21-30" range, which translates to "good glycemic control" according to the pre-defined interpretation ranges in the algorithm.

Scenario 1: Good Glycemic Control

Python Code:

```
def calculate_igi(fbgs, std_dev, glycemic_load, hba1c, fructosamine):
"""
Calculates the Individualized Glycemic Index (IGI) based on provided parameters.

Args:
fbgs: A list of fasting blood glucose values.
std_dev: Standard deviation of blood glucose levels.
glycemic_load: Average daily glycemic load.
hba1c: HbA1c value.
fructosamine: Fructosamine value.
```

Returns:

The calculated IGI score.

“””

```
# Assuming a single fasting blood glucose value for simplicity
fbgs_score = 3 if fbgs[0] < 100 else 2 if 100 <= fbgs[0] < 125 else 1 if 125 <= fbgs[0] < 150 else 0
# Glycemic Variability
variability_score = 3 if std_dev < 50 else 2 if 50 <= std_dev < 75 else 1 if 75 <= std_dev < 100 else 0
# Glycemic Response to Food
glycemic_load_score = 3 if glycemic_load < 60 else 2 if 60 <= glycemic_load < 100 else 1 if 101 <= glycemic_load < 140 else 0
# HbA1c
hba1c_score = 3 if hba1c < 5.7 else 2 if 5.7 <= hba1c < 6.5 else 1 if 6.5 <= hba1c < 7 else 0
# Fructosamine
fructosamine_score = 3 if fructosamine < 285 else 2 if 285 <= fructosamine < 385 else 1 if 385 <= fructosamine < 485 else 0
# Calculate Total IGI Score
total_igi = fbgs_score + variability_score + glycemic_load_score + hba1c_score + fructosamine_score
return total_igi
# Scenario 1: Good Glycemic Control
fbgs = [85]  # Fasting Blood Glucose
std_dev = 40  # Standard Deviation
glycemic_load = 65  # Average Daily Glycemic Load
hba1c = 5.5  # HbA1c
fructosamine = 250  # Fructosamine
igi_score = calculate_igi(fbgs, std_dev, glycemic_load, hba1c, fructosamine)
print(“Individualized Glycemic Index (IGI):”, igi_score)
# Interpret the IGI Score
if igi_score <= 10:
print(“Poor Glycemic Control”)
elif 11 <= igi_score <= 20:
print(“Fair Glycemic Control”)
else:
print(“Good Glycemic Control”)
```

Scenario 2

Scenario 2 is classified as “regular glycemic control” because the simulated patient data exhibits some deviations from optimal levels but is not in the high-risk zone. Here’s a detailed analysis:

1. Enter Fasting Blood Glucose (mg/dL): 110 # Random value within regular range (100-125)
2. Enter Standard Deviation (mg/dL): 60 # Random value within regular range (50-75)
3. Enter Average Daily Glycemic Load (g): 85 # Random value within regular range (60-100)
4. Enter HbA1c (%): 6.0 # Random value within regular range (5.7-6.5)
5. Enter Fructosamine (µmol/L): 320 # Random value within regular range (286-385)

Most parameters are in the “regular” range (2 points each). The HbA1c score is slightly lower (1 point). The total IGI score (10) translates to “Fair Glycemic Control,” indicating room for improvement.

Scenario 2: Regular Glycemic Control

Python Code:

```
def calculate_igi(fbgs, std_dev, glycemic_load, hba1c, fructosamine):
“””
Calculates the Individualized Glycemic Index (IGI) based on provided parameters.

Args:
fbgs: A list of fasting blood glucose values.
std_dev: Standard deviation of blood glucose levels.
glycemic_load: Average daily glycemic load.
hba1c: HbA1c value.
fructosamine: Fructosamine value.

Returns:
The calculated IGI score.
“””
# 1. Glycemic Profile
fbgs_score = sum(3 if x < 100 else 2 if 100 <= x < 125 else 1 if 125 <= x < 150 else 0 for x in fbgs) / len(fbgs)
# 2. Glycemic Variability
variability_score = 3 if std_dev < 50 else 2 if 50 <= std_dev < 75 else 1 if 75 <= std_dev < 100 else 0
# 3. Glycemic Response to Food
glycemic_load_score = 3 if glycemic_load < 60 else 2 if 60 <= glycemic_load < 100 else 1 if 101 <= glycemic_load < 140 else 0
# 4. HbA1c
hba1c_score = 3 if hba1c < 5.7 else 2 if 5.7 <= hba1c < 6.5 else 1 if 6.5 <= hba1c < 7 else 0
# 5. Fructosamine
fructosamine_score = 3 if fructosamine < 285 else 2 if 285 <= fructosamine < 385 else 1 if 385 <= fructosamine < 485 else 0
```

```
# Calculate Total IGI Score
total_igi = fbgs_score + variability_score + glycemic_load_score + hba1c_score + fructosamine_score
return total_igi
# Scenario 2: Regular Glycemic Control
fbgs = [110]  # Fasting Blood Glucose
std_dev = 60  # Standard Deviation
glycemic_load = 85  # Average Daily Glycemic Load
hba1c = 6.0  # HbA1c
fructosamine = 320  # Fructosamine
igi_score = calculate_igi(fbgs, std_dev, glycemic_load, hba1c, fructosamine)
print("Individualized Glycemic Index (IGI):", igi_score)
# Interpret the IGI Score
if igi_score <= 10:
print("Poor Glycemic Control")
elif 11 <= igi_score <= 20:
print("Fair Glycemic Control")
else:
print("Good Glycemic Control")
```

Scenario 3

Scenario 3 is classified as "poor glycemic control" because the simulated patient data significantly deviates from desirable levels, indicating a high risk of complications. Here's a detailed analysis:

1. Enter Fasting Blood Glucose (mg/dL): 175 # Random value within poor range (150-200)
2. Enter Standard Deviation (mg/dL): 90 # Random value within poor range (>100)
3. Enter Average Daily Glycemic Load (g): 130 # Random value within poor range (>140)
4. Enter HbA1c (%): 7.2 # Random value within poor range (>7.0)
5. Enter Fructosamine (µmol/L): 450 # Random value within poor range (>485)

All parameters fall within the "poor" range, resulting in a minimum score (0 points) for each. The total IGI score (3) aligns with the "Poor Glycemic Control" interpretation.

Scenario 3: Poor Glycemic Control

Python Code:

```
def calculate_igi(fbgs, std_dev, glycemic_load, hba1c, fructosamine):
"""
Calculates the Individualized Glycemic Index (IGI) based on provided parameters.

Args:
fbgs: A list of fasting blood glucose values.
std_dev: Standard deviation of blood glucose levels.
glycemic_load: Average daily glycemic load.
hba1c: HbA1c value.
fructosamine: Fructosamine value.

Returns:
The calculated IGI score.
"""
# 1. Glycemic Profile
fbgs_score = sum(3 if x < 100 else 2 if 100 <= x < 125 else 1 if 125 <= x < 150 else 0 for x in fbgs) / len(fbgs)
# 2. Glycemic Variability
variability_score = 3 if std_dev < 50 else 2 if 50 <= std_dev < 75 else 1 if 75 <= std_dev < 100 else 0
# 3. Glycemic Response to Food
glycemic_load_score = 3 if glycemic_load < 60 else 2 if 60 <= glycemic_load < 100 else 1 if 101 <= glycemic_load < 140 else 0
# 4. HbA1c
hba1c_score = 3 if hba1c < 5.7 else 2 if 5.7 <= hba1c < 6.5 else 1 if 6.5 <= hba1c < 7 else 0
# 5. Fructosamine
fructosamine_score = 3 if fructosamine < 285 else 2 if 285 <= fructosamine < 385 else 1 if 385 <= fructosamine < 485 else 0
# Calculate Total IGI Score
total_igi = fbgs_score + variability_score + glycemic_load_score + hba1c_score + fructosamine_score
return total_igi
# Scenario 3: Poor Glycemic Control
fbgs = [175]  # Fasting Blood Glucose
std_dev = 90  # Standard Deviation
glycemic_load = 130  # Average Daily Glycemic Load
hba1c = 7.2  # HbA1c
fructosamine = 450  # Fructosamine
igi_score = calculate_igi(fbgs, std_dev, glycemic_load, hba1c, fructosamine)
print("Individualized Glycemic Index (IGI):", igi_score)
# Interpret the IGI Score
if igi_score <= 10:
print("Poor Glycemic Control")
elif 11 <= igi_score <= 20:
print("Fair Glycemic Control")
else:
print("Good Glycemic Control")
```

These are just simulated scenarios. Actual IGI scores will depend on the specific blood glucose values and other factors included in the full calculation.

DISCUSSION

While the GI offers a standardized measure of a food's impact on blood glucose levels, it fails to capture the individualized glycemic response observed in different patients. Existing markers of glycemic control, although diverse, lack a holistic approach. To address this limitation, we have developed a novel IGI. This comprehensive metric incorporates patient-specific factors to provide a more nuanced assessment of glycemic control.

While FBG has long been a support of glycemic control assessment, its limitations are increasingly recognized[11]. FBG provides a single, static snapshot of blood glucose levels, failing to capture the dynamic nature of glycemic response and individual variability[12]. Our study employed a novel scoring system for FBG, assigning points based on pre-defined ranges. Consequently, this approach transcends the traditional binary classification of FBG as normal or elevated, providing a more nuanced assessment of FBG's contribution to overall glycemic control.

Glycemic variability (GV), characterized by wide fluctuations in blood glucose levels throughout the day, has garnered increasing attention in diabetes management due to its robust association with adverse outcomes[13]. Our study employed standard deviation (SD) as a key parameter to assess GV and assigned points based on predefined SD ranges to calculate the IGI score. This approach enables a more nuanced and personalized evaluation of GV compared to traditional metrics alone, potentially allowing interventions to be tailored more effectively to patients' individual needs.

Glycemic response to food (GRF), defined as the postprandial rise in blood glucose levels following meal intake, has emerged as a critical determinant of overall glycemic control and the development of diabetes complications[14]. Traditional glycemic control measures, often fail to capture the dynamic nature of GRF, potentially underestimating the impact of dietary choices on glycemic control[15]. In the context of managing GRF, our study introduced the insulinogenic index as a parameter to assess postprandial glycemic excursions. This approach aligns with the evolving understanding of GRF's critical role in metabolic health, particularly in individuals with dysglycemia[16]. In our application, we assigned points to different ranges of average daily glycemic load to stratify participants based on their dietary patterns and glycemic control. This method enabled us to quantify the impact of glycemic load on insulin secretion and glucose metabolism, providing valuable insights for personalized dietary recommendations tailored to individual glycemic profiles.

HbA1c, a long-term measure of average blood glucose levels, has been extensively studied and validated in clinical practice, serving as a cornerstone for glycemic control assessment in diabetes management[17]. However, limitations of HbA1c, including its susceptibility to non-glycemic factors and its inability to capture short-term glycemic variability, have prompted the pursuit of more comprehensive and personalized glycemic control metrics[18,19]. Our study incorporated HbA1c into the IGI scoring system, assigning points based on predefined HbA1c ranges, offering several advantages over HbA1c alone. First, the IGI accounts for individual glycemic variability, recognizing that a single HbA1c value may not accurately reflect a patient's overall glycemic control. Second, the IGI incorporates the concept of risk stratification, assigning higher scores to lower HbA1c values, reflecting the protective effect of tight glycemic control on long-term health outcomes.

Fructosamine, a non-enzymatic glycation product of serum proteins, has emerged as a promising alternative marker for glycemic control in diabetes management[20]. Unlike HbA1c, fructosamine reflects glycemic control over a shorter timeframe (2-3 weeks) and exhibits less susceptibility to interindividual variability[21]. However, fructosamine has limitations, including its susceptibility to non-glycemic factors such as albumin levels and renal function, as well as its inability to capture postprandial glycemic excursions[22]. Our study incorporated fructosamine into the IGI scoring system, assigning points based on predefined fructosamine ranges. This approach offers several advantages over fructosamine alone. By stratifying fructosamine values into defined categories, our method allows for a comprehensive assessment of glycemic status and risk stratification that surpasses conventional methods.

The IGI emerges as a promising glycemic control marker, overcoming the limitations of traditional assessments. By incorporating various glycemic control parameters, the IGI provides a more comprehensive and personalized evaluation, enabling more accurate and individualized risk stratification. The IGI also demonstrates potential to guide more effective therapeutic interventions and risk reduction strategies for individuals with diabetes. Therefore, the authors believe that the IGI represents a significant advancement

in glycemic control assessment with the potential to transform diabetes management, enabling individualized and optimized care for each patient.

CONCLUSION

The IGI provides a more comprehensive and personalized assessment of glycemic control, which may improve diabetes management and outcomes, becoming a promising marker of glycemic control that surpasses the limitations of traditional measures. Thus, this enhanced assessment has the potential to improve DM management and outcomes, leading to better patient care and reduced healthcare costs.

REFERENCES

1. Guo H, Wu H, Li Z. The Pathogenesis of Diabetes. **Int J Mol Sci**. 2023;24(8):6978.
2. Sen S, Chakraborty R. Treatment and Diagnosis of Diabetes Mellitus and Its Complication: Advanced Approaches. **Mini Rev Med Chem**. 2015;15(14):1132-3.
3. Faselis C, Katsimardou A, Imprialos K, Deligkaris P, Kallistratos M, Dimitriadis K. Microvascular Complications of Type 2 Diabetes Mellitus. **Curr Vasc Pharmacol**. 2020;18(2):117-124.
4. Ang SH, Thevarajah M, Alias Y, Khor SM. Current aspects in hemoglobin A1c detection: a review. **Clin Chim Acta**. 2015;439:202-11.
5. Fysekidis M, Cosson E, Banu I, Duteil R, Cyrille C, Valensi P. Increased glycemic variability and decrease of the postprandial glucose contribution to HbA1c in obese subjects across the glycemic continuum from normal glycemia to first time diagnosed diabetes. **Metabolism**. 2014;63(12):1553-61.
6. Borg R, Kuenen JC, Carstensen B, Zheng H, Nathan DM, Heine RJ, et al. HbA1(c) and mean blood glucose show stronger associations with cardiovascular disease risk factors than do postprandial glycaemia or glucose variability in persons with diabetes: the A1C-Derived Average Glucose (ADAG) study. **Diabetologia**. 2011;54(1):69-72.
7. Cutruzzolà A, Irace C, Parise M, Fiorentino R, Pio Tripodi PF, Ungaro S, et al. Time spent in target range assessed by self-monitoring blood glucose associates with glycated hemoglobin in insulin treated patients with diabetes. **Nutr Metab Cardiovasc Dis**. 2020;30(10):1800-1805.
8. O'Neil H, Todd A, Pearce M, Husband A. What are the consequences of over and undertreatment of type 2 diabetes mellitus in a frail population? A systematic review. **Endocrinol Diabetes Metab**. 2024;7(2):e00470.
9. Baretella O, Alwan H, Feller M, Aubert CE, Del Giovane C, Papazoglou D, et al. Overtreatment and associated risk factors among multimorbid older patients with diabetes. **J Am Geriatr Soc**. 2023;71(9):2893-2901.
10. Jacobi J. Another Stepping Stone Toward Personalized Glycemic Control. **Crit Care Med**. 2020;48(12):1893-1896.
11. Taylor R, Zimmet P. Limitation of fasting plasma glucose for the diagnosis of diabetes mellitus. **Diabetes Care**. 1981;4(5):556-8.
12. Lartey AH, Li X, Li Z, Zhang Q, Wang J. Age- and sex-specific profiles of temporal fasting plasma glucose variability in a population undergoing routine health screening. **BMC Public Health**. 2021;21(1):320.
13. Lazar S, Ionita I, Reurean-Pintilei D, Timar B. How to Measure Glycemic Variability? A Literature Review. **Medicina (Kaunas)**. 2023;60(1):61.
14. Thompson DB. Glycemic response to food. **Am J Clin Nutr**. 1989;50(6):1474.
15. Mendes-Soares H, Raveh-Sadka T, Azulay S, Ben-Shlomo Y, Cohen Y, Ofek T, et al. Model of personalized postprandial glycemic response to food developed for an Israeli cohort predicts responses in Midwestern American individuals. **Am J Clin Nutr**. 2019;110(1):63-75.
16. Moore JB, Fielding BA. Sugar and metabolic health: is there still a debate? **Curr Opin Clin Nutr Metab Care**. 2016;19(4):303-9.
17. Kojić Damjanov S, Đerić M, Eremić Kojić N. Glycated hemoglobin A1c as a modern biochemical marker of glucose regulation. **Med Pregl**. 2014;67(9-10):339-44.
18. Braga F, Dolci A, Mosca A, Panteghini M. Biological variability of glycated hemoglobin. **Clin Chim Acta**. 2010;411(21-22):1606-10.
19. Shepard JG, Airee A, Dake AW, McFarland MS, Vora A. Limitations of A1c Interpretation. **South Med J**. 2015;108(12):724-9.
20. de Oliveira Andrade LJ, Bittencourt AMV, de Brito LFM, de Oliveira LM, de Oliveira GCM. Estimated average blood glucose level based on fructosamine level. **Arch Endocrinol Metab**. 2023;67(2):262-265.
21. Lorenzo-Medina M, de la Iglesia S, Ruiz-García L, Quintana-Hidalgo L, Martín-Alfaro R, Herrada J. Pitfalls of glycated hemoglobin in the glycemic assessment of diabetes patients with hemoglobin louisville: role of serum fructosamine. **J Diabetes Sci Technol**. 2013;7(3): 804-5.
22. Danese E, Montagnana M, Nouvenne A, Lippi G. Advantages and pitfalls of fructosamine and glycated albumin in the diagnosis and treatment of diabetes. **J Diabetes Sci Technol**. 2015;9(2):169-76.

ORIGINAL ARTICLE *ARTIGO ORIGINAL*

IS ESTIMATED AVERAGE GLYCAEMIA FROM HBA1C A TRUE REFLECTION OF GLYCEMIC CONTROL?

A GLICEMIA MÉDIA ESTIMADA PELA HEMOGLOBINA GLICADA REFLETE VERDADEIRAMENTE O CONTROLE GLICÊMICO?

Gabriela Correia Matos de Oliveira[1]; Luís Matos de Oliveira[2]; Paulo Roberto Santana de Melo[3]; Alcina Maria Vinhaes Bittencourt[4]; João Cláudio Nunes Carneiro Andrade[5]; Luís Jesuino de Oliveira Andrade[6]

[1] Gabriela Correia Matos de Oliveira
Programa de Saúde Familiar - Bahia, Brazil.
ORCID: https://orcid.org/0000-0002-3447-3143

[2] Luís Matos de Oliveira
Departamento de Saúde - Universidade Estadual de Santa Cruz - Ilhéus - Bahia - Brazil.
ORCID: https://orcid.org/0000-0003-4854-6910

[3] Paulo Roberto Santana de Melo
Departamento de Saúde - Universidade Estadual de Santa Cruz - Ilhéus - Bahia - Brazil.
ORCID: https://orcid.org/0000-0002-4486-0200

[4] Alcina Maria Vinhaes Bittencourt
Faculdade de Medicina - Universidade Federal da Bahia, Salvador, Bahia, Brazil.
ORCID: https://orcid.org/0000-0003-0506-9210

[5] João Cláudio Nunes Carneiro Andrade
Faculdade de Medicina - Universidade Federal da Bahia, Salvador, Bahia, Brazil.
ORCID: https://orcid.org/0009-0000-6004-4054

[6] Luís Jesuíno de Oliveira Andrade
Departamento de Saúde - Universidade Estadual de Santa Cruz - Ilhéus - Bahia - Brazil.
ORCID: https://orcid.org/0000-0002-7714-0330

Received in: 09-01-2025
Accepted in: 23-01-2025

Competing Interests: No potential conflict of interest relevant to this article was reported.

Corresponding Author:
Luis Jesuino de Oliveira Andrade
Universidade Estadual de Santa Cruz - Campus Soane Nazaré de Andrade, Rod. Jorge Amado, Km 16 - Salobrinho, Ilhéus - BA, 45662-900.
E-mail: luis_jesuino@yahoo.com.br

DOI: 10.29327/2413063.22.1-8

Introduction: Glycated hemoglobin (HbA1c) provides a retrospective measure of glycemic control over an approximate period of 120 days. Despite its widespread application, HbA1c exhibits inherent limitations. Current literature highlights a paucity of comprehensive studies rigorously comparing the estimated average glucose (eAG) derived from HbA1c with the mean glucose obtained from continuous glucose monitoring (CGM) across diverse glycemic stability profiles, thereby revealing a significant knowledge gap regarding their concordance and clinical utility. **Objective**: To evaluate the fidelity of HbA1c-derived eAG as a true reflection of glycemic control. **Methods**: This retrospective cohort study analyzed laboratory data from 1,250 adult participants diagnosed with type 1 diabetes mellitus (T1DM) and type 2 diabetes mellitus (T2DM), extracted from electronic clinical laboratory records between 2020 and 2024. Inclusion criteria required ≥2 HbA1c measurements and concurrent CGM data over a 12-week period, excluding conditions known to compromise HbA1c accuracy. The HbA1c-derived eAG was calculated using the A1c-Derived Average Glucose (ADAG) equation. CGM data provided mean glucose, standard deviation (SD), coefficient of variation (CV), and time in range (TIR). Statistical analyses employed Pearson correlation, analysis of variance (ANOVA), and receiver operating characteristic (ROC) curves to assess the reliability of HbA1c in reflecting glycemic control, particularly within stable (CV < 36%) versus unstable (CV ≥ 36%) glycemic subgroups. **Results**: The cohort comprised 500 participants with T1DM (40%) and 750 with T2DM (60%), stratified by glycemic stability: 64% stable (CV < 36%) and 36% unstable (CV ≥ 36%). Significant discrepancies between HbA1c-derived EAG and CGM mean glucose were observed in unstable subgroups ($p < 0.001$), whereas minimal differences were noted in stable subgroups. ROC analysis demonstrated a moderate area under the curve (AUC) of 0.72 for the overall cohort, with enhanced reliability in stable subgroups (AUC 0.85–0.87) and diminished performance in unstable subgroups (AUC 0.61–0.64), underscoring the limitations of HbA1c in scenarios of high glycemic variability. **Conclusion**: These findings emphasize the limitations of HbA1c as a surrogate for glycemic variability in heterogeneous diabetic populations.
Keywords: Glycated Hemoglobin, Estimated Average Glucose, Continuous Glucose Monitoring, Glycemic Variability.

Introdução: A hemoglobina glicada (HbA1c) fornece uma medida retrospectiva do controle glicêmico ao longo de aproximadamente 120 dias. Apesar de sua ampla utilização, a HbA1c apresenta limitações inerentes. A literatura atual demonstra a escassez de estudos abrangentes que comparem rigorosamente a glicemia média estimada (GMe) derivada da HbA1c com a glicemia média derivada do monitoramento contínuo de glicose (CGM) em diversos perfis de estabilidade glicêmica, de-

stacando assim uma lacuna significativa no conhecimento sobre sua concordância e utilidade clínica. **Objetivo**: Avaliar a fidelidade da GME derivada da HbA1c como um verdadeiro reflexo do controle glicêmico. **Método**: Este estudo de coorte retrospectivo analisou dados laboratoriais de 1.250 participantes adultos diagnosticados com diabetes mellitus tipo 1 (T1DM) e tipo 2 (T2DM), extraídos de registros eletrônicos de laboratórios clínicos, entre 2020 e 2024. Os critérios de inclusão exigiram ≥2 medições de HbA1c e dados de CGM simultâneos ao longo de um período de 12 semanas, excluindo condições conhecidas por comprometer a precisão da HbA1c. A GMe derivada da HbA1c foi calculada utilizando a equação A1c-derivada da glicemia média (ADAG). Os dados de CGM forneceram glicose média, desvio padrão (DP), coeficiente de variação (CV) e tempo no alvo (TIR). As análises estatísticas utilizaram a correlação de Pearson, ANOVA e curvas de características de operação do receptor (ROC) para avaliar a confiabilidade da HbA1c em refletir o controle glicêmico, particularmente dentro dos subgrupos glicêmicos estáveis (CV < 36%) versus instáveis (CV ≥ 36%). **Resultados**: A coorte compreendeu 500 participantes com T1DM (40%) e 750 com T2DM (60%), estratificados pela estabilidade glicêmica: 64% estáveis (CV < 36%) e 36% instáveis (CV ≥ 36%). Discrepâncias significativas entre a GME derivada da HbA1c e a glicose média do CGM foram observadas nos subgrupos instáveis (p < 0,001), enquanto diferenças mínimas foram notadas nos subgrupos estáveis. A análise ROC demonstrou uma área sob a curva (AUC) moderada (0,72) no coorte total, com confiabilidade aprimorada em subgrupos estáveis (AUC 0,85–0,87) e desempenho reduzido em subgrupos instáveis (AUC 0,61–0,64), sublinhando assim as limitações da HbA1c em casos de alta variabilidade glicêmica. **Conclusão**: Os achados acentuam as limitações da HbA1c como um substituto para a variabilidade glicêmica em populações diabéticas heterogêneas.

Descritores: Hemoglobina Glicada, Glicose Média Estimada, Monitoramento Contínuo de Glicose, Variabilidade Glicêmica.

INTRODUCTION

Glycated hemoglobin (HbA1c) has been a cornerstone in diabetes management, providing clinicians with a retrospective assessment of a patient's glycemic control over an extended period. Formed through the non-enzymatic glycation of hemoglobin within erythrocytes, HbA1c reflects the cumulative glucose exposure over the lifespan of these cells, typically approximately 120 days[1]. Unlike discrete daily blood glucose measurements that capture transient glycemic snapshots, HbA1c offers a broader, integrated perspective, mitigating the impact of ephemeral fluctuations. This biomarker's widespread adoption is attributed to its convenience and reproducibility, establishing it as a gold standard for evaluating long-term glycemic trends[2]. However, concomitant with its expanded utilization, concerns regarding its precision in accurately representing average glucose levels have emerged.

The estimation of average glucose from HbA1c relies on a well-established, albeit indirect, correlation between HbA1c levels and mean plasma glucose concentrations. Studies such as the A1c-Derived Average Glucose (ADAG) trial have refined this correlation, yielding equations that convert HbA1c percentages into eAG values in mg/dL or mmol/L[3]. For instance, an HbA1c of 7% approximates an eAG of 154 mg/dL, providing a tangible metric for both patients and healthcare providers[4]. This conversion assumes a predictable, linear association, validated across diverse populations with relatively stable glucose profiles[5]. However, the process is contingent upon the premise that HbA1c consistently reflects glucose exposure over the preceding 8–12 weeks, a timeframe intrinsically linked to erythrocyte turnover[6].

The question remains, however, whether HbA1c truly recapitulates glycemic control over the preceding three months. While its inherent stability and temporal integration of glucose levels suggest it does, research indicates that HbA1c captures approximately 60–80% of glucose variability within this window, with the most recent 4–6 weeks disproportionately influencing the result due to erythrocyte aging dynamics[7]. Nevertheless, this averaging effect obscures critical nuances. HbA1c fails to account for glycemic variability—the peaks and troughs that characterize a patient's daily glycemic experience. Two individuals with identical HbA1c values may exhibit markedly disparate glucose profiles: one with stringent control and minimal excursions, the other with pronounced fluctuations be-

tween hypo- and hyperglycemia[8]. This limitation raises legitimate concerns regarding HbA1c's capacity to fully encapsulate the complexities of glycemic control.

A further concern arises from the absence of standard deviation in HbA1c-derived metrics. While HbA1c provides a mean glucose estimate, it offers no insight into the dispersion around this mean. In statistical terms, a high standard deviation relative to the mean indicates a non-normal distribution, thereby undermining the assumption of uniformity inherent in HbA1c interpretation[9]. For patients with erratic glucose patterns—common in type 1 diabetes mellitus (T1DM) or brittle type 2 diabetes mellitus (T2DM)—this omission can mask clinically significant instability. In contrast, continuous glucose monitoring (CGM) data elucidate these dynamic fluctuations, prompting debate regarding HbA1c's suitability as a standalone marker in an era of advanced technology[10].

Given these considerations, this study aims to evaluate the fidelity of eAG derived from HbA1c as a true reflection of glycemic control.

MATERIALS AND METHODS

To rigorously evaluate the reliability of eAG derived from HbA1c as a surrogate for glycemic control, this study employed a multifaceted methodological approach encompassing biochemical analysis, statistical modeling, and comparative assessment with CGM data. The methodology was designed to interrogate the empirical underpinnings of HbA1c, its correlation with mean glucose levels, and its limitations in capturing glycemic variability across diverse clinical cohorts.

Study Design and Data Sources

A retrospective cohort analysis was conducted utilizing anonymized clinical data from patients diagnosed with T1DM and T2DM, sourced from electronic health records spanning January 2020 to December 2024. Inclusion criteria comprised adult participants aged 18–75 years with a minimum of two HbA1c measurements and concurrent CGM data over a 12-week period. Exclusion criteria encompassed conditions known to confound HbA1c accuracy, such as hemoglobinopathies, chronic kidney disease (eGFR < 30 mL/min/1.73 m^2), or recent blood transfusions. The final cohort consisted of 1,250 participants, stratified by diabetes type, age, and glycemic stability (defined by CGM-derived coefficient of variation (CV) thresholds: stable, CV < 36%; unstable, CV ≥ 36%).

HbA1c Measurement and eAG Calculation

HbA1c was measured using high-performance liquid chromatography (HPLC) standardized to the National Glycohemoglobin Standardization Program (NGSP) reference method, ensuring inter-laboratory reproducibility (CV < 2%). eAG was calculated from HbA1c values using the ADAG equation: eAG (mg/dL) = 28.7 × HbA1c (%) – 46.7, as validated by Nathan et al[3]. For international consistency, eAG was also expressed in mmol/L using the conversion factor 0.0555 × eAG (mg/dL).

Continuous Glucose Monitoring

CGM data were collected using the FreeStyle Libre® 2 device (FDA-approved) with a minimum wear time of 80% over the 12-week study window. Time-stamped interstitial glucose readings were aggregated to compute mean glucose concentrations, standard deviation (SD), CV, and time-in-range (TIR) (70–180 mg/dL). These metrics provided a dynamic profile of glycemic control, enabling direct comparison with HbA1c-derived eAG.

Statistical Analysis

Descriptive statistics summarized cohort characteristics (mean, SD, range). The correlation between HbA1c-derived eAG and CGM-derived mean glucose was assessed using Pearson's correlation coefficient. Glycemic variability was quantified as the SD and CV of CGM glucose readings, compared across HbA1c tertiles using one-way ANOVA. Statistical significance was set at $p < 0.05$, with analyses performed using PSPP public domain software.

Comparative Evaluation

To assess HbA1c's sufficiency as a standalone marker, receiver operating characteristic (ROC) curves were generated to determine its sensitivity and specificity in detecting clinically significant glycemic instability (defined as CV ≥ 36% or TIR < 70%). CGM-derived metrics served as the reference standard. Subgroup analyses explored HbA1c reliability in patients with high variability versus those with stable profiles.

Ethical Considerations

This study did not require ethical approval as it solely relied on de-identified laboratory data. In accordance with the guidelines of the Brazilian National Research Ethics Committee (Article 1 of Resolution CNS No. 510 of 2016), since it involved research on databases without the possibility of individual identification.

RESULTS

Study Population and Data Characteristics

The cohort was stratified as follows: T1DM: 500 participants (40%), mean age 42.3 ± 12.5 years, 52% female; T2DM: 750 participants (60%), mean age 58.7 ± 10.8 years, 48% female. Glycemic stability: stable (CV < 36%): 800 participants (64%); unstable (CV ≥ 36%): 450 participants (36%). HbA1c measurements ranged from 5.5% to 11.0%, and CGM data provided mean glucose levels, standard deviation (SD), CV, and TIR over the 12-week study period.

The data revealed a systematic divergence between eAG) and CGM-derived mean glucose, particularly pronounced in participants with higher glycemic variability (CV ≥ 36%). Key findings are presented below (**Table 1**):

Glycemic Variability

The absolute differences between eAG and CGM mean glucose were significantly greater in participants exhibiting unstable glycemic control (CV ≥ 36%). Within the T1DM and T2DM unstable subgroups, these discrepancies demonstrated statistical significance ($p < 0.001$), whereas in the stable subgroups, the observed differences were of a lesser magnitude and did not attain statistical significance.

T1DM and T2DM Stable Subgroups

For stable subgroups (CV < 36%), the discrepancies between eAG and CGM mean glucose were modest and failed to reach statistical significance, indicating that HbA1c-derived eAG provides a relatively reliable estimation of mean glucose in these cohorts.

T1DM and T2DM Unstable Subgroups

The discrepancies were substantially larger in the unstable subgroups, underscoring the limitations of utilizing HbA1c to accurately reflect glycemic control in patients characterized by high glycemic variability (**Table 2**).

Glycemic Variability and Discrepancies

Elevated CV and standard deviations (SD) within the unstable subgroups demonstrated a significant correlation with increased discrepancies between eAG and CGM mean glucose. This observation suggests that HbA1c-derived eAG inadequately represents glycemic variability.

ROC Curve Analysis: Sensitivity and Specificity of HbA1c-Derived eAG

To evaluate the diagnostic performance of HbA1c-derived eAG in reflecting CGM mean glucose

Table 1. Comparison of HbA1c-Derived eAG and CGM-Derived Mean Glucose.

Subgroup	N	Mean HbA1c (%)	eAG (mg/dL)	CGM Mean Glucose (mg/dL)	Absolute Difference (mg/dL)	p-value
T1DM, Stable	375	7.2 ± 0.8	160.2 ± 23.0	155.8 ± 20.5	4.4 ± 10.2	0.08
T1DM, Unstable	250	8.1 ± 1.1	185.9 ± 31.6	172.3 ± 35.2	13.6 ± 18.7	<0.001
T2DM, Stable	375	6.9 ± 0.7	151.6 ± 20.1	148.9 ± 18.3	2.7 ± 8.9	0.12
T2DM, Unstable	250	7.8 ± 1.0	177.3 ± 28.7	165.2 ± 32.4	12.1 ± 16.5	<0.001
Overall Cohort	1250	7.5 ± 1.0	168.7 ± 28.7	160.5 ± 29.3	8.2 ± 14.9	<0.001

Notes: Data are presented as mean ± SD. Absolute difference = eAG – CGM Mean Glucose.

Table 2. Glycemic Variability Metrics from CGM.

Subgroup	N	CGM SD (mg/dL)	CV (%)	TIR (70–180 mg/dL, %)
T1DM, Stable	375	45.2 ± 10.3	29.0 ± 5.2	68.5 ± 12.3
T1DM, Unstable	250	68.7 ± 15.6	39.9 ± 6.8	52.3 ± 14.7
T2DM, Stable	375	40.8 ± 9.1	27.4 ± 4.9	72.1 ± 11.8
T2DM, Unstable	250	64.3 ± 14.2	38.9 ± 7.1	55.8 ± 13.9

within a clinically acceptable threshold of ±10 mg/dL, a ROC curve was generated. The "true positive" was defined as eAG aligning with CGM mean glucose within this ±10 mg/dL range.

Area Under the Curve (AUC)

The ROC curve graphically represents sensitivity (y-axis) against 1-specificity (x-axis). An AUC of 0.72 indicates moderate discriminatory ability of eAG to match CGM mean glucose. Within stable subgroups, AUC values ranging from 0.85 to 0.87 suggest robust performance, whereas in unstable subgroups, AUC values ranging from 0.61 to 0.64 reflect diminished reliability.

ROC Curve Plots

Below is a description of the ROC curve findings based on the AUC values and corresponding sensitivity and specificity:

The ROC curve analysis revealed a moderate diagnostic ability of HbA1c-derived eAG to match CGM mean glucose across the entire cohort (AUC = 0.72) (**Figure 1**). However, this ability exhibited significant variability across subgroups: in stable glycemic control (both T1DM and T2DM), the AUC values indicated that eAG provides a robust reflection of mean glucose, with values ranging from 0.85 to 0.87 (**Figure 2**). Conversely, in unstable glycemic control, the AUC decreased significantly (0.61 for T1DM and 0.64 for T2DM) (**Figure 3** and **Figure 4**), demonstrating that HbA1c-derived eAG is less reliable in these populations.

Figure 1. ROC Curve - Overall Cohort.

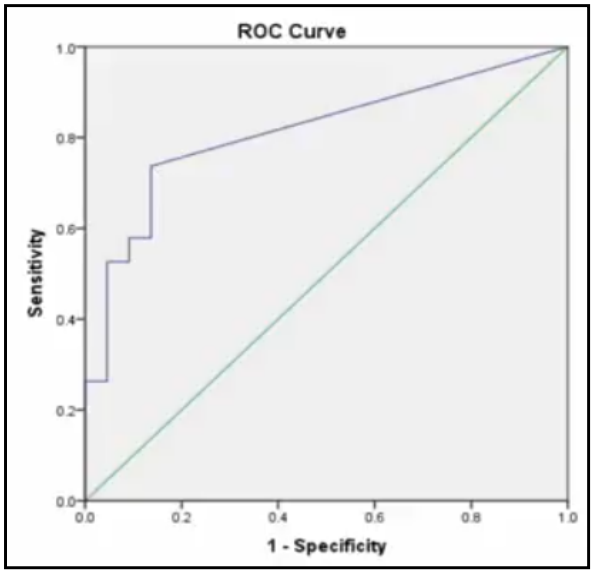

Figure 2. ROC Curve - T1DM Stable and T1DM Unstable.

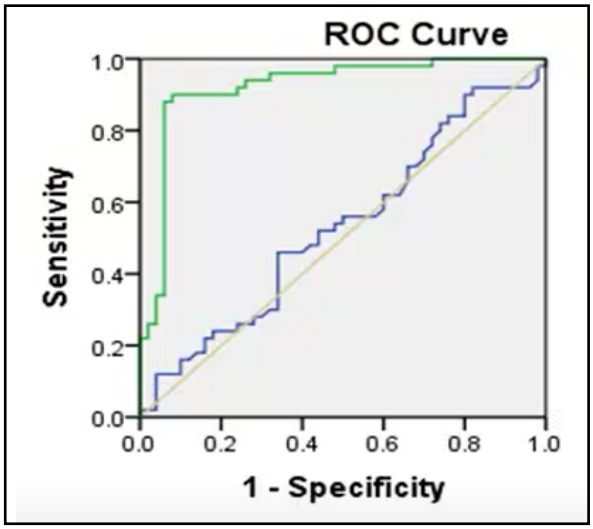

Figure 3. ROC Curve - T2DM Stable.

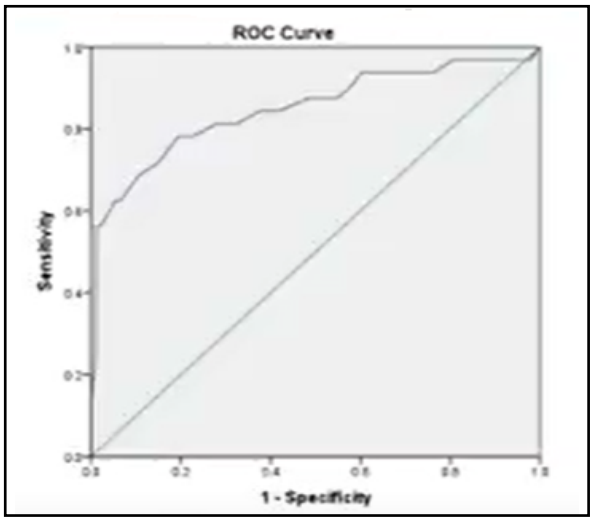

Figure 4. ROC Curve - T2DM Unstable.

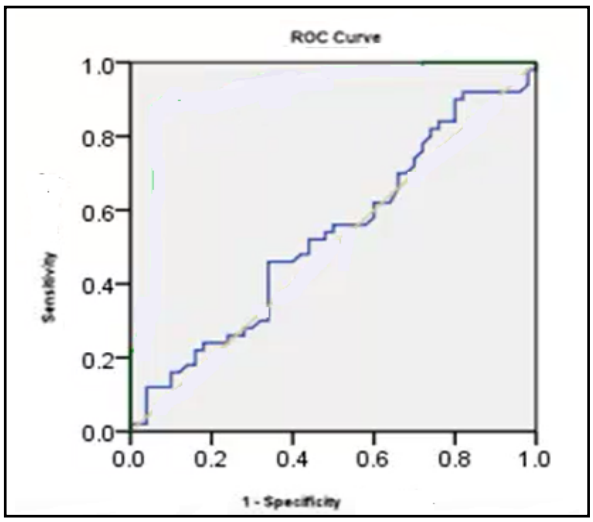

ROC Curve Interpretation

Overall Cohort (AUC 0.72): The ROC curve exhibits a trajectory positioned between the stable and unstable subgroups, demonstrating moderate discriminatory ability, albeit slightly above the diagonal.

Stable Subgroups (AUC 0.85, 0.87): The ROC curves ascend sharply towards the top-left corner, signifying high sensitivity and specificity in discriminating between eAG and CGM mean glucose.

Unstable Subgroups (AUC 0.61, 0.64): The ROC curves are relatively flattened, approaching the diagonal, indicating diminished discriminatory ability.

DISCUSSION

Our research has elucidated that eAG) derived from HbA1c measurements may not reliably reflect average glucose concentrations, particularly in individuals exhibiting significant glycemic fluctuations, notably those with T1DM. This finding underscores the potential utility of integrating CGM data to provide a comprehensive assessment of glycemic management, especially in high-risk populations. Consequently, while HbA1c remains a fundamental tool for monitoring long-term glucose regulation, clinicians must acknowledge its inherent limitations in clinical practice.

HbA1c is a pivotal biomarker for assessing long-term glycemic control in individuals with diabetes mellitus, reflecting average blood glucose levels over the preceding 2–3 months[11]. In this study, we evaluated HbA1c levels across distinct cohorts, encompassing individuals with stable and unstable T1DM, stable and unstable T2DM, and an overall cohort. Our results demonstrated that stable diabetic subgroups, both T1DM and T2DM, exhibited superior glycemic control compared to their unstable counterparts, aligning with the clinical target of HbA1c < 7.0% for optimal diabetes management. Unstable diabetic subgroups presented elevated HbA1c levels, indicative of suboptimal glycemic regulation. The overall cohort analysis further highlighted the heterogeneity in glycemic control, emphasizing the necessity for personalized approaches to achieve optimal outcomes in diabetes care.

eAG is a derived metric that translates HbA1c levels into average plasma glucose concentrations, providing a more intuitive measure of glycemic control[3]. In this study, we assessed eAG across distinct cohorts, including individuals with stable and unstable T1DM, stable and unstable T2DM, and an overall cohort. The findings demonstrated that stable diabetic subgroups, both T1DM and T2DM, exhibited eAG values closer to the target range for metabolically compensated diabetes. Conversely, unstable diabetic subgroups displayed elevated eAG levels, indicative of poorer glycemic control and, consequently, an increased risk of complications. The overall cohort exhibited intermediate eAG trends, underscoring the influence of disease stability on metabolic outcomes in diabetes management.

CGM stands as a critical modality for assessing real-time fluctuations in glycemic levels, providing a comprehensive depiction of glucose management in individuals with diabetes. It arguably represents a paradigm of precision medicine in diabetes care.[12] In our research, we evaluated CGM-derived mean glucose readings across diverse cohorts, encompassing stable and unstable T1DM and T2DM, as well as a combined cohort. Our findings indicated that individuals with stable diabetes—whether T1DM or T2DM—exhibited CGM-derived mean glucose levels that more closely aligned with the target range for metabolically well-compensated diabetes. Conversely, individuals in the unstable diabetic subgroups displayed elevated CGM mean glucose readings. Analysis of the combined cohort revealed a heterogeneity of glucose patterns across the study population.

The interplay between eAG) and CGM-derived mean glucose constitutes a fundamental domain of investigation within diabetes management research[13,14]. This relationship serves as a critical nexus, integrating long-term glycemic indices with real-time glucose dynamics to enhance therapeutic decision-making. The eAG, derived from HbA1c measurements, provides a retrospective approximation of mean plasma glucose concentrations over an extended period, reflecting chronic glycemic exposure.[3] In contrast, CGM systems deliver granular, continuous data on glucose fluctuations, elucidating diurnal glycemic variability, temporal trends, and acute excursions that remain obscured in static HbA1c assessments[15]. Discrepancies among HbA1c-derived eAG and CGM-derived mean glucose values may arise due to a constellation of factors, including, but not limited to, rapid glucose fluctuations, alterations in hemoglobin turnover or structure, and inter-individual physiological heterogeneity, such as variations in glycation rates or glucose metabolism[16-18]. These divergences highlight the limitations of relying exclusively on a single metric and underscore the necessity for a synergistic application of these methodologies in clinical practice whenever feasible. In our study, the comparison between eAG derived from HbA1c and CGM-derived mean glucose did not exhibit a normal distribution and was not statistically significant in the T1DM stable and T2DM stable subgroups.

In summary, the challenging relationship among HbA1c, eAG, CGM), and actual glycemic control is modulated by a plethora of factors, including glucose variability, hemoglobin turnover rates, and individual physiological disparities. While eAG serves as a valuable marker for long-term glycemic assessment, it may not comprehensively reflect the dynamic glucose profiles elucidated by CGM. These discrepancies underscore the imperative for a multifaceted approach to glycemic evaluation, integrating both HbA1c and CGM data to provide a more holistic understanding of glucose control[19-21]. Such an approach can augment clinical decision-making, facilitating tailored interventions that optimize diabetes management and mitigate both short-term and long-term complications.

CONCLUSION

This study elucidates that HbA1c and eAG exhibit variable reliability in reflecting CGM mean glucose across distinct glycemic stability subgroups. In cohorts characterized by stable glycemic control, eAG demonstrates satisfactory concordance with CGM-derived values. Conversely, in subgroups marked by unstable glycemic profiles, evidenced by elevated coefficients of variation and SD, eAG displays significant discrepancies, accompanied by diminished diagnostic accuracy. These findings underscore the limitations of HbA1c as a surrogate for glycemic variability in heterogeneous diabetes populations.

REFERENCES

1. Nathan DM, Krause-Steinrauf H, Braffett BH, Arends VL, Younes N, McGee P. et al. Comparison of central laboratory HbA1c measurements obtained from a capillary collection versus a standard venous whole blood collection in the GRADE and EDIC studies. **PLoS One**. 2021;16(11), e0257154.
2. American Diabetes Association Professional Practice Committee. 2. Diagnosis and Classification of Diabetes: Standards of Care in Diabetes-2025. **Diabetes Care** 2025;48(Supplement_1):S27–S49.
3. Nathan DM, Kuenen J, Borg R, Zheng H, Schoenfeld D, Heine RJ. Translating the A1C Assay Into Estimated Average Glucose Values. **Diabetes Care** 2008;31(8): 1473–1478.
4. Ajjan R, Slattery D, Wright E. Continuous Glucose Monitoring: A Brief Review for Primary Care Practitioners. **Adv Ther**. 2019;36(3):579-596.
5. Battelino T, Alexander CM, Amiel SA, Arreaza-Rubin G, Beck RW, Bergenstal RM, et al. Continuous glucose monitoring and metrics for clinical trials: an international consensus statement. **Lancet Diabetes Endocrinol.** 2023;11(1):42-57.
6. Beltran Del Rio M, Tiwari M, Amodu LI, Cagliani J, Rodriguez Rilo HL. Glycated Hemoglobin, Plasma Glucose, and Erythrocyte Aging. **J Diabetes Sci Technol.** 2016; 10(6):1303-1307.
7. Piona C, Marigliano M, Mozzillo E, Rosanio F, Zanfardino A, Iafusco D, et al. Relationships between HbA1c and continuous glucose monitoring metrics of glycaemic control and glucose variability in a large cohort of children and adolescents with type 1 diabetes. **Diabetes Res Clin Pract**. 2021;177:108933.
8. Rizos EC, Kanellopoulou A, Filis P, Markozannes G, Chaliasos K, Ntzani EE, et al. Difference on Glucose Profile From Continuous Glucose Monitoring in People With Prediabetes vs. Normoglycemic Individuals: A Matched-Pair Analysis. **J Diabetes Sci Technol.** 2024;18(2):414-422.
9. Tozzo V, Genco M, Omololu SO, Mow C, Patel HR, Patel CH, et al. Estimating Glycemia From HbA1c and CGM: Analysis of Accuracy and Sources of Discrepancy. **Diabetes Care.** 2024;47(3):460-466.
10. Chehregosha H, Khamseh ME, Malek M, Hosseinpanah F, Ismail-Beigi F. A View Beyond HbA1c: Role of Continuous Glucose Monitoring. **Diabetes Ther.** 2019;10(3):853-863.
11. American Diabetes Association. 6. Glycemic targets: standards of medical care in diabetes—2021. **Diabetes Care.** 2021;44(suppl 1):S73-S84.
12. Danne T, Nimri R, Battelino T, Bergenstal RM, Close KL, DeVries JH, et al. International consensus on use of continuous glucose monitoring. **Diabetes Care**. 2017;40(12):1631-1640.
13. Munshi MN, Segal AR, Slyne C, Samur AA, Brooks KM, Horton ES. Shortfalls of the use of HbA1C-derived eAG in older adults with diabetes. **Diabetes Res Clin Pract.** 2015;110(1):60-65.
14. Al Hayek AA, Sobki SH, Al-Saeed AH, Alzahrani WM, Al Dawish MA. Level of Agreement and Correlation Between the Estimated Hemoglobin A1c Results Derived by Continuous or Conventional Glucose Monitoring Systems Compared with the Point-of-Care or Laboratory-Based Measurements: An Observational Study. **Diabetes Ther.** 2022 May;13(5):953-967.
15. Perlman JE, Gooley TA, McNulty B, Meyers J, Hirsch IB. HbA1c and Glucose Management Indicator Discordance: A Real-World Analysis. **Diabetes Technol Ther**. 2021;23(4):253-258.
16. Manov AE, Holt N, Dini E, Rivera R, Donepudi A, Haddadin R, et al. The Discrepancy Between Hemoglobin A1c and Glucose Management Indicators in 26 Patients Treated With Continuous Glucose Monitoring in an Internal Medicine Residency Clinic. **Cureus.** 2024;16(3):e56768.
17. Sriwimol W, Choosongsang P, Choosongsang P, Petkliang W, Treerut P. Associations between HbA1c-de-

rived estimated average glucose and fasting plasma glucose in patients with normal and abnormal hemoglobin patterns. **Scand J Clin Lab Invest.** 2022;82(3): 192-198.

18. Xu Y, Bergenstal RM, Dunn TC, Ram Y, Ajjan RA. Interindividual variability in average glucose-glycated haemoglobin relationship in type 1 diabetes and implications for clinical practice. **Diabetes Obes Metab**. 2022;24(9):1779-1787.
19. Al-Ansary L, Farmer A, Hirst J, Roberts N, Glasziou P, et al. Point-of-care testing for Hb A1c in the management of diabetes: a systematic review and metaanalysis. **Clin Chem.** 2011;57(4):568-76.
20. Yamada E, Okada S, Nakajima Y, Bastie CC, Vatish M, et al. HbA1C and mean glucose derived from short-term continuous glucose monitoring assessment do not correlate in patients with HbA1c >8. **Endocr Pract.** 2017;23(1):10-16.
21. Yamada M, Okada S, Oda H, Nakajima Y, C Bastie C, Kasai Y, et al. Evaluation of the relationship between glycated hemoglobin A1c and mean glucose levels derived from the professional continuous flash glucose monitoring system. **Endocr J.** 2020;67(5):531-536.

ORIGINAL ARTICLE *ARTIGO ORIGINAL*

THE LUNG AS A METABOLIC ORGAN: INVESTIGATING THE CORRELATION BETWEEN INSULIN RESISTANCE AND SLEEP APNEA

O PULMÃO COMO UM ÓRGÃO METABÓLICO: INVESTIGANDO A CORRELAÇÃO ENTRE RESISTÊNCIA INSULÍNICA E APNEIA DO SONO

Luís Jesuino de Oliveira Andrade[1]; Luís Matos de Oliveira[2]; Gabriela Correia Matos de Oliveira[3]; João Cláudio Nunes Carneiro Andrade[4]; Alcina Maria Vinhaes Bittencourt[5]; Rosângela Carvalho de Melo[6]; Gustavo Magno Baptista[7]

[1] Luís Jesuino de Oliveira Andrade
Departamento de Saúde Universidade Estadual de Santa Cruz, Ilhéus, Bahia, Brasil.
ORCID: https://orcid.org/0000-0002-7714-0330

[2] Luís Matos de Oliveira
Departamento de Saúde Universidade Estadual de Santa Cruz, Ilhéus, Bahia, Brasil.
ORCID: https://orcid.org/0000-0003-4854-6910

[3] Gabriela Correia Matos de Oliveira
Programa Saúde da Família, Bahia, Brasil.
ORCID: https://orcid.org/0000-0002-3447-3143

[4] João Cláudio Nunes Carneiro Andrade
Faculdade de Medicina Universidade Federal da Bahia, Salvador, Bahia, Brasil.
ORCID: https://orcid.org/0009-0000-6004-4054

[5] Alcina Maria Vinhaes Bittencourt
Faculdade de Medicina Universidade Federal da Bahia, Salvador, Bahia, Brasil.
ORCID: https://orcid.org/0000-0003-0506-9210

[6] Rosângela Carvalho de Melo
Departamento de Saúde Universidade Estadual de Santa Cruz, Ilhéus, Bahia, Brasil.
ORCID: https://orcid.org/0009-0008-0816-3783

[7] Gustavo Magno Baptista
Clínica Médica e de Pneumologia, Itabuna, Bahia, Brasil.
ORCID: https://orcid.org/0000-0001-8462-1098

Received in: 20-11-2024
Reviewed in: 06-12-2024
Accepted in: 20-12-2024

Competing Interests: None declared.

Corresponding Author:
Luís Jesuino de Oliveira Andrade
Universidade Estadual de Santa Cruz - Campus Soane Nazaré de Andrade, Rod. Jorge Amado, Km 16 - Salobrinho, Ilhéus - BA, 45662-900.
E-mail: luis_jesuino@yahoo.com.br

DOI: 10.29327/2413063.22.1-9

Objective: To examine the correlation between insulin resistance (IR) and the severity of sleep apnea (SA), as well as the potential impact of IR on pulmonary function. **Methods**: A cross-sectional analysis was conducted on 72 individuals diagnosed with SA. Demographic data, fasting blood glucose, triglycerides, and glycated hemoglobin were collected. IR was assessed using the triglyceride glucose index (TyG index). Polysomnography and spirometry were performed. Logistic regression analysis was employed to evaluate the association between IR, SA severity, and pulmonary function. **Results:** The study population consisted of 37 females and 35 males with a mean age of 45.31 years. IR was present in 66% of participants. The mean Epworth sleepiness score was 12.89 ± 4.54. The apnea-hypopnea index (AHI) revealed 19.40% normal, 30.60% mild, 27.80% moderate, and 22.20% severe. A significant association was found between IR and both Epworth score (PR 60.50%, OR 1.243, P = 0.0001) and AHI (PR 65.50%, OR 4.750, P = 0.014). However, no significant association was observed between IR and mild AHI. **Conclusion:** This study demonstrates a significant association between IR and the severity of SA, particularly moderate and severe AHI. These results underscore the importance of considering IR as a potential risk factor for SA and suggest the possibility of pulmonary IR in situ.
Keywords: Insulin resistance, Sleep apnea; Pulmonary function; TyG index.

Objetivo: Examinar a correlação entre resistência insulínica (RI) e a gravidade da apneia do sono (AS), bem como o impacto potencial da RI na função pulmonar. **Métodos**: Foi realizada uma análise transversal com 72 indivíduos diagnosticados com AS. Dados demográficos, glicemia de jejum, triglicerídeos e hemoglobina glicada foram coletados. A RI foi avaliada utilizando o índice triglicerídes-glicose (índice TyG). Foram realizadas polissonografia e a espirometria. A análise de regressão logística foi empregada para avaliar a associação entre RI, gravidade da AS e função pulmonar. **Resultados:** A população do estudo consistiu em 37 mulheres e 35 homens, com idade média de 45,31 anos. A RI esteve presente em 66% dos participantes. A média do escore de sonolência de Epworth foi de 12,89 ± 4,54. O índice apneia-hipopneia (IAH) revelou 19,40% de normal, 30,60% leve, 27,80% moderada e 22,20% grave. Foi encontrada uma associação significativa entre a RI e o escore de Epworth (PR 60,50%, OR 1,243, P = 0,0001) e o IAH (PR 65,50%, OR 4,750, P = 0,014). No entanto, nenhuma associação significativa foi observada entre RI e IAH leve. **Conclusão**: Este estudo demonstra uma associação significativa entre a RI e a gravidade da AS, particularmente nos casos de IAH moderado e grave. Esses resultados destacam a importância de considerar a RI como um possível fator de risco para a AS e sugerem a possibilidade de RI pulmonar in situ.
Descritores: Resistência à insulina, Apneia do sono, Função pulmonar, Índice TyG.

INTRODUCTION

Pulmonary insulin resistance (IR) refers to the decreased responsiveness of lung tissues to insulin's effects, has emerged as a focal point of respiratory research. While the presence of insulin receptors within the lungs underscores the direct influence of insulin on pulmonary function, IR compromises these effects, leading to impaired lung performance[1]. The mechanisms underlying pulmonary IR remain an active area of investigation, although several factors have been implicated in its pathogenesis. Chronic inflammation, a hallmark of numerous diseases, has been consistently linked to IR in various organs, including the lungs. Inflammatory mediators, released in response to chronic inflammation, can disrupt insulin signaling pathways, thereby promoting resistance[2]. Oxidative stress, another potential contributor to pulmonary IR, arise from an imbalance between the production of reactive oxygen species and the body's antioxidant defenses. This oxidative stress can interfere with insulin signaling and impair lung function. Environmental factors such as exposure to pollutants and smoking, both of which are known to elevate the risk of respiratory diseases, can contribute to oxidative stress and, consequently, pulmonary IR[3].

The expression of insulin receptors within pulmonary tissue suggests a direct link between insulin signaling and lung health. Impaired IR has been implicated as an independent risk factor for the development of respiratory morbidities[4].

Sleep apnea (SA), a sleep-related disorder characterized by recurrent episodes of upper airway obstruction leading to intermittent hypoxia, has been increasingly recognized as a risk factor for a multitude of comorbidities, including cardiovascular disease, cerebrovascular disease, dementia, and metabolic syndrome. IR has been implicated as a key pathogenic mechanism linking SA to its associated comorbidities[5]. Consequently, there has been a concerted effort to identify accurate and accessible methods for assessing IR. Among the various indices employed, the triglyceride glucose (TyG) index has emerged as a convenient and cost-effective surrogate marker for IR. Its diagnostic and prognostic value has been shown to be comparable to more established methods such as the homeostasis model assessment of IR (HOMA-IR) and the hyperinsulinemic-euglycemic clamp, which is considered the gold standard for IR assessment[6].

The systemic nature of IR can manifest in the respiratory system, leading to a heightened susceptibility to respiratory diseases. Pulmonary IR can exacerbate disease severity and may limit the effectiveness of usual therapeutic approaches. This study aims to explore the relationship between the lung and IR. By investigating the correlation between pulmonary IR and SA, we seek to elucidate the role of the lung as a metabolic organ.

MATERIAL AND METHODS

Study Design and Participants:

This study included a cross-sectional analysis of 72 participants with a clinical diagnosis of SA. The study protocol was approved by the Ethics Committee.

Clinical and Laboratory Assessments:

Baseline demographic information, including age, gender, and body mass index, was collected. Fasting blood samples were obtained from each participant for comprehensive laboratory evaluation. Serum levels of fasting glucose, triglycerides, and glycated hemoglobin were measured using standardized laboratory methods.

Assessment of Insulin Resistance

The IR was evaluated using the TyG index and, representing a reliable threshold for predicting the onset of diabetes mellitus and aligning with the hyperglycemic-hyperinsulinemic clamp method (gold standard).

The TyG index, calculated as the natural logarithm of the product of fasting triglycerides (mg/dL) and fasting glucose (mg/dL) divided by 2: Ln[fasting triglycerides (mg/dL) fasting glucose (mg/dL)/2]. A TyG index value of 4.49 serves as a benchmark for identifying IR[7].

Overnight Polysomnography Assessment

A multidisciplinary LAMARCK SC810 polysomnograph was employed, featuring 24 amplifier channels, a 16-bit analog-to-digital converter resolution, and a sampling rate of 1024 samples per second per channel. This device concurrently assessed the following parameters: electroencephalography, electrooculography, electromyography, electrocardiogram, respiratory channels, straps, position sensors, and pulse oximetry.

Spirometry

A Koko PFT System nSpire Health 2010 spirometer was utilized, employing disposable nSpire filters. Patients were instructed to perform a forced vital capacity (FVC) maneuver. This involves a maximal inspiration followed by a maximal forced expiration. The following

parameters were assessed: FVC, forced expiratory volume in one second (FEV1), and the FEV1/FVC ratio, all expressed in liters or as a percentage.

After the initial three FVC maneuvers, patients were administered 400 micrograms of salbutamol via inhaler and allowed to rest for 20 minutes before repeating the procedure. This test allows for the detection of obstructive diseases (such as asthma and chronic obstructive broncho-pulmonary disease) and restrictive diseases (such as interstitial lung diseases, chest wall restrictions, or obesity-induced restrictions). The bronchodilator challenge reveals bronchoreversibility, a characteristic feature of obstructive diseases, particularly asthma.

Statistical Analysis

Descriptive statistics were summarized as mean ± standard deviation or median (interquartile range) for continuous variables and as percentages for categorical variables. The relationship among IR, pulmonary function, and SA severity was evaluated using logistic regression analysis, adjusting for potential confounding factors. Statistical significance was considered at a P-value threshold of less than 0.05.

Ethical Considerations

This study adhered to the ethical principles outlined in the Declaration of Helsinki. The study protocol was approved by the National Commission for Research Ethics (Opinion number: 2,464,513) in Brazil, and informed consent was obtained from all participants prior to their involvement in the study. Strict confidentiality of personal information was maintained throughout the study, and all data were analyzed and reported in an aggregated and anonymized format.

RESULTS

A sample of 72 individuals underwent a comprehensive assessment. The group was evenly divided between females (n=37) and males (n=35), with a mean age of 45.31 years. Fasting glucose and triglyceride concentrations were measured, revealing mean values of 106.90 mg/dL and 124.84 mg/dL, respectively. The prevalence of IR, as determined by the TyG index, was substantial, affecting 66% of the cohort (**Table 1**).

The mean absolute Epworth Sleepiness Scale (ESS) was 12.89 ± 4.54 (probability of dozing 1-24) (**Graph 1**). The apnea-hypopnea index (AHI) revealed 19.40% (14/72) normal, 30.60% (22/72) mild, 27.80% (20/72) moderate, and 22.20% (16/72) severe AHI (**Graph 2**).

Table 1. Demographic and biochemical date.

Gender	Females: 37 (51.40%) Males: 35 (48.60%)
Age (years)	45.31 ± 13.72
Fasting glucose	106.90 ± 23.24
Tryglicerides	124.84 ± 66.63
TyG index	4.64 ± 0.30

Graph 1. Absolute Epworth.

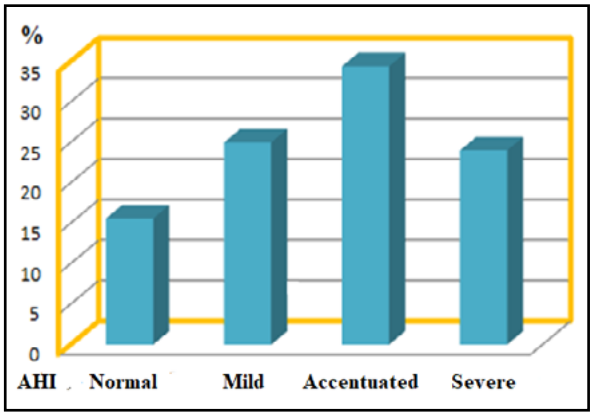

Graph 2. Apnea-hypopnea index.

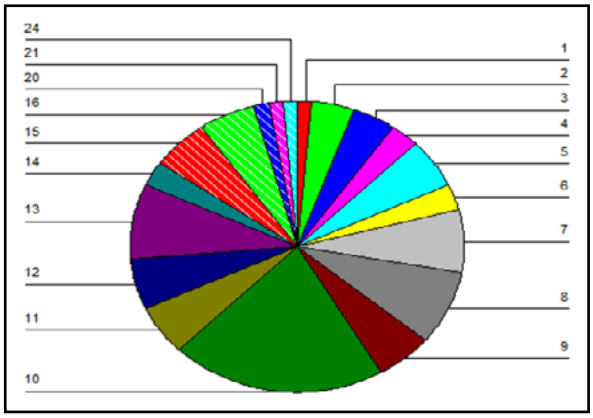

A prevalence ratio (PR) of 60.50% (OR 1.243, 95% CI: 0.479-3.225) was found between excessive daytime sleepiness, EES and IR. This association was statistically significant (P = 0.0001).

There was a significant correlation between absolute AHI and IR (P = 0.013). Similarly, a significant association was observed between AHI ≥ 5 and IR (P = 0.014), with a PR of 65.50% (OR 4.750, 95% CI: 1.321-17.079). Although a PR of 54.50% (OR 0.800, 95% CI: 0.291-2.201) was found between mild AHI and IR, this association was not statistically significant. Moderate AHI was significantly associated with IR (P = 0.020), with a PR of 70.00% (OR 2.000, 95% CI: 0.665-6.013).

A similar significant association was found between severe AHI and IR (P = 0.020), with a PR of 75.00% (OR 2.600, 95% CI: 0.747-9.052) (**Table 2**).

Table 2. Association between AHI and IR.

Association	Prevalence ratio (%)	Estimated risk (OR)
IAH ≥ 5 / IR	65.50	4.750 (1.321-17.070)
IAH Leve / IR	54.50	0.800 (0.291-2.201)
IAH Moderada / IR	70.00	2.000 (0.665-6.013)
IAH Severa / IR	75.00	2.600 (0.747-9.052)

Oxygen Desaturation Index (ODI) showed that oxygen desaturation ≤ 90% was significantly associated with IR (P = 0.001).

A logistic regression analysis was conducted to investigate whether IR was a risk factor for AHI. After adjusting for gender and age, the TyG index was significantly associated with AHI (OR 5.75, 95% CI 2.9-15.00, P = 0.021).

DISCUSSION

This study provides evidence supporting the association between IR and SA severity. Our results highlight the potential for pulmonary IR to play a important role in the development and progression of SA. The pulmonary IR has garnered significant attention in respiratory research due to its impact on lung function. The presence of insulin receptors in the lungs highlights the direct influence of insulin, but IR hampers this response, leading to compromised pulmonary performance. This study establishes a link between IR and the severity of SA, especially in cases of moderate and severe AHI. Thus, these results emphasize the importance of recognizing IR as a potential contributing factor to SA risk and suggest the plausibility of localized pulmonary IR.

TyG index can serve as a practical alternative of IR measurement, and previous studies showed that a higher TyG index showed a higher risk of obstructive SA[8]. Chronic intermittent hypoxia, a hallmark pathophysiological consequence of SA, is a primary mechanism underlying the development of IR[9]. Additionally, sleep fragmentation and deprivation may also contribute to the pathogenesis of IR in this context[10]. Moreover, genetic and epigenetic factors play a significant role in modulating the relationship between the TyG index and SA[11]. Our study evaluated the correlation between IR, using the TyG index, and SA. We employed logistic regression analysis to investigate whether IR was a risk factor for SA, adjusted for age and gender. Our findings revealed a significant association between the TyG index and SA.

The ESS, a self-reported questionnaire designed to gauge the propensity for napping during routine activities, has become the gold standard for quantifying daytime sleepiness in clinical and research settings[12]. The ESS is a concise, self-administered questionnaire comprising eight items, designed to quantify daytime somnolence across various levels of arousal. With a total score ranging from 0 to 24, a score of 10 or greater is indicative of excessive daytime sleepiness, a clinical hallmark of numerous sleep disorders.[(13)] Our study demonstrated a significant association between the ESS and IR, independent of gender and age. The ESS has been widely employed to assess subjective daytime sleepiness in other studies[14].

The AHI, calculated as the sum of hypopneas and apneas per hour of sleep, is the gold standard for quantifying the severity of SA. AHI values categorize SA into mild (5-14 events/h), moderate (15-29 events/h), and severe (>30 events/h) categories[15]. Hypertriglyceridemia is strongly linked to IR and can mask the underlying impact of AHI on insulin sensitivity. The lipolytic action of insulin, coupled with increased sympathetic tone induced by arousals and intermittent hypoxia associated with SA, contributes to the development of dyslipidemia and further exacerbates IR[16]. Our findings align with a growing body of literature that underscores the strong association between SA, as quantified by the AHI and IR. Consistent with previous studies[17,18], we observed a correlation between increasing AHI severity and the frequency of IR. The significant positive association between moderate and severe AHI and IR, in particular, highlights the potential clinical implications of this relationship.

The ODI is calculated as the number of oxygen desaturations of ≥3% (over the last 120 seconds) that lasts for at least 10 seconds per hour of sleep, is a commonly used metric in sleep medicine. However, the ODI has several limitations, including its reliance on an arbitrary desaturation threshold and its inability to accurately reflect the severity or frequency of hypoxic events. Furthermore, the ODI may be influenced by factors such as arousal thresholds and the presence of underlying medical conditions[19]. Our study demon-

strated a clinically significant link between an ODI of 10 or more events per hour and IR.

Thus, our study underscores the relationship between IR and SA, reinforcing the notion that pulmonary IR may play a pivotal role in the development and progression of this disorder. The presence of insulin receptors within the lung tissue highlights the organ's direct susceptibility to insulin's influence. However, impaired insulin sensitivity within the lungs can lead to compromised pulmonary function, ultimately contributing to the severity of SA. The significant association observed between IR, as assessed by the TyG index, and SA severity, particularly in cases of moderate and severe AHI, further supports this hypothesis. These results emphasize the importance of considering IR as a potential risk factor for SA and suggest the need for a more comprehensive approach to managing this condition, encompassing both respiratory and metabolic aspects.

CONCLUSION

This study demonstrates a significant association between IR and the severity of SA, particularly moderate and severe AHI. These results emphasize the importance of considering IR as a potential risk factor for SA and underscore the need for a more comprehensive approach to managing this condition, encompassing both respiratory and metabolic aspects. Thus, our results highlight the importance of considering IR as a potential risk factor for SA and suggest the possibility of pulmonary IR in situ.

REFERENCES

1. Sagun G, Gedik C, Ekiz E, Karagoz E, Takir M, Oguz A. The relation between insulin resistance and lung function: a cross sectional study. **BMC Pulm Med**. 2015;15:139. https://doi.org/10.1186/s12890-015-0125-9.
2. Karlina R, Flexeder C, Musiol S, Bhattacharyya M, Schneider E, Altun I, et al. Differential effects of lung inflammation on insulin resistance in humans and mice. **Allergy**. 2022;77(8):2482-2497. https://doi.org/10.1111/all.15226.
3. Haberzettl P, O'Toole TE, Bhatnagar A, Conklin DJ. Exposure to Fine Particulate Air Pollution Causes Vascular Insulin Resistance by Inducing Pulmonary Oxidative Stress. **Environ Health Perspect**. 2016;124(12):1830-1839. https://doi.org/10.1289/EHP212.
4. Shapiro DL, Livingston JN, Maniscalco WM, Finkelstein JN. Insulin receptors and insulin effects on type II alveolar epithelial cells. **Biochim Biophys Acta**. 1986;885(2): 216-20. https://doi.org/10.1016/0167-4889(86)90091-1.
5. Ercolano E, Bencivenga L, Palaia ME, Carbone G, Scognamiglio F, et al. Intricate relationship between obstructive sleep apnea and dementia in older adults. **Geroscience**. 2024;46(1):99-111. https://doi.org/10.1007/s11357-023-00958-4.
6. Luo P, Cao Y, Li P, Li W, Song Z, Fu Z, et al. TyG Index Performs Better Than HOMA-IR in Chinese Type 2 Diabetes Mellitus with a BMI < 35 kg/m2: A Hyperglycemic Clamp Validated Study. **Medicina (Kaunas)**. 2022;58(7):876. https://doi.org/10.3390/medicina58070876.
7. Guerrero-Romero F, Simental-Mendía LE, González-Ortiz M, Martínez-Abundis E, Ramos-Zavala MG, Hernández-González SO, et al. The product of triglycerides and glucose, a simple measure of insulin sensitivity. Comparison with the euglycemic-hyperinsulinemic clamp. **J Clin Endocrinol Metab**. 2010;95(7):3347-51. https://doi.org/10.1210/jc.2010-0288.
8. Kang HH, Kim SW, Lee SH. Association between triglyceride glucose index and obstructive sleep apnea risk in Korean adults: a cross-sectional cohort study. **Lipids Health Dis**. 2020;19(1):182. https://doi.org/10.1186/s12944-020-01358-9.
9. Lindberg E, Theorell-Haglöw J, Svensson M, Gislason T, Berne C, Janson C. Sleep apnea and glucose metabolism: a long-term follow-up in a community-based sample. **Chest.** 2012;142(4):935-942. https://doi.org/10.1378/chest.11-1844.
10. Mesarwi O, Polak J, Jun J, Polotsky VY. Sleep disorders and the development of insulin resistance and obesity. **Endocrinol Metab Clin North Am**. 2013;42(3):617–34. https://doi.org/10.1016/j.ecl.2013.05.001.
11. Tramunt B, Smati S, Grandgeorge N, Lenfant F, Arnal JF, Montagner A, et al. Sex differences in metabolic regulation and diabetes susceptibility. **Diabetologia**. 2020;63(3):453–61. https://doi.org/10.1007/s00125-019-05040-3.
12. Johns MW. A new method for measuring daytime sleepiness: the Epworth sleepiness scale. **Sleep.** 1991;14(6): 540-5. https://doi.org/10.1093/sleep/ 14.6.540.
13. Bulcun E, Ekici M, Ekici A. Disorders of glucose metabolism and insulin resistance in patients with obstructive sleep apnoea syndrome. **Int J Clin Pract**. 2012;66(1):91-7. https://doi.org/10.1111/j.1742-1241.2011.02795.x.
14. Barceló A, Barbé F, de la Peña M, Martinez P, Soriano JB, Piérola J, et al. Insulin resistance and daytime sleepiness in patients with sleep apnoea. **Thorax**. 2008;63(11):946-50. https://doi.org/10.1136/thx.2007.093740.
15. Blekic N, Bold I, Mettay T, Bruyneel M. Impact of Desaturation Patterns versus Apnea-Hypopnea Index in the Development of Cardiovascular Comorbidities in Obstructive Sleep Apnea Patients. **Nat Sci Sleep**. 2022;14:1457-1468. https://doi.org/10.2147/NSS.S374572.
16. Vacelet L, Hupin D, Pichot V, Celle S, Court-Fortune I, Thomas T, et al. Insulin Resistance and Type 2 Diabe-

tes in Asymptomatic Obstructive Sleep Apnea: Results of the PROOF Cohort Study After 7 Years of Follow-Up. **Front Physiol**. 2021;12:650758. https://doi.org/10.3389/fphys.2021.650758

17. Huang T, Sands SA, Stampfer MJ, Tworoger SS, Hu FB, Redline S. Insulin Resistance, Hyperglycemia, and Risk of Developing Obstructive Sleep Apnea in Men and Women in the United States. **Ann Am Thorac Soc**. 2022;19(10):1740-1749. https://doi.org/10.1513/AnnalsATS.202111-1260OC
18. Michalek-Zrabkowska M, Macek P, Martynowicz H, Gac P, Mazur G, Grzeda M, et al. Obstructive Sleep Apnea as a Risk Factor of Insulin Resistance in Nondiabetic Adults. **Life (Basel)**. 2021;11(1):50. https://doi.org/10.3390/life11010050
19. Ioachimescu OC. Obstructive sleep apnoea, oxygen desaturation and hypoxic burden: pebble, rock or boulder? **Respirology.** 2024;29(9):761-764. https://doi.org/10.1111/resp.14801

OPINION IN REAL WORLD *OPINIÃO NO MUNDO REAL*

DIETARY FLEXIBILITY AS A STRATEGY FOR BETTER TREATMENT ADHERENCE IN PATIENTS WITH TYPE 1 DIABETES MELLITUS

A FLEXIBILIDADE NA DIETA COMO ESTRATÉGIA PARA MELHOR ADESÃO AO TRATAMENTO EM PACIENTES COM DIABETES MELLITUS TIPO 1

Leticia Fuganti Campos[1]; Katiuci Zorzi Moronte[2]

[1] Leticia Fuganti Campos
Departamento de Nutrição , Endocrinologia e Diabetes - Projeto DOCE - Faculdade Evangélica Mackenzie do Paraná (FEMBPAR) - Curitiba - PR - Brazil.
ORCID: https://orcid.org/0000-0001-9663-1867.

[2] Katiuci Zorzi Moronte
Departamento de Psicologia, Endocrinologia e Diabetes - Projeto DOCE, Faculdade Evangélica Mackenzie do Paraná (FEMPAR) - Curitiba - PR - Brazil
ORCID: https://orcid.org/0000-0002-7699-3542

Received in 28-11-2024
Reviewed in : 03-12-2024
Accepted in: 16-12-2024

Corresponding author:
Leticia Fuganti Campos
Rua Dona Alice Tibiriça 455, ap 701 – Curitiba – PR – Brazil
E-mail: le_campos@hotmail.com

DOI: 10.29327/2413063.22.1-11

Current evidence on nutrition in diabetes management highlights the importance of considering dietary flexibility, which takes into account patient preference and may aid adherence on the treatment, what helps achieving glycemic control. In this real-world opinion paper we discuss our experience encouraging flexibility on day-to-day self-management in a type 1 diabetes mellitus service.
Keywords: Nutrition in diabetes, dietary flexibility, adherence to diabetes treatment, carbohydrate counting.

As evidências atuais em nutrição no gerenciamento do diabetes destacam a importância de considerar a flexibilidade na dieta, o que considera a preferência do paciente e pode auxiliar na adesão ao tratamento, ajudando a atingir o controle glicêmico. Neste artigo de opinião do mundo real, discutimos nossa experiência em encorajar a flexibilidade no autogerenciamento diário em um serviço de Diabetes Mellitus tipo 1.
Palavras-chave: Nutrição no diabetes, flexibilidade na dieta, adesão no tratamento do diabetes, contagem de carboidratos.

Diabetes mellitus (DM) is a prevalent chronic disease, and nutrition is a corner stone of diabetes management to prevent/delay complications. Besides the 21st century modern technology, insulin remains the only treatment for type 1 DM (T1DM). An intensive regimen with multiple daily insulin injections guided by self-monitoring of blood glucose and adequate diet has positive effects on postprandial hyperglycemia, which improves glycated haemoglobin (HbA_{1c})[1,2].

The current advice for nutrition in diabetes management should focus on maintaining appropriate body weight, ingesting right amounts of macro and micronutrients, benefits with different dietary patterns and also the lifestyle context. More recent evidence on topics indicates that flexibility can be recommended, which enables patient preference and may aid adherence[2].

Day-to-day self-management is fundamental in T1DM to achieve glycemic control and prevent acute and chronic complications, but active self-management is still suboptimal. Glucose control and diabetes outcomes are still dependent on food choices. Achieving knowledge and the ability for empowering people to actively participate in decision making

regarding their self-care is the best option for optimal self-management[3].

Projeto Doce is a outpatient clinic of the Faculdade Evangélica Mackenzie do Paraná (FEMPAR, Curitiba, Brazil) that provides clinical treatment for T1DM patients since 2005. The project offers multidisciplinary care, with a diabetologist, residents in endocrinology, a dietitian and a psychologist, and is based on the DAFNE study principles, always seeking for a greater flexibility in the diet of patients with T1DM[4].

The DAFNE study[4], which included 169 adults with T1DM and moderate or poor glycaemic control, showed that after 6 months of a course providing the skills to enable patients to replace insulin matching it to desired carbohydrate intake on a meal-by-meal basis resulted in significantly better HbA1c in participants attending training immediately (immediate DAFNE patients, mean 8.4%), than in those acting as waiting list controls (delayed DAFNE patients, 9.4%) (t=6.1, P < 0.0001). The impact of diabetes on dietary freedom was significantly improved in immediate DAFNE patients compared with delayed DAFNE patients (t= −5.4, p<0.0001), as well as the impact of diabetes on overall quality of life (t=2.9, p< 0.01).

In clinical practice we can verify what the studies prove: allowing more flexibility results in more confidence and improves the patient-healthcare relationship. From the moment the patient understands that he/she can do something, the chance of listening the following information increases. And when the patient understands that has this flexibility, he/she feel comfortable to tell that a mistake happened, to try to improve in future situations. If there is no flexibility, there is a higher risk that the patient will not reveal the error.

Today's patients seek information about DM on a daily basis, and find it in many places, what results in patient's empowerment. Detailing explanations of the reason for each conduct and let the patient participates in these decisions are fundamental. In our service, we try to involve the patients to dietary treatments to seek better results.

There is an array of individual factors, such as motivation, self-efficacy, coping skills, locus of control, sense of coherence, psychological characteristics, but also environmental factors, such as social support, and factors related to provider of care, that influence the management and outcomes of T1DM[3].

Carbohydrate counting is considered the ideal way to calculate meal-related insulin doses as it allows greater flexibility in the diet, as it is a major determinant of postprandial blood glucose[5-8]. Carbohydrate counting is a planning strategy that may also reduce the burden of the disease [1,4,9,10].

All guidelines also emphasizes the importance of the individualized nutrition therapy, and to achieve this individualization it is essential to analysis eating habits, to evaluate history of weight management and to consider physical activity, medications in use (doses and times), occurrence and times of hypo and hyperglycemia, as well as to understand patient preferences, access to food and the ability and availability to promote behavioral changes[7,11]. All people with diabetes should be advised to participate in developmentally and culturally appropriate diabetes self-management education and support to facilitate informed decision-making, self-care behaviors, problem-solving, and active collaboration with the health care team[11]. Projeto Doce is well compromised with this ideal, to promote education on diabetes, but always based on individual's needs.

Another important topic is that the incentive for a healthy diet for those with DM is also appropriate to be also recommend for their families and the general population[2]. This is also an important conduct that we adopt in our service, which increases adherence to treatment, and flexibility facilitates the adoption of a single diet for the whole family.

To conclude, the presence of a multidisciplinary team is essential for the successful treatment of patients with T1DM, and the dietitian has a fundamental role in ensuring adherence to treatment to achieve glycemic control. All health care professionals should refer people with diabetes for individualized nutrition therapy provided by a dietitian who is experienced and skilled in providing diabetes-specific, at diagnosis and as needed throughout the life span[11]. The dietitian that works with T1DM should contemplate nutrition therapy with diet flexibly and the individualization in every treatment conduct.

REFERENCES

1. Builes-Montaño CE, Ortiz-Cano NA, Ramirez-Rincón A, Rojas-Henao NA. Efficacy and safety of carbohydrate counting versus other forms of dietary advice in patients with type 1 diabetes mellitus: a systematic review and meta-analysis of randomized clinical trials. **J Hum Nutr Diet** 2022; 35(6):1030-42. Doi: 10.1111/jhn.13017.
2. Reynolds A, Mann J. Update on Nutrition in Diabetes Management. **Med Clin North Am** 2022; 106(5):865-79. Doi: 10.1016/j.mcna.2022.03.003.
3. Barlovic DP, Harjutsalo V, Groop PK. Exercise and nutrition in type 1 diabetes: Insights from the FinnDiane

cohort. **Front Endocrinl** (Lausanne) 2022;13:1064185. doi: 10.3389/fendo.2022.1064185.

4. DAFNE Study Group. Training in flexible, intensive insulin management to enable dietary freedom in people with type 1 diabetes: dose adjustment for normal eating (DAFNE) randomized controlled trial. **BMJ** 2002;325(7367):746. doi: 10.1136/bmj.325.7367.746.
5. Subramanian S, Khan F, Hirsch IB. **New advances in type 1 diabetes**. BMJ 2024;384:e075681. doi: 10.1136/bmj-2023-075681.
6. Builes-Montaño CE, Ortiz-Cano NA, Ramirez-Rincón A, Rojas-Henao NA. Efficacy and safety of carbohydrate counting versus other forms of dietary advice in patients with type 1 diabetes mellitus: a systematic review and meta-analysis of randomised clinical trials. **J Hum Nutr Diet** 2022; 35(6):1030-42. doi: 10.1111/jhn.13017.
7. Scavone GA, Manto A, Potocco D, Gagliardi L et al. Effect of carbohydrate counting and medical nutritional theraopy on glycaemic control in type 1 diabetic subjects: a pilot study. **Diabet Med** 2010;27(4):477-9. doi: 10.1111/j.1464-5491.2010.02963.
8. Campos LF, Hafez VCB, Barreto PA, Gonzalez MC et al. Diretriz BRASPEN de Terapia Nutricional no Diabetes Mellitus. **BRASPEN J** 2020; 35 (Supl 4). doi: 10.37111/braspenj.diretrizDM2020
9. Hayes RL, Garnett SP, Clarke SL, Harkin NM et al. A flexible diet using an insulin to carbohydrate ratio for adolescents with type 1 diabetes – a pilot study. **Clin Nutr** 2012;31(5):705-9. doi: 10.1016/j.clnu.2012.02.012.
10. Bell KJ, Barclay AW, Petocz P, Colagiuri S, Brand-Miller JC. Efficacy of carbohydrate counting in type 1 diabetes: a systematic review and meta-analysis. **Lancet Diabetes Endocrinol**. 2014;2(2):133-40. doi: 10.1016/S2213-8587(13)70144-X.
11. American Diabetes Associations 2025. Facilitating positive health behaviors and well-being to improve health outcomes: Standards of Care in Diabetes 2025. **Diabetes Care** 2025;48(1):286-127. doi:org/10.2337/dc25-S005.

OPINION IN REAL WORLD *OPINIÃO NO MUNDO REAL*

WHAT IS OBSERVED IN PATIENTS WITH TYPE I DIABETES MELLITUS IN A MULTIDISCIPLINARY TEAM

O QUE SE OBSERVA EM PACIENTES COM DIABETES MELLITUS TIPO I EM UMA EQUIPE MULTIDISCIPLINAR

Katiuci Zorzi Moronte, LMHC[1]; Letícia Fuganti Campos, RD, PhD[1]

[1] Leticia Fuganti Campos
Departamento de Endocrinologia e Diabetes - Projeto DOCE - Faculdade Evengélica Mackenzie do Paraná - (FEMPAR) Curitiba - PR - Brazil.
ORCID: https://orcid.org/0000-0001-9663-1867

[2] Katiuci Zorzi Moronte
Departamento de Endocrinologia e Diabetes - Projeto DOCE - Faculdade Evengélica Mackenzie do Paraná - (FEMPAR) Curitiba - PR - Brazil.
ORCID: https://orcid.org/0000-0002-7699-3542

Received in: 06-01-2025
Reviewed in: 1-01-2025
Accepted in: 29-01-2025

Corresponding author:
Katiuci Zorzi Moronte
Rua Waldomiro Antonio Dalarmi, 160, 6, Santa Felicidade, Curitiba – PR
CEP: 82015-700
ORCID: 0009-0004-0469-3673
E-mail: katiuci,zorzi@hotmail.com

DOI: 10.29327/2413063.22.1-12

This article aims to describe, based on the experience of listening to patients with Type 1 Diabetes Mellitus, by a psychology professional, the possible profile of these patients regarding diagnosis and treatment, and the importance of a multidisciplinary team in monitoring these patients and their families.
Keywords: Diagnosis; Type 1 Diabetes Mellitus; Psychology

Este artigo tem como objetivo descrever, a partir da experiência de escuta nos atendimentos a pacientes com Diabetes Mellitus tipo 1, pelo profissional de psicologia, o possível perfil destes pacientes frente ao diagnóstico e tratamento, e a importância de uma equipe multidisciplinar no acompanhamento destes pacientes e seus familiares.
Palavras-chave: Diagnóstico; Diabetes Mellitus tipo 1; Psicologia

We know Type I Diabetes Mellitus T1DM as a condition that affects the pancreas, where it no longer produces the insulin necessary for the body or produces it in small quantities[1,2]. Thus turns this individual dependent on external insulin, that is, insulin-dependent, so that it meets the body's need for insulin, helping the individual to avoid being affected by the possible complications of T1DM [2].

As a psychologist working for almost two years [still in progress] in a multidisciplinary team, within the DOCE Extension Project, registered at the medical specialties outpatient clinic of the Mackenzie Evangelical College of Paraná [FEMPAR], coordinated by Professor Dr. Mirnaluci Paulino Ribeiro Gama, it has been possible to receive different profiles of patients who were diagnosed with T1DM. Some patients have been diagnosed for a few years, while others for a few months.

This multidisciplinary team is made up of an endocrinologist who coordinates the service, six endocrinology residents, a dietitian and a psychologist, who carries out their practice from a psychoanalytic perspective.

The psychologist, as part of the multidisciplinary team, can help to welcome patients diagnosed with T1DM, listen to their suffering, their doubts regarding the diagnosis and treatment, and sometimes listen to their family members, especially when the patient is a minor.

The psychologist, can help to bring greater results to the treatment of patients by being able to treat the individuality of each case, promoting this action through active listening[3]. The work of the psychologist also aims to open a space so that the patient who is suffering has someone to direct their suffering[4].

During the monitoring of patients treated at this outpatient clinic, it has been possible to notice the different patient profiles, that is, the different ways of dealing with the diagnosis. Patients diagnosed more recently sometimes present better acceptance and less difficulty with treatment, while other patients diagnosed more recently sometimes present denial, non-acceptance and difficulty with the treatment of T1DM.

We can think about this difficulty considering that the diagnosis is often experienced by the patient as a trauma [in addition to possibly having arisen after a traumatic event]. Trauma can be understood as something that is outside of the programming, which is not symbolized by the patient[5] .

It is also possible to notice that some parents/guardians have difficulty accepting the diagnosis and managing their child's treatment, which implies some difficulties in the child himself/herself, an insecurity, which is sometimes accompanied by the feeling of "pity" of the parents/guardians, due to the need to measure the child's blood glucose several times a day and the daily and repeated use of insulin, for example.

The lives of patients with T1DM, whether children and their parents/guardians, or adolescents and adults, change from the moment of diagnosis. Important changes occur that must be worked out by both parties, which include changes in diet, insulin routine, among others.

It is difficult for parents when the child deviates from the imaginary ideal; the diagnosis makes this child no longer perfect for the parents, and the child may feel this way, feeling unwanted, thinking that he or she no longer corresponds to what his or her parents expect[6]. This can also lead to feelings of guilt in the patient, for not having corresponded to the expectations of the parents/guardians [when the child has T1DM][7].

Despite the quality of treatment provided by the multidisciplinary team, there is never a guarantee that patients with T1DM will not suffer from the possible discomfort caused by hyper or hypoglycemia. T1DM has a very heavy burden, a burden that can appear as a secondary traumatic aspect for the patient and those around them[8], so it is important that these patients have a space so that their suffering is heard.

REFERENCES

1. Sol, H.; Saeedi , P.; Karuranga , S.; Pinkepank , M.; Ogurtsova , K.; Duncan, B.B.; Stein, C.; Basit , A.; Chan, J.C.N.; Mbanya , J.C.; et al. IDF Diabetes Atlas: Global, regional, and national diabetes prevalence estimates for 2021 and projections to 2045. **Diabetes Res. Clin . Pract.** 2022, *183*, 109119.
2 **Available at: https://diabetes.org.br**
3. Langaro, F.; Santos, AH; Adherence to Treatment in High-Risk Pregnancy**. Psychology: Science and Profession**, Santa Catarina, v. 34, n.3, p. 625-642, 2014.
4. Belaga , G. (2006). Presentation . In G. Belaga (Org.). The generalized urgency: there practice en el hospital (2nd ed., pp. 11-12). **Buenos Aires: Grama Ediciones**.
5. Laurent, E. (2006). Hijos del trauma. In G. Belaga (Org.). The generalized urgency: there practice en el hospital (pp. 23-29, 2nd ed.). **Buenos Aires: Grama Ediciones**.
6. Andrade, AK The child with chronic illness and the hospital: the contributions of psychoanalysis. Analytica, São João del -Rei, v.8, n.14, January/June 2019, p. 1-13.
7. Ferreira, AM. From excess sugar in the blood to lack of sugar in the mouth. GHC Journal – **Moment and Perspective in Health**. 2009;22(25-31).
8. Debray R. Psychosomatic balance and a study in diabetics. **Editora Casa do Psicologia**, SP, 1995. 1st edition.

MINI REVIEW *MINI REVISÃO*

AMERICAN THYROID ASSOCIATION (ATA) 2024 HIGHLIGHTS: CAN WE EXPECT AN IMPROVEMENT ON CLINICAL MANEGEMENT FOR THYROID NODULE DIAGNOSIS IN ADULTS IN 2025?

DESTAQUES DA AMERICAN THYROID ASSOCIATION (ATA) 2024: PODEMOS ESPERAR UM APRIMORAMENTO NO MANEJO CLÍNICO NO DIAGNÓSTICO DO NÓDULO DE TIREOIDE EM ADULTOS EM 2025?

Ricardo Ribeiro Gama

Ricardo Ribeiro Gama
Hospital do Câncer de Barretos. Departamento de Cirurgia de Cabeça e Pescoço - Barretos - SP - Brazil.
ORCID: 0000-0003-4406-8958
LATTES: http://lattes.cnpq.br/3059638519748785
E-mail: ricardorgama@yahoo.com.br

Received in: 17-11-2024
Accepted: 28-11-2024

Corresponding author:
Ricardo Ribeiro Gama
Rua Fábio Junqueira Franco, 195, Bairro Exposição. Barretos CEP 14783-040
SP - Brazil

DOI: 10.29327/2413063.22.1-13

Introduction: The most recent update from the American Thyroid Association (ATA) regarding the clinical management of thyroid nodules in adults was published in 2016. Since then, clinicians and surgeons worldwide have been anticipating the release of new ATA guidelines aimed at improving the clinical management of patients with thyroid nodules. This mini-review addresses key topics including the estimated risk of malignancy based on ultrasound characteristics, fine-needle aspiration (FNA) recommendations, the management of non-biopsied nodules, follow-up strategies for nodules with benign cytology, and preliminary insights into the forthcoming recommendations for indeterminate cytology and molecular testing. **Objective:** The objective of this mini-review is to present selected highlights from the plenary session of the 2024 ATA Congress held in Chicago, with the aim of providing readers with an early overview of anticipated updates in the forthcoming ATA guidelines for the clinical management of thyroid nodules in adults. **Conclusion:** The upcoming 2025 ATA guidelines are expected to offer a comprehensive framework for stratifying all thyroid nodules detected on ultrasound into a malignancy risk scale, with FNA indications based on both risk category and nodule size, while incorporating clinical factors and patient preferences. The updated malignancy risk categories reflect the inclusion of previously unclassified nodules from the 2015 guidelines, aligning more closely with current evidence in the literature.
Key-words: Thyroid Nodule; Clinical Diagnosis; Adult.

Introdução: A última atualização da *American Thyroid Association* (ATA) em relação ao manejo clínico dos nódulos de tireoide em adultos, foi publicada em 2016. Desde então, clínicos e cirurgiões de todo o mundo aguardam a publicação pela ATA de novos guidelines que possam aprimorar o manejo clínico de pacientes com nódulos de tireoide. O que será discorrido ao longo desta *minireview* abrange o risco estimado de malignidade dos nódulos baseado em características ultrassonográficas, as recomendações de citopunção, conduta com nódulos não puncionados, seguimento dos nódulos com citologia benigna e parte do que será publicado sobre conduta com citologia indeterminada e testes moleculares. **Objetivo:** O objetivo desta *mini review* é apresentar parte do que foi mostrado e debatido na plenária do congresso da ATA em Chicago em 2024, com o objetivo de antecipar aos leitores, o que está por vir nas novas diretrizes de manejo clínico do nódulo de tireoide em adultos. **Conclusão:** A nova versão da ATA 2025 procurará abranger todos os nódulos de tireoide ao ultrassom em uma escala de risco de malignidade e a indicação

de citopunção dos mesmos baseada nesta escala e no tamanho do nódulo, em conjunto com fatores clínicos e preferência do paciente. Os novos riscos de malignidade categorizados ao ultrassom, refletem a inclusão de nódulos não previamente classificados na ATA 2015, o que vem de encontro com a literatura.
Descritores: Nódulo da Glândula Tireoide; Diagnóstico Clínico; Adulto.

INTRODUCTION

The most recent American Thyroid Association (ATA) meeting was held in Chicago, USA, during october and november 2024, bringing together thousands of attendees from various medical specialties and allied health fields to discuss updates across multiple areas of thyroidology. One of the most anticipated sessions was the plenary presentation outlining the preliminary version of the forthcoming 2025 ATA guidelines for the clinical management of thyroid nodules in adults, presented by the doctors Susan J. Mandel and Lisa A. Orloff, members of the ATA Thyroid Nodule Task Force.

It was evident that the task force had worked tirelessly to complete the guidelines in time for the event, though final publication was not yet possible. The intention, as emphasized by the presenters, is to release the updated guidelines in 2025, following an extensive review and synthesis of the current literature across the various topics to be addressed. It was explicitly stated that the content presented during the session represented a draft version and remains subject to further revisions before its official publication.

The purpose of this mini-review is to share key elements presented and discussed during the plenary session in Chicago, offering readers an early overview of the expected updates to the ATA guidelines for the clinical management of thyroid nodules in adults. The figures presented herein reflect those shown during the session, with minimal adaptations that preserve the integrity of the original content. All visual materials and information were derived directly from the presentation, and not produced by the author, thus adhering to ethical standards regarding authorship and intellectual contribution.

Throughout the presentation, it was noted that most recommendations are accompanied by a strength of recommendation (strong or conditional) and a corresponding level of evidence (high, moderate, low, or very low). All proposed recommendations are based on a comprehensive literature review conducted up to october 2023, with the exception of molecular testing data, which was updated through july 2024. The majority of the evidence stems from systematic reviews and meta-analyses published in high-impact, peer-reviewed journals, retrieved from multiple scientific databases.

The following sections of this review summarize key aspects regarding the estimated malignancy risk of thyroid nodules based on ultrasound features, fine-needle aspiration (FNA) recommendations, management of non-biopsied nodules, follow-up strategies for nodules with benign cytology, and preliminary insights into the proposed approach to indeterminate cytology and molecular testing.

ATA 2025 objectives and ultrasound-based risk of malignancy (ROM)

The most recent ATA guideline update on the clinical management of adult thyroid nodules was published in 2016[1]. Since then, clinicians and surgeons worldwide have been awaiting the release of new guidelines aimed at optimizing patient care.

The 2016 ATA guidelines introduced a risk of malignancy (ROM) stratification system for thyroid nodules identified on ultrasound, based on sonographic features. This system classified nodules into five categories according to their estimated risk of malignancy: high suspicion (ROM 70–90%), intermediate suspicion (ROM 10–20%), low suspicion (ROM 5–10%), very low suspicion (ROM <3%), and benign (ROM <1%). The indication for FNA was determined by the nodule size in relation to its risk category: for high and intermediate suspicion nodules, FNA was recommended for nodules ≥1 cm; for low suspicion nodules, ≥1.5 cm; for very low suspicion nodules, ≥2 cm or observation; and for benign-appearing nodules, FNA was not indicated. The final decision regarding FNA was guided not only by the ultrasound-based suspicion category, but also by clinical judgment, the presence of suspicious cervical lymph nodes (on clinical examination or ultrasound), and patient preferences. **Figure 1** illustrates this ultrasound-based risk stratification model as published in the 2016 ATA guidelines, modified to include nodule size thresholds corresponding to each malignancy risk category for FNA indication.

The ATA 2025 aims to enhance the ultrasound classification system for thyroid nodules by incorporating all relevant sonographic features and possible combinations, ensuring that every nodule can be accurate-

Figure 1. American Thyroid Association sonographic patterns and risk of malignancy associated with indication of fine-needle aspiration (FNA) based on the largest dimension (cm) of the nodule.

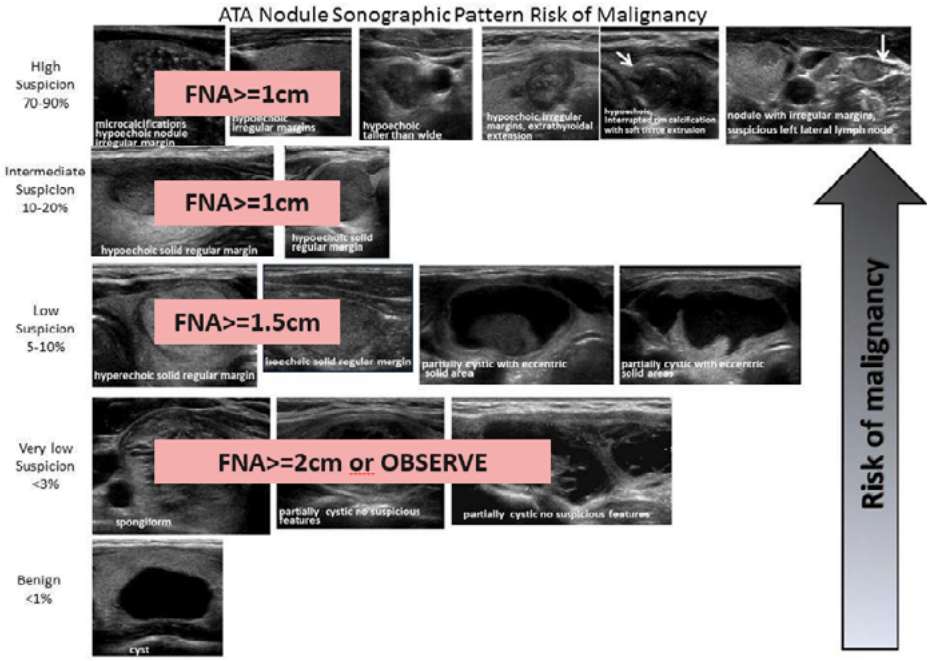

ATA: American Thyroid Association, FNA: fine-needle aspiration. This figure was extracted from ATA 2015 publication (1), with minimal modification by the authors.

ly categorized. Additionally, the ATA intends to provide an updated estimated risk of malignancy (ROM) based on the current literature, expand the photographic atlas, and introduce an intuitive and accessible algorithm that supports stratified ROM assessment through an online application (app).

This algorithm is structured according to a stepwise evaluation based on nodule composition, echogenicity, and the presence or absence of suspicious sonographic features (SSFs). According to ATA 2025, the following are defined as SSFs in solid nodules: irregular margins or halo (spiculated, lobulated, or jagged), a taller-than-wide shape (round configuration), presence of punctate echogenic foci (microcalcifications), or macrocalcifications. Notably, findings such as abnormal cervical lymph nodes or overt extrathyroidal extension will always be classified as high suspicion and are now excluded from the algorithm used for calculating the ROM of thyroid nodules.

Kwon et al.[2] reported in a systematic review and meta-analysis that approximately 7.8% of thyroid nodules could not be classified into any risk category using the 2015 ATA ultrasound criteria. The pooled risk of malignancy for these unclassifiable nodules was 20.3%. Among all unclassifiable nodules, 44% were mixed solid-cystic nodules with suspicious ultrasound features, 29% had undefined composition or echogenicity, and 27% were hyperechoic or isoechoic nodules with suspicious sonographic features.

With the incorporation of previously unclassifiable nodules into the new framework, the ROM distribution has become more continuous and proportionally spread across the 1–100% scale (**Figure 2**). For example, in the 2015 ATA guidelines, nodules with intermediate suspicion were assigned a ROM of 10–20%, while the next higher category, high suspicion, jumped to a ROM of 70–90%, leaving a wide gap without representation in the 21–70% range. In the upcoming 2025 ATA guidelines, this classification is expected to be revised, with intermediate suspicion nodules assigned a ROM of 20–50%, and high suspicion nodules defined as having a ROM greater than 50%.

Diagnostic assessment of solid thyroid nodules on ultrasound

Solid thyroid nodules on ultrasound can be classified as isoechoic, hyperechoic, hypoechoic, or markedly hypoechoic. Hypoechoic and markedly hypoechoic nodules are associated with a higher likelihood of malignancy. Some nodules may exhibit mixed echogenicity, in which case the dominant echogenicity should be used for classification.

Figure 2. Thyroid nodule risk of malignancy (ROM) according to ATA 2015 and ATA 2025.

BENIGN – ATA 2015 (<1%) ---------- **ATA 2025 (<1%)**

VERY LOW SUSPICION– ATA 2015 (<3%) ---------- **ATA 2025 (<3%)**

LOW SUSPICION– ATA 2015 (5-10%) ---------- **ATA 2025 (3-20%)**

INTERMEDIATE SUSPICION- ATA 2015 (10-20%) ---------- **ATA 2025 (20-50%)**

HIGH SUSPICION– ATA 2015 (>70-90%) ---------- **ATA 2025(>50%)**

ATA: American Thyroid Association. Adapted from ATA 2024 presentation.

A key distinction between the 2015 and 2025 ATA guidelines regarding echogenicity-based classification lies in the integration of echogenicity with the presence or absence of suspicious sonographic features (SSFs). For example, under the 2015 ATA guidelines, a hypoechoic nodule without any SSFs was classified as having an intermediate risk of malignancy (ROM 10–20%). However, under the 2025 ATA framework, this same nodule must exhibit at least one SSF to be considered intermediate risk, otherwise, it is reclassified as low risk, with an adjusted ROM range of 3–20%. To classify a hypoechoic nodule as high suspicion in the 2025 ATA model, it must present two or more SSFs, corresponding to a ROM >50%.

Hyperechoic and isoechoic nodules, which were previously considered low risk (ROM 5–10%) under the 2015 guidelines, remain in the low-risk category but with a revised ROM of 3–20%. Importantly, in the 2025 ATA guidelines, these nodules may now be reclassified as intermediate risk if they are associated with one or more SSFs, resulting in a ROM of 20–50%, a classification not previously defined in the 2015 guidelines.

Markedly hypoechoic nodules with one or more SSFs will be classified as high suspicion (ROM >50%), while those without any SSFs will remain classified as intermediate suspicion, but with an updated ROM range from 10–20% (ATA 2015) to 20–50% (ATA 2025).

Mixed echogenicity nodules without SSFs, previously unclassified, will now be categorized as low suspicion with a ROM of 3–20% (**Figure 3**).

Diagnostic assessment of cystic thyroid nodules on ultrasound

Cystic thyroid nodules can be categorized as completely cystic (which are benign, with a ROM <1%), spongiform, or partially cystic (**Figure 3**).

Spongiform or microcystic nodules are defined by the presence of interspersed solid components within microcystic areas. When more than 50% of the nodule volume is composed of microcystic spaces, the nodule is classified as spongiform. If less than 50% is microcystic and the remainder is cystic, it is considered microcystic. Although this classification may appear somewhat ambiguous, it reflects the criteria presented at the 2024 ATA conference and may be subject to revision in the final guideline version.

In the 2015 ATA guidelines, spongiform and microcystic nodules were considered very low suspicion, with a ROM <3%, a classification supported by high-level scientific evidence. In the 2025 ATA revision, these nodules will remain in this category unless they exhibit one or more of the following features: irregular margins or halo, or the presence of macrocalcifications[3]. In such cases, they will be reclassified as low suspicion with an adjusted ROM of 3–20%. However, this proposed change, aimed at including previously unclassified nodules, is supported by low-level scientific evidence.

Partially cystic (non-spongiform) nodules are considered high suspicion (ROM >50%) when they exhibit strong predictors of malignancy, such as irregularity at the solid–cystic interface (e.g., acute-angled, or jagged soft tissue protrusions or spiculated projections into the cystic component) and presence of echogenic foci, and/or macrocalcifications within the solid component. These findings are particularly suggestive of cystic papillary thyroid carcinoma and were not previously classified in the 2015 guidelines.

Importantly, typical SSFs used for solid nodules (such as margin irregularity or a taller-than-wide shape) should not be applied to partially cystic nodules when estimating ROM. Other partially cystic nodules, regardless of the presence of features such as macrocalcification or irregular external margins with lobulated interface with the cystic portion, or isolated angulated solid components, or lobulated solid part

with echogenic foci, are still classified as low or very low suspicion. However, their ROM has been adjusted from 5–10% (ATA 2015) to 3–20% (ATA 2025), since many of these nodules were previously unclassifiable. Despite this revision, the level of evidence supporting the new ROM estimates in this context remains low to very low.

Diagnostic assessment of nodules with unassessable composition due to dense peripheral calcifications

Nodules in which composition cannot be assessed due to dense peripheral calcifications will be classified as low suspicion (ROM 3–20%) if the calcification rim is thin, regular, and without soft tissue protrusions. When peripheral calcifications are irregular but still without soft tissue protrusion, the nodule will be categorized as intermediate suspicion with a ROM of 20–50%. Finally, nodules with peripheral calcifications that exhibit protrusion into the adjacent soft tissue will be classified as high suspicion, with a ROM >50% (**Figure 3**).

Fine-needle aspiration (FNA) recommendations for thyroid nodules in the ATA 2025 guidelines

Figure 4 outlines the ATA 2025 recommendations for fine-needle aspiration (FNA) of thyroid nodules, based on the estimated ultrasound suspicion category and the corresponding risk of malignancy (ROM). The figure presents the size thresholds for FNA indication and the recommended range of nodule diameter at which FNA may be considered, accompanied by the strength of recommendation and the level of scientific evidence.

The decision to perform FNA at the lower or upper end of the suggested size range should be individualized according to patient-specific clinical features and patient preferences, as detailed in **Figure 5**.

For instance, high-suspicion nodules, defined by the ATA 2025 guidelines as having a ROM >50%, are generally recommended for FNA when they measure ≥1.5 cm in maximum diameter. This recommendation is considered strong and supported by moderate-quality evidence. However, FNA may be considered for nodules as small as 1.0 cm in the presence of specific clinical factors; these include: young age, associated risk factors for thyroid cancer, absence of comorbidities, high-risk sonographic features, incidental detection on FDG-PET, presence of symptoms, posterior or isthmic location, or patient preference to proceed with early diagnostic evaluation rather than prolonged surveillance due to anxiety regarding the possibility of nodule growth.

Follow-up interval and management of non-aspirated nodules smaller than the cutoff value for Fine-Needle Aspiration (FNA)

Figure 6 illustrates the nodules that, due to their suspicion risk on ultrasound, did not reach the recommended size for fine-needle aspiration (FNA). The

Figure 3. Thyroid nodules risk of malignancy (ROM) stratification according to ultrasound nodule composition.

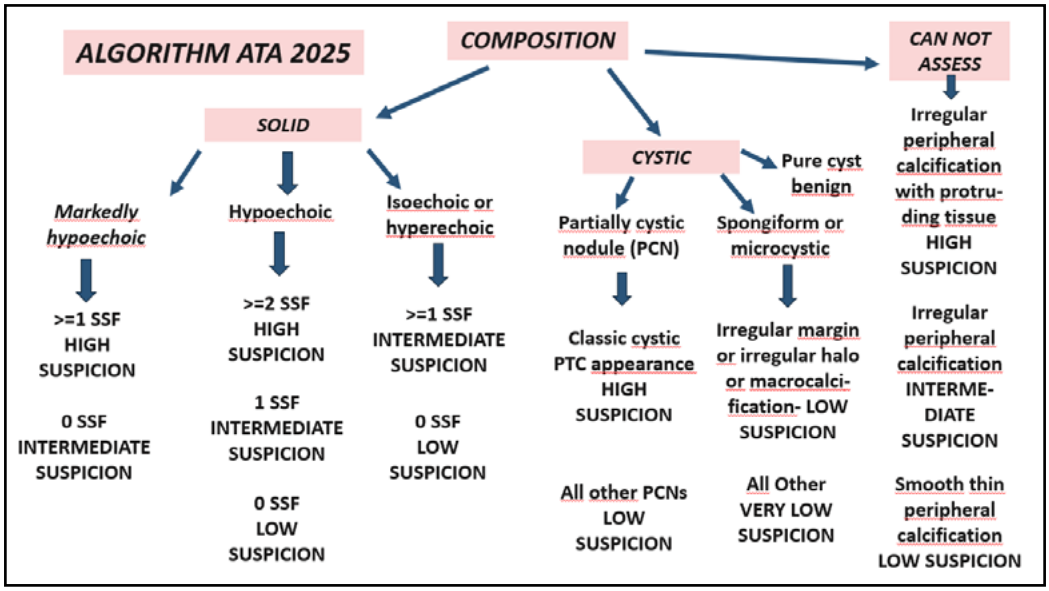

SSF: Solid nodule Suspicious Features; PTC: papillary thyroid carcinoma; PCN: partially cystic nodule, ATA: American Thyroid Association. Adapted from ATA 2024 presentation.

Figure 4. Recommendation of fine-needle aspiration of thyroid nodules based on their size in the largest dimension or size ranges and strenght of recommendation and quality of evidence.

ATA sonographic pattern and risk of malignancy (ROM)	FNA size cut-off (largest dimension) and range to consider FNA (largest dimension)	Strenght of recommendation/ quality of evidence
HIGH SUSPICION(>50%)	>=1.5cm (1-1.5cm)	STRONG / MODERATE
INTERMEDIATE SUSPICION (>20-50%)	>=2cm (1-2cm)	CONDITIONAL / MODERATE
LOW SUSPICION (3-20%)	>=2.5cm (1.5-2.5cm)	CONDITIONAL / MODERATE
VERY LOW SUSPICION (<3%)	No FNA	STRONG / MODERATE
BENIGN (<1%)	No FNA	STRONG / MODERATE

FNA: fine-needle aspiration, ATA: American Thyroid Association. Adapted from ATA 2024 presentation.

Figure 5. Factors influencing decision making for nodule fine-needle aspiration within the recommended nodule size ranges.

FACTORS	FAVORS SMALLER SIZE	FAVORS LARGER SIZE
Age	YOUNGER	OLDER
Personal risk factors for thyroid cancer (irradiation at childhood, genetic syndrome)	PRESENT	ABSENT
Comorbidities	ABSENT	PRESENT
Evidence for sonographic pattern ROM	STRONG	WEAK
FDG or Galio-68 dotatate avidity (incidental finding)	PRESENT	ABSENT
Symptoms attributable to nodule	PRESENT	ABSENT
Nodule location	Isthmus, posterior	OTHER

ROM: risk of malignancy, FDG: fluorodeoxyglucose. Adapted from ATA 2024 presentation.

figure details the ultrasound follow-up intervals and the actions to be taken based on observed variations during this follow-up, along with the strength of the recommendation and the level of scientific evidence. It is evident that many of these actions are based on performing FNA in response to nodule growth. It is important to note that nodule growth is defined as an increase of ≥3 mm in one dimension for nodules with high suspicion on ultrasound, and a 50% increase in nodule volume or a 20% increase in at least two dimensions for nodules with intermediate or low suspicion on ultrasound.

For non-sampled nodules with intermediate or low suspicion on ultrasound that are smaller than the upper cutoff limit for FNA and remain stable in size and ultrasound patterns after 5 years, ultrasound follow-up may be discontinued in the absence of individual high-risk criteria. This ATA recommendation is considered conditional, with very low-quality scientific evidence.

Non-sampled nodules that are classified as high risk on ultrasound should follow active surveillance recommendations for papillary microcarcinoma. This ATA recommendation is considered strong, with moderate-quality scientific evidence.

Figure 6. Surveillance intervals and management of unsampled nodules smaller than the fine-needle aspiration size cut-off and strenght of recommendation and quality of evidence.

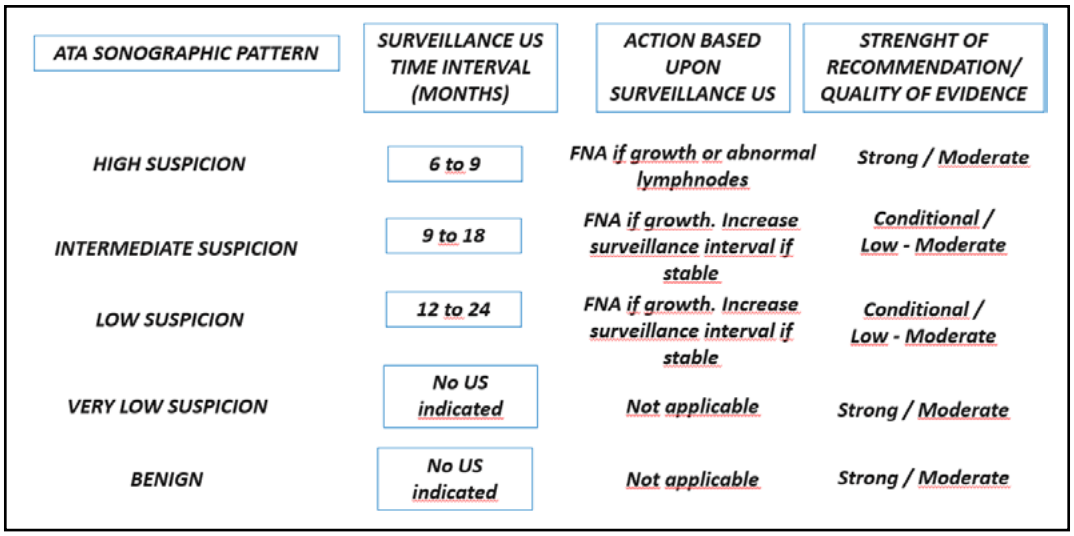

ATA SONOGRAPHIC PATTERN	SURVEILLANCE US TIME INTERVAL (MONTHS)	ACTION BASED UPON SURVEILLANCE US	STRENGHT OF RECOMMENDATION/ QUALITY OF EVIDENCE
HIGH SUSPICION	6 to 9	FNA if growth or abnormal lymphnodes	Strong / Moderate
INTERMEDIATE SUSPICION	9 to 18	FNA if growth. Increase surveillance interval if stable	Conditional / Low - Moderate
LOW SUSPICION	12 to 24	FNA if growth. Increase surveillance interval if stable	Conditional / Low - Moderate
VERY LOW SUSPICION	No US indicated	Not applicable	Strong / Moderate
BENIGN	No US indicated	Not applicable	Strong / Moderate

US: ultrasound, FNA: fine-needle aspiration, ATA: American Thyroid Association. Adapted from ATA 2024 presentation.

Figure 7. Follow-up period for benign cytology nodules and action based on their ultrasound risk of malignancy linked to strenght of recommendation and quality of evidence.

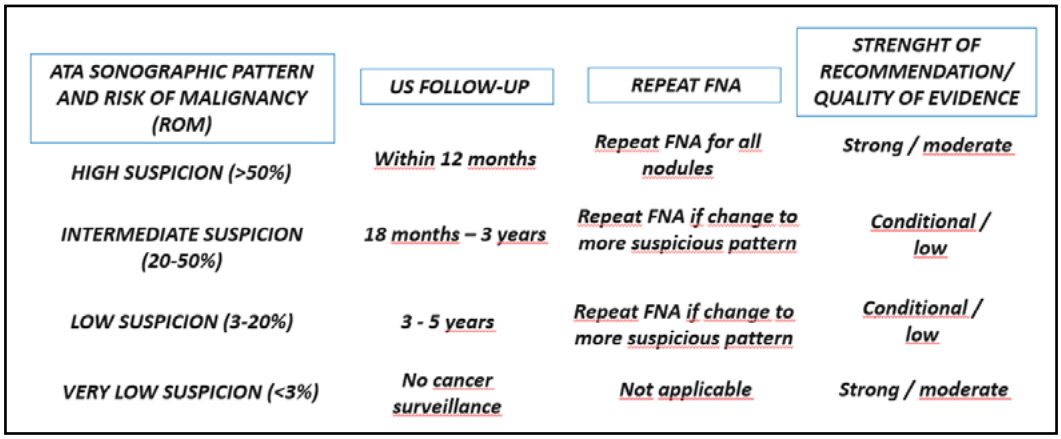

ATA SONOGRAPHIC PATTERN AND RISK OF MALIGNANCY (ROM)	US FOLLOW-UP	REPEAT FNA	STRENGHT OF RECOMMENDATION/ QUALITY OF EVIDENCE
HIGH SUSPICION (>50%)	Within 12 months	Repeat FNA for all nodules	Strong / moderate
INTERMEDIATE SUSPICION (20-50%)	18 months – 3 years	Repeat FNA if change to more suspicious pattern	Conditional / low
LOW SUSPICION (3-20%)	3 - 5 years	Repeat FNA if change to more suspicious pattern	Conditional / low
VERY LOW SUSPICION (<3%)	No cancer surveillance	Not applicable	Strong / moderate

ATA: American Thyroid Association, US: ultrasound, FNA: fine-needle aspiration. Adapted from ATA 2024 presentation.

Follow-up of Nodules with Benign Cytology

In cases of nodules with benign cytology, management should be guided by the ultrasound appearance within the follow-up interval. Nodules that exhibit high suspicion of malignancy on ultrasound should have fine-needle aspiration (FNA) always repeated. Conversely, nodules with intermediate or low suspicion should only be aspirated if there is a change in nodule characteristics toward a more suspicious appearance.

Nodule growth alone should not be used as an indication for repeat FNA[4]. The literature lacks robust evidence to establish a clear link between the growth of nodules with benign cytology and the risk of malignancy. **Figure 7** illustrates the aforementioned points.

Management of indeterminate nodules on Fine-Needle Aspiration (FNA): Bethesda III and IV

Patients whose FNA results are compatible with atypia of undetermined significance (AUS), classified as Bethesda III[5], present a range of management options. These options vary from clinical observation in nodules with a very low suspicion ultrasound pattern to surgery in nodules with high suspicion on ultrasound, nodule growth, or the presence of local compressive symptoms. Decisions regarding management should always be done in collaboration with the patient, ensuring they are informed about the possible approaches, along with their respective advantages

and disadvantages. It is important to note that the risk of malignancy for a Bethesda III nodule is approximately 22% (ranging from 13% to 30%)[5], depending on clinical variables, ultrasound features, cytological architectural and cellular aspects, molecular findings, and the experience of the cytopathologist.

For patients with nodules classified as Bethesda IV (follicular neoplasm) on FNA, management involves either molecular testing or surgery. This recommendation stems from the fact that the malignancy risk for these lesions is more consistent, reaching up to 30% (ranging from 23% to 34%)[5]. Thus, diagnostic clarification is recommended through molecular testing (typically employed to exclude malignancy in nodules with low ultrasound or clinical suspicion) or surgery in cases with higher ultrasound or clinical suspicion. Surgery is also advised when appropriate molecular testing is unavailable, regardless of ultrasound or clinical findings. It is essential to emphasize that the selection of a molecular test in a clinical setting should consider the results and quality of validation studies, as well as publications demonstrating the test's performance in a real-world practice setting that aligns with the specific clinical environment. **Figure 8** details the possible management strategies for Bethesda III and IV nodules, along with the corresponding strength of recommendations and level of evidence.

The preferred surgical approach for Bethesda III or IV nodules (with or without molecular testing) is diagnostic lobectomy for nodules with a high-suspicion ultrasound pattern, any nodule growth pattern, presence of symptoms, or patient preference. Patients should be informed about the possibility of conversion to total thyroidectomy or the subsequent need for completion thyroidectomy if high-risk factors are identified intraoperatively or postoperatively (conditional recommendation / moderate-quality evidence). Potential modifiers for diagnostic lobectomy include substantial contralateral nodular disease, nodule size, coexisting Graves' disease, history of childhood irradiation, family history of thyroid cancer, patient preference, and, if performed, a high-risk molecular test result. It is important to note that total thyroidectomy is indicated when there is evidence of extrathyroidal extension on imaging or intraoperatively, or in the presence of suspicious cervical lymph nodes.

CONCLUSION

It is anticipated that the final version of the ATA guidelines, to be published in the coming months, regarding the clinical management of adult thyroid nodules, will aim to classify all thyroid nodules on ultrasound within a malignancy risk scale. The updated malignancy risk categories reflect the inclusion of previously unclassified nodules from the 2015 ATA guidelines, aligning with current literature. The photographic atlas will be maintained with the addition of a malignancy risk algorithm and the incorporation of FNA indications based on larger nodule size thresholds, as well as range variations on nodule size, considering clinical criteria and patient preference. The new version will also include follow-up intervals

Figure 8. Option strategies for Bethesda III and IV cytology nodules and their respective strenght of recommendation and quality of evidence.

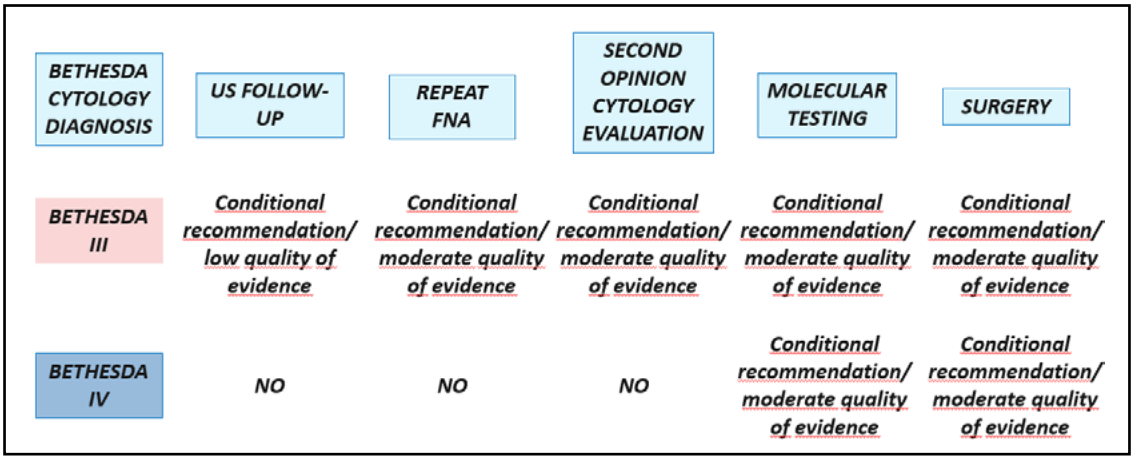

US: ultrasound. Adapted from ATA 204 presentation.
FNA: fine-needle aspiration.

and management strategies, along with guidance for discontinuing follow-up for nodules with benign cytology and for non-aspirated nodules of low or intermediate suspicion that have not reached the size threshold for FNA.

The ATA aims to integrate, in the future, a management strategy in synergy with the American College of Radiology (ACR) and the TIRADS (Thyroid Imaging Reporting and Data System classification)[6]. At present, this integration is not yet feasible, as ATA members believe that the TIRADS classification considers only the ultrasound appearance of the nodule, whereas the ATA's malignancy risk assessment incorporates both ultrasound features and patient clinical and risk factors. Consequently, the members of ATA believe their guidelines have greater potential for practical application when deciding on FNA indication for a given nodule in collaboration with the patient.

In its 2024 presentation, the ATA did not address the following topics: initial evaluation of patients with nodules (including discussions on thyroid nodule screening), FNA techniques and specimen preparation, management of nondiagnostic nodules on FNA, follow-up of benign nodules in molecular tests, and the management of thyroid nodules in specific populations such as older adults, pregnant women, children, and others.

REFERENCES

1. Haugen BR, Alexander EK, Bible KC, Doherty GM, Mandel SJ, Nikiforov YE, et al. 2015 American Thyroid Association Management Guidelines for Adult Patients with Thyroid Nodules and Differentiated Thyroid Cancer: The American Thyroid Association Guidelines Task Force on Thyroid Nodules and Differentiated Thyroid Cancer. **Thyroid.** 2016;26(1):1-133. doi: 10.1089/thy.2015.0020.
2. Kwon D, Kulich M, Mack WJ, Monedero RM, Joyo E, Angell TE. Malignancy Risk of Thyroid Nodules That Are Not Classifiable by the American Thyroid Association Ultrasound Risk Stratification System: A Systematic Review and Meta-Analysis. **Thyroid**. 2023;33(5):593-602. doi:10.1089/thy.2022.0672.
3. Kobaly K, Kim CS, Langer JE, Mandel SJ. Macrocalcifications Do Not Alter Malignancy Risk Within the American Thyroid Association Sonographic Pattern System When Present in Non-High Suspicion Thyroid Nodules. **Thyroid**. 2021;31(10): 1542-1548. doi: 10.1089/ thy. 2021. 0140.
4. Ospina NS, Brito JP, Maraka S, de Ycaza AEE, Rodriguez-Gutierrez R, Gionfriddo MR. Diagnostic accuracy of ultrasound-guided fine needle aspiration biopsy for thyroid malignancy: systematic review and meta-analysis. **Endocrine**. 2016;53(3):651-61. doi: 10.1007/ s12020-016-0921-x.
5. Ali SZ, Baloch ZW, Cochand-Priollet B, Schmitt FC, Vielh P, VanderLaan PA. The 2023 Bethesda System for Reporting Thyroid Cytopathology. **Thyroid**. 2023;33(9):1039-1044. doi: 10.1089/thy.2023.0141.
6. Tessler FN, Middleton WD, Grant EG, Hoang JK, Berland LL, Teefey SA, et al. ACR Thyroid Imaging, Reporting and Data System (TI-RADS): White Paper of the ACR TI-RADS Committee. **J Am Coll Radiol**. 2017;14(5):587-595. doi: 10.1016/j.jacr.2017.01.046.

CASE REPORT *RELATO DE CASO*

A GESTURE OF AFFECTION AND ITS DELETERIOUS OUTCOME: ADULT-CHILD CONTAMINATION BY SEX STEROIDS – A CASE REPORT?

UM GESTO DE CARINHO E SEU DESFECHO DELETÉRIO: CONTAMINAÇÃO ADULTO-CRIANÇA POR ESTERÓIDES SEXUAIS

Lucianna Ribeiro Thá[1]; Caio Yutaka Hayashi[2]; Mirnaluci Paulino Ribeiro Gama[3]

[1] Lucianna Ribeiro Thá
Grupo de Estudos dos Exs. Residentes do Serviço de Endocrinologia e Diabetes - Hospital Universitário Evangélico Mackenzie of Curitiba - PR - Brazil.
ORCID: 0009-0004-0046-7847

[2] Caio Yutaka Hayashi
Serviço de Endocrinologia e Diabetes - Hospital Universitário Evangélico Mackenzie de Curitiba - PR - Brazil.
ORCID: 0009-0000-0550-1435

[3] Mirnaluci Paulino Ribeiro Gama
Serviço de Endocrinologia e Diabetes - Hospital Universitário Evangélico Mackenzie de Curitiba - PR - Brazil - Faculdade Evangélica Mackenzie do Paraná - Brazil.
ORCID: 0000-0601-7639-1579

Received in: 10-01-2025
Reviewed in: 16-01-2025
Accepted in: 24-01-2025

The authors of this work have no conflicts of interest.

Corresponding author:
Lucianna Ribeiro Thá
Unidade de Diabetes do Hospital Universitário Evangélico Mackenzie de Curitiba - PR
Rua Augusto Stelfeld 1908 - Bigorrilho - Curitiba, PR - Brazil. CEP: 80730-50
E- mail:

DOI: 10.29327/2413063.22.1-14

Incidental contamination with sex steroids, particularly testosterone gel, is a rare but significant cause of precocious puberty. This case report details a 7-year-old girl presenting with premature pubarche, initially without other signs of virilization. Despite normal initial exams, persistent pubic hair prompted further investigation. Subsequent evaluations revealed elevated testosterone and dehydroepiandrosterone sulfate (DHEAS), leading to concerns for adrenal tumors. However, imaging and hormonal tests ruled out these pathologies. The source of exposure was ultimately identified as topical testosterone used by the grandmother. Following cessation of exposure, the patient's hormone levels normalized, and breast development regressed. This case highlights the importance of considering exogenous sex steroid exposure in children with isolated premature pubarche, even when initial parental denial is encountered.

Keywords: Premature Pubarche, Sex Steroid Contamination, Testosterone Gel, Childhood Virilization

A contaminação incidental por esteroides sexuais, particularmente gel de testosterona, é uma causa rara, mas significativa, de puberdade precoce. Este relato de caso detalha uma menina de 7 anos apresentando pubarca precoce, inicialmente sem outros sinais de virilização. Apesar dos exames iniciais normais, a persistência de pelos pubianos motivou uma investigação mais aprofundada. Avaliações subsequentes revelaram testosterona e sulfato de deidroepiandrosterona (SDHEA) elevados, levantando preocupações sobre tumores adrenais. No entanto, exames de imagem e hormonais descartaram essas patologias. A fonte de exposição foi finalmente identificada como testosterona tópica usada pela avó. Após a cessação da exposição, os níveis hormonais da paciente normalizaram e o desenvolvimento mamário regrediu. Este caso destaca a importância de considerar a exposição a esteroides sexuais exógenos em crianças com pubarca precoce isolada, mesmo quando ocorre negação inicial por parte dos pais.

Descritores: Pubarca Precoce, Contaminação por Esteroides Sexuais, Gel de Testosterona, Virilização na Infância

INTRODUCTION

Incidental contamination by sex steroids is rare, but an important cause of iso or heterosexual precocious puberty. This diagnosis should be considered in a child with premature pubarche without other features of virilization or isosexual puberty. In the vast majority of cases, especially the

child's parents are not warned and have no idea what may happen with the topical use of sex steroids[1].

Testosterone gel is the most commonly used steroid by both men and women. Its use may be inappropriate or not, and it is often obtained without a prescription. In Brazil, ANVISA (Agência Nacional de Vigilância Sanitária) – the National Health Surveillance Agency, requires, in the package insert, an alert about passive skin-to-skin adult-child contamination. This demonstrates the need for a thorough medical history and insistence by the physician in questioning and explaining the danger of contamination. This would avoid subjecting the child to unnecessary tests with their preparation requirements , like hormonal assays, ultrasounds and radiation from other imaging exams[2].

From 2012 to 2019, 19 articles were reported, totaling 28 cases of contamination through family members[2,3,4,5,6]. Childhood exposure to endogenous sex steroids is associated with the development of precocious puberty and the following pathologies:

- Congenital adrenal hyperplasia
- Adrenal tumors
- McCune-Albright syndrome
- Virilizing ovarian tumors

And much rarer, in males, pathogenic variations of the LHCGR gene leading to familial gonadotropin-independent precocious puberty[2,7].

The most common signs and symptoms are premature pubarche, accelerated growth, advanced bone age, clitoral enlargement (heterosexual) and penile enlargement (isosexual)[2,3].

Testosterone levels, especially in girls, are variable, reaching pubertal levels in most cases in both sexes[4]. However, upon withdrawal of the steroid, laboratory levels fall rapidly. Unfortunately, there may be irreversible changes, such as advanced bone age, which can lead to a decrease in final height[2,3,4,5,6].

CASE DESCRIPTION

Female patient, GDBW, currently 8 years and 3 months old. At 7 years and 7 months old, she started with adrenarche. There was no thelarche or axillary odor. Parents denied the use of testosterone or estrogen gel in the anamnesis of the first consultation. The child is previously healthy. She was born at term, appropriate for gestational age, without complications.

On physical examination, she presented a normal segmental examination. Blood pressure was normal, without acne, without signs of Cushing, and pubertal staging M1P2. Her height was 128.5cm (50th percentile) and weight 27.3kg (50th percentile).

Some complementary exams were requested: complete blood count, fasting glucose, glycated hemoglobin, creatinine, liver function, thyroid function, lipid profile, and vitamin D within normal limits. Adrenal evaluation: DHEAS = 146 µg/dL, 17-OHP 76 ng/dL, basal cortisol = 10.6 µg/dL, total testosterone = 7.3 ng/dL, and androstenedione = 0.3 ng/mL. Bone age 8 years and 6 months.

After 4 months, the child returned for a new evaluation. The mother reported increased pilosity, without other associated complaints. The physical examination showed pubertal progression to M2 P3. Adrenal exams were repeated, and a significant increase in DHEAS and total testosterone levels was observed. The DHEAS result was greater than 1000 µg/dL, and the testosterone was 12 ng/dL. The DHEAS exam was repeated in another laboratory and was 790 µg/dL after several progressive dilutions. Basal LH was measured and found to be 0.2 mUI/mL, FSH 4.3 mUI/mL, and estradiol 14 ng/dL.

Subsequently, a suppression test with 1 g of dexamethasone was performed, which was normal, and a total abdominal CT scan with emphasis on the adrenals, which was also normal. Pelvic ultrasound showed a uterus of 3.5 cm^3, right ovary with 1.4 cm^3, and left ovary with 1.4 cm^3, both of them without a stimulated follicle. There was no advancement of bone age in this period.

After further questioning about the use of hormone gels, the parents reported that the grandmother was using a compounded gel cream containing 2 mg of testosterone, 1 mg of estradiol, and 100 mg of progesterone. She applied the cream upon waking, and the child stayed at the grandmother's house every day in the morning. We hypothesized contamination from the gel cream used by the grandmother. The grandmother stopped using the gel cream immediately.

Two months after stopping use, we repeated the DHEAS, which was 169.7 µg/dL. After another 2 months, there was no increase in the child's pilosity, and the breast regressed. The DHEAS resulted in 144.7 µg/dL (reference value = 108 µg/dL), and the child's bone age at this time is 8 years and 10 months.

DISCUSSION

Our patient's history begins at 7 years and 7 months, prolonging for 1 year until the definitive di-

agnosis. It is known that adrenarche can begin 2 years before puberty, however, the case was investigated at the insistence of the patient's mother. In the first contact with the specialist, she brought exams that were normal. There was nothing important in the history, but the mother insisted on very thick pubic hair. On physical examination, the patient was healthy, bone age compatible with chronological age, and without any signs or symptoms of virilization. Pubertal staging M1 P2.

A return was requested with repetition of the simplest exams. She returned 4 months later with pubertal staging M2 P3, LH normal for age, as well as FSH at the elevated limit of normal for age. Dehydroepiandrosterone sulfate was very elevated, as was testosterone. The increase in DHEAS made us think of an adrenal tumor, however, the clinical picture was normal, without virilization or Cushingoid habitus.

The gold standard test dexametazone suppression, for hypercortisolism, was negative. Adrenal tomography was normal, pelvic ultrasound showed unstimulated and prepubertal ovaries and the uterus volume was borderline for pubertal age, remaining within normal limits (<3cm³).

After we insisted again and the parents vehemently denied the use of testosterone by them once more, they subsequently discovered its use by the child's grandmother. And after the withdrawal of the steroid, the laboratory values of testosterone and DHEAS quickly returned to normal. The breast involuted to M1 and there was no increase in bone age.

In this patient, the only complaint was pubarche; the slight stimulation of the hypothalamic-pituitary axis is due to a priming effect by the steroid on the hypothalamus, so much so that withdrawal triggered breast involution[2,3,4,5,6,7]. Breast growth may also have been caused by the estrogen contained in the formulation used by the grandmother. It is also questioned whether estrogen was the protective factor against virilization by testosterone.

On rare occasions, it has been reported that contamination with testosterone can mask the diagnosis of adrenal tumors[8]. Our patient will be observed annually given the very high values of DHEAS and testosterone.

CONCLUSION

A child presenting with premature pubarche, even in the absence of other clinical signs of virilization, warrants thorough investigation for potential exposure to exogenous sex steroids. Early identification and cessation of exposure are crucial to prevent irreversible consequences such as accelerated bone maturation and compromised final height.

Increased awareness of the potential for inadvertent sex steroid exposure in children is crucial for early detection and intervention. Healthcare providers should maintain a high index of suspicion for this etiology in cases of premature pubarche, even when initial parental denial is encountered.

REFERENCES

1. Yakovenko V, Choukair D, Duffert C, Mittnacht J, Klose D and Bettendorf M Pseudo-Precocious Puberty in Children Triggered by Incidental Transdermal Contamination with Topical Sex Steroids Through Parents ESPE2019 Poster Category 2 Sex Differentiation, Gonads and Gynaecology or Sex Endocrinology **ESPE Abstracts** 2019; **92**, P2-269
2. Svetlana Azova, Joseph Wolfsdorf Precocious sexual development in a male toddler caused by unrecognized transdermal exposure to testosterone: case report and review of the literature **J Pediatr Endocrinol Metab**. 2021 Mar 3;34(5):675-678.
3. Garcia Garcia E, Jimenez Varo I. Potential consequences in children of a testosterone gel used by their fathers. **Endocrinol Diabetes Nutr** 2017;64:278–80.
4. Martinez-Pajares JD, Diaz-Morales O, Ramos-Diaz JC, Gomez-Fernandez E. Peripheral precocious puberty due to inadvertent exposure to testosterone: case report and review of the literature. **J Pediatr Endocrinol Metab** 2012;25:1007–12
5. 3. Brachet C, Heinrichs C. Central precocious puberty after interpersona transfer of testosterone gel: just a coincidence? J Pediatr Endocrinol Metab 2012;25:757–60.
6. Ramos CO, Macedo DB, Bachega T, Nascimento ML, Madureira G, Latronico AC, et al. Premature pubarche due to exogenous testosterone gel or intense diaper rash prevention cream use: a case series. **Horm Res Paediatr** 2019;91:411–5.
7. Cabrera SM, Rogol AD Testosterone exposure in childhood: discerning pathology from physiology **Expert Opin Drug Saf** 2013 May;12(3):375-88.
8. Green AL, Srivatsa A, Rodriguez-Galindo C. Delayed diagnosis and false relapse due to paternal testosterone use in adrenocortical carcinoma. **Pediatrics** 2014; 133:e1772–6.

CASE REPORT *RELATO DE CASO*

SGLT2 INHIBITOR AND TYPE 2 DIABETES: WHEN THE DUO BECOMES AN ISSUE

INIBIDOR SGLT2 E DIABETES TIPO 2: QUANDO A DUPLA TORNA-SE UM PROBLEMA

Emanuelle Leonel Ferreira[1], Maryna Rodrigues Gonçalves[2], Aline Maciel Gouveia[3], Caio Yutaka Hayashi[4], Heloisa Lima[5], Isadora Bulati[6], Mirnaluci P. Ribeiro Gama[7]

[1] Emanuelle Leonel Ferreira
Departamento de Endocrinologia e Diabetes - Hospital Universitário Evangélico Mackenzie (HUEM) Curitiba - PR - Brazil.
ORCID: https://orcid.org/0000-0003-0408-6131

[2] Maryna Rodrigues Gonçalves
Departamento de Endocrinologia e Diabetes - Hospital Universitário Evangélico Mackenzie (HUEM), Curitiba-PR, Brazil.
ORCID: https://orcid.org/0000-0003-1219-3076

[3] Aline Maciel Gouveia
Departamento de Endocrinologia e Diabetes - Hospital Universitário Evangélico Mackenzie (HUEM), Curitiba-PR, Brazil.
ORCID: https://orcid.org/0000-0002-5157-1431

[4] Caio Yutaka Hayashi
Departamento de Endocrinologia e Diabetes - Hospital Universitário Evangélico Mackenzie (HUEM), Curitiba-PR, Brazil.
ORCID: https://orcid.org/0009-0000-0550-1435

[5] Heloisa Moreira de Lima
Departamento de Endocrinologia e Diabetes - Hospital Universitário Evangélico Mackenzie (HUEM), Curitiba-PR, Brazil.
ORCID: https://orcid.org/0009-0005-1117-5273

[6] Isadora Bulati
Departamento de Endocrinologia e Diabetes - Hospital Universitário Evangélico Mackenzie (HUEM), Curitiba-PR, Brazil.
ORCID: https://orcid.org/0000-0003-1260-8198

[7] Mirnaluci P. Ribeiro Gama
Chefe do Departamento de Endocrinologia e Diabetes – Hospital Universitário Evangélico Mackenzie (HUEM), Faculdade Evangélica Mackenzie do Paraná - Curitiba-PR, Brazil.
ORCID: https://orcid.org/0000-0601-7639-1579

Received in: 14-01-2025
Accepted in: 24-01-2025

Corresponding author:
Emanuelle Leonel Ferreira
R. Monsenhor Manoel Vicente, 1138. 80620230. Curitiba, PR.

DOI: 10.29327/2413063.22.1-10

Euglycemic ketoacidosis is a potentially serious condition that can occur in patients with or without diabetes. It is characterized by ketonemia and metabolic acidosis, but with normal or only slightly elevated blood glucose levels. Its early diagnosis is a challenge, not only because it is an uncommon condition, but also because the absence of significant hyperglycemia can delay its identification and, consequently, appropriate management. Considering its relevance, especially in an intra-hospital setting, this report aims to reduce the threshold of clinical suspicion in the medical field for this potentially fatal condition, review its possible etiologies and highlight the potential risk of the duo: type 2 diabetes + sodium-glucose cotransporter 2 inhibitors (SGLT2i) precipitating such an event.

A cetoacidose euglicêmica é uma condição potencialmente grave que pode ocorrer em pacientes com ou sem diabetes. É caracterizada por cetonemia e acidose metabólica, porém com níveis normais ou apenas ligeiramente elevados de glicose no sangue. Seu diagnóstico precoce é um desafio, não só por ser condição pouco comum, mas também porque a ausência de hiperglicemia significativa, pode atrasar sua identificação, e por consequência, o manejo adequado. Considerando sua relevância, em especial em contexto intra hospitalar, este relato tem como objetivo reduzir o limiar de suspeição clínica na área médica para essa condição potencialmente fatal, revisar sobre suas possíveis etiologias e destacar o risco potencial da dupla: diabetes tipo 2 + inibidores do cotransportador de sódio-glicose tipo 2 (iSGLT-2) precipitar tal evento.

Keywords: Euglycemic diabetic ketoacidosis (eDKA); Sodium-glucose cotransporter 2 inhibitors (SGLT2i); Type 2 diabetes
Descritores: Cetoacidose diabética euglicêmica; Inibidores do co-transporte sódio-glicose; Diabetes tipo 2

INTRODUCTION

Initially described in 1973 in a case series in people with type 1 diabetes[1], euglycemic ketoacidosis (EKA) is defined as a medical emergency characterized by ketoacidosis with normal or only slightly elevated blood glucose levels, usually below 200 mg/dL (11.1 mmol/L)[2].

This phenomenon can be associated with the use of sodium-glucose cotransporter type 2 inhibitors (SGLT2i), medications approved worldwide for the treatment of type 2 diabetes and, in some cases, for heart failure[3].

According to the medical literature, the prevalence of EKA among patients hospitalized with diabetic ketoacidosis (DKA) was 10.8% in a retrospective study conducted in the Catholic Health Initiatives-Omaha healthcare system between 2018 and 2023[4], and this increased prevalence is associated with the use of sodium-glucose cotransporter type 2 inhibitors (SGLT2i), which are known to increase the risk of DKA and EKA, especially, but not only, in patients with type 1 diabetes[3].

In addition, in patients undergoing pancreaticoduodenectomy, the prevalence of EKA was 11.1% in a study investigating this metabolic condition after surgery[5]. In pregnant and postpartum women with severe COVID-19, the prevalence of EKA was reported as 5.94% in an observational study[6].

Furthermore, recent evidence also suggests that the occurrence of EKA in individuals with type 2 diabetes is rare when treated with SGLT2i[7,8].

This prevalence indicates that EKA is a relevant condition in certain groups of patients, especially in hospitalized patients, and this report highlights those using SGLT2i, describing the case of a female patient with in-hospital EKA after use of dapagliflozin and reviewing the multiple mechanisms involved in the induction of ketoacidosis by SGLT2 inhibitors.

CASE REPORT

A 78-year-old white female patient from Curitiba was admitted to the Mackenzie University Hospital in Curitiba-PR-Brazil due to abdominal pain that had started approximately 10 days ago, in the upper abdomen, with cramping pain, worsening after meals, associated with vomiting and diarrhea.

At the time, she also reported unquantified weight loss during the period and polyuria. She had a previous history of hypertension, dyslipidemia, valvular heart disease, hypothyroidism and diabetes mellitus, and was taking dapagliflozin and insulin therapy.

On physical examination upon admission, she was in regular general condition, dehydrated, oriented, thin (estimated weight of 45 kilograms and height of 160 centimeters), with a painful abdomen without peritonism.

Complementary tests showed a complete blood count with leukocytes of 4,660/mm3 (VR: 3,500-11,000), urea = 58 mg/dL, creatinine = 1.79 mg/dL. The partial urine test showed glycosuria +++ and ketonuria +.

A tomography of the abdomen and pelvis was performed without significant changes.

The patient developed an episode of psychomotor slowing and reduced food intake. Given the clinical suspicion, ketonemia was collected: High (**Figure 1**), and there was: dextrose 120 mg/dL, blood gas analysis with pH = 7.26, bicarbonate (BIC) = 10.6 mEq/L, anion gap = 15 mmol/L, potassium = 2.9 mEq/L and sodium = 136 mEq/L.

Figura 1. Cetonemia HIGH da paciente VSB.

A diagnosis of euglycemic ketoacidosis was made and management was initiated with prompt suspension of SGLT2i; intravenous (IV) hydration, IV insulin infusion, IV glucose infusion and hydroelectrolytic control.

The patient was subsequently transferred to ICU care and developed ketoacidosis resolution criteria.

DISCUSSION

This report describes the clinical case of an elderly aged female patient with diabetes, using insulin and dapagliflozin; with a history of low food intake; weight loss/low body mass index (BMI); renal injury and in metabolic stress: all documented risk factors for euglycemic ketoacidosis. Other risk factors, although not present in this case, described are: reductions in insulin dose, increased insulin demand, and latent autoimmune diabetes (LADA) of adulthood[9].

Although this is an uncommon condition, due to its potential for morbidity and mortality, clinical suspicion at the hospital level should be high[7].

Regarding the etiology, the causes of euglycemic ketoacidosis are varied and include:

1. **Sodium-glucose cotransporter type 2 inhibitors (SGLT-2i):** a well-documented cause, SGLT-2i are characterized by being selective, highly potent and agents that bind reversibly to their receptor[10].

Considering the relevance of the kidney in glucose homeostasis, through gluconeogenesis and reabsorption of filtered glucose, and the fact that 90% of glucose reabsorption in the renal proximal tubules occurs mediated by sodium-glucose cotransporter 2 (SGLT2), through a transmembrane sodium gradient, blocking SGLT2 has become a potent therapeutic target[11].

Approximately 160 to 180 grams of glucose are filtered by the kidneys each day and it is well known that in patients with type 2 diabetes the release of renal glucose is increased in both the postabsorptive and postprandial states[11].

These medications, in the kidney, promote the excretion of glucose in the urine, reduction in lipolysis and a subsequent increase in ketone reabsorption (especially of acetoacetate by increasing the sodium concentration, mediated by an electrochemical gradient, in the renal tubular fluid). This drug can limit hyperglycemia, but, also, in the pancreas, induce the production of ketone bodies due to reduced insulin and increased glucagon (generating a decreased insulin-glucagon ratio), through a direct action on pancreatic α cells, where SGLT2 is expressed[8,11], leading, finally, to a state of hepatic lipolysis (increase the production of free fatty acids, which are converted to ketone bodies by beta-oxidation in the liver) and ketosis even with normal blood glucose levels.

It is known that the use of SGLT-2 inhibitors in patients with type 1 diabetes is also associated with an increased risk[1,12].

2. **Fasting or Reduced Caloric Intake:** In states of prolonged fasting or insufficient caloric intake, there is a decrease in hepatic glucose production and this can precipitate this condition, especially in patients who are already in a state of mild ketosis due to other conditions, such as the use of SGLT-2 inhibitors[3,10,13].
3. **Pregnancy:** a condition that may predispose, possibly due to hormonal and metabolic changes that occur during this period: increased glucose utilization by the placenta and fetus; relative insulin deficiency and increased production of free fatty acids, which are converted to ketone bodies in the liver[2,14].
4. **Excessive Alcohol Consumption**: Alcohol abuse can lead to alcoholic ketosis, which, in combination with other factors, can result in this condition[15].
5. **Pancreatitis and Chronic Liver Disease:** Conditions such as pancreatitis and chronic liver disease can alter carbohydrate and fat metabolism, contributing to the development of euglycemic ketoacidosis[15].
6. **Infections and Physiological Stress:** Infections and other physiological stress conditions can increase the production of counter-regulatory hormones, such as glucagon, that promote ketogenesis[13].

It is noteworthy that, in some literature, half of the cases did not identify a precipitating factor for DKA[11].

Its diagnosis is made by clinical and laboratory evaluation. Clinically: early signs and symptoms of diabetic ketoacidosis include polyuria, breathing difficulties, nausea, vomiting and anorexia, excessive thirst, abdominal pain, confusion, unusual asthenia, and sleepiness. More severe symptoms are dehydration, difficulty breathing, confusion, and coma[4,10,13]. Laboratory tests involve the presence of metabolic acidosis (pH < 7.3 or BIC < 15-18 mEq/L) with increased anion gap (> 10-12 mmol/L), presence of ketosis (ketonemia - > 1.6 mmol/L - or ketonuria) and normal glucose levels[12]. The patient described above presented all the criteria and the measurement of ketonemia was especially important in this case because the patient was using SGLT2 inhibitors: a situation in which there may be a reduction in ketonuria due to increased tubular reabsorption of acetoacetate, despite the increase in ketonemia.

Treatment involves the administration of intravenous fluids, insulin and, often, glucose to interrupt ketogenesis and correct the electrolyte imbalance.

It is crucial to identify and treat the underlying cause of ketoacidosis to avoid complications[12]; in this case, the conduct of suspending the drug was a priority, with resolution of the condition afterwards.

CONCLUSION

Awareness of EKA is essential, especially in patients taking SGLT-2 inhibitors, to ensure early diagnosis and appropriate treatment.

Due to its unique biochemical profile and the potential for delayed diagnosis, it is important that clinicians are alert to this condition and aware of potential etiological triggers in susceptible individuals, actively ruling out other differentials, thus minimizing the time required for diagnosis of EKA.

REFERENCES

1. Munro JF, Campbell IW, McCuish AC, Duncan LJP. Euglycaemic Diabetic Ketoacidosis. **Br Med J.** 9 de junho de 1973;2(5866):578–80.

2. American Diabetes Association Professional Practice Committee. 6. Glycemic Goals and Hypoglycemia: Standards of Care in Diabetes-2025. **Diabetes Care.** 2025 Jan 1;48(Supplement_1):S128-S145. doi: 10.2337/dc25-S006. PMID: 39651981; PMCID: PMC11635034.
3. Garg R, Sood N, Bansal O, Hoskote A. Euglycemic Ketoacidosis Associated with SGLT-2 Inhibitors in Non-diabetic Patients-A Narrative Review. **J Gen Intern Med.** 2025;40(2):437-442. doi:10.1007/s11606-024-09073-2.
4. Schutte B, Savage K, Merwin M, et al. Euglycemic diabetic ketoacidosis: Rising incidence, diagnostic delays, and the impact of SGLT2 inhibitors in hospitalized patients. **J Hosp Med**. Published online February 19, 2025. doi:10.1002/jhm.70015.
5. Sholevar C, Torjani A, Kavanagh TR, et al. Euglycemic diabetic ketoacidosis (EDKA) after pancreaticoduodenectomy: An under-recognized metabolic abnormality with outcome implications. **Surgery**. 2023;173(4):888-893. doi:10.1016/j.surg.2022.07.009.
6. Melo Mendes IC, Martins de Oliveira AL, Pinheiro Trindade PM, et al. Metabolic acidosis with elevated anion gap and euglycemic ketoacidosis in pregnant and postpartum women with severe Covid-19. **Ann Med**. 2025;57(1):2445189. doi:10.1080/07853890.2024.2445189.
7. Barski L, Eshkoli T, Brandstaetter E, Jotkowitz A. Euglycemic diabetic ketoacidosis. **Eur J Intern Med**. maio de 2019;63:9–14.
8. Peters AL, Buschur EO, Buse JB, Cohan P, Diner JC, Hirsch IB. Euglycemic Diabetic Ketoacidosis: A Potential Complication of Treatment With Sodium-Glucose Cotransporter 2 Inhibition. **Diabetes Care**. 2015;38(9):1687-1693. doi:10.2337/dc15-0843.
9. Qiu H., Novikov A., Vallon V. Ketosis and diabetic ketoacidosis in response to SGLT2 inhibitors: Basic mechanisms and therapeutic perspectives. **Diabetes Metab. Res. Rev.** 2017;33:e2886.
10. Di Mauro G , Mascolo A, Gaio M, Rafaniello C, De Angelis A et als The Reporting Frequency of Ketoacidosis Events with Dapagliflozin from the European Spontaneous Reporting System: The DAPA-KETO **Study Pharmaceuticals** (Basel) 2022; 25;15(3):286.
11. Maadarani O, Bitar Z and Alhamdan R Dapagliflozin- Induced Severe Ketoacidosis Requiring Hemodialysis *Med* **Rev Case Rep** 2016, 3:150 Volume 3 | Issue 12.
12. Zhao Z, Zhan Y, Hu X, Tian C, Fei Jin P Liu D, Risk factors of dapagliflozin-associated diabetic ketosis/ketoacidosis in patients with type 2 diabetes mellitus: A matched case-control study **Diabetes Research and Clinical Practice** 2023;Volume 196 2023, 11023.
13. Long B, Lentz S, Koyfman A, Gottlieb M. Euglycemic diabetic ketoacidosis: Etiologies, evaluation, and management. **Am J Emerg Med**. 2021;44:157-160. doi:10.1016/j.ajem.2021.02.015.
14. Mehta AE, Zimmerman R. Classic diabetic ketoacidosis and the euglycemic variant: Something old, something new. **Cleve Clin J Med**. 2025;92(1):33-39. Published 2025 Jan 2. doi:10.3949/ccjm.92a.24075.
15. Han HJ, Cole AE, Verma A. Euglycemic Diabetic Ketoacidosis Caused by Alcoholic Pancreatitis and Starvation Ketosis. **J Gen Intern Med**. 2023;38(5):1299-1301. doi:10.1007/s11606-022-07993-5.

Instructions for the Publication of the Journal Endocrinology & Diabetes Clinical and Experimental

The journal follows the International Committee of Medical Journal Editors.

01 All the manuscripts will be published in English. The journal accepts original articles, preliminary notes, case reports, review articles, updates and letters to editor. There a topic dedicate to internal medicine linking endocrinology and medical clinic. The journal strongly encourages on line submissions of manuscripts. Those should be accompanied by a title, keywords and an abstract in English for the purposes of international registration. Abstracts in other languages may also be attached.

02 The articles received by the Editor will be analyzed with the Assistance of the Editorial Board. Minor changes to "copy desk" can be effective with the purpose of standardizing the articles, without subs tantial changes in original text.

03 Manuscripts can be sent on CD or via on line to publicacao@revistaendocrino.com. The text should be typed on pages containing 20 to 24 rows and rows with 70 to 75 spaces, with the objective of enabling the diagramming the calculation of space required for each article. The word processor used must be either Microsoft Windows compatible program (Word, Write etc.).

04 The article must have title, full name of the authors; quote from site (full address) where out performed the work; full titles of authors, key words (or "keywords") without exceeding a limit of 250 words; introduction; material or material and methods or description of the case; results; discussion and/or comments (when applicable); conclusions (when applicable); summary (summary in English), consisting in the correct version of the summary, not exceeding 250 words; references (as quoted below in item 08) in alphabetical order; the accompanying illustrations must follow appropriate rules, described in item 07.

05 Illustrations are of figures and graphs referred to in Arabic numerals (example: fig. 3, graph 7), in the form of ink drawings photographs ECG EEG etc. When possible must be submitted in original form. The illustrations will be accepted only allow good reproduction. Should not be glued in the middle of the article text and it must be attached with the respective legends typed on the bottom of the same (one sheet for each illustration). Must take care to number each illustration on the back of the same and indicate the correct place where should be introduced. Tables and frames are specified in Arabic numerals, consisting always the respective title, accurately. Tables and frames without its description in the text and are intended to summarize the article. The units used to express the results (m, g, g/100 ml, etc.) will appear at the top of each column. It will be up to the Editor to judge excessive illustrations (figures, tables, graphs, tables etc.), deleting the redundant.

06 The references must follow the alphabetical order or the order of appearance in the text. Showing them all authors cited in the text. It must be contain: name of author, name of the journal abbreviated in accordance with the criteria used in the Index Medicus (www.nlm.nih.gov/tsd/serials/lji.html). Papers accepted but not yet published may be included in the references. You should avoid using as reference poster or free themes from conferences unless they are of high relevance. Articles published online may be cited in the references and should bear the name of the site as well as the date of access.Chapter of Book: Ruch, TC.Somatic Sensation. In Ruch T C et al. Neurophysiology. Philadelphia Saunders 1963; 330-332 Journal article: R.W.G Gruessner, Sutherland D.E.R, Najarian j. S, et al. Solitary pancreas transplantation for non uremic patients with insulin-dependent diabetes mellitus labile. Transplantation 1997; 64: 1572-77.

07 The names of drugs cited in the text (names of fantasy, officers, patented, and acronyms of chemical research) shall comply with corresponding regulations of the World Health Organization, according to rules summarised by KOROLKOVAS, a.-Regulatory Editorial Nomenclature-Names of drugs (Drug Nomenclature). Rev. Bras. Clin. Terap. 5: 1976 (February).

08 The authors will receive ten copies of the issue in which their work was published (for reprints), which will be sent directly to the place where the work performed. Reprints must be ordered and previously combined with the Commercial Direction.

09 The manuscripts that don't fit the standards or that does not suit the needs of the journal editorials may be forwarded to the authors to carry out the necessary adjustments that will be indicated in the personal letter from the Editor. Will be mentioned the dates of receipt and approval of work for publication, in order to safeguard the interests of the author's priority. In the case of re-routing of work to adapt to our rules for publication, the date cited is always receive the first forwarding of work. The content of the articles is the responsibility of the authors. The link between the author (s) and pharmaceutical laboratories, as well as another source that is generating resources must always be quoted by author (s). The copyright of the manuscripts are of the magazine in question.

10 Will be given top priority in the publication of articles and/or notes that they concerned about matters directly or indirectly related to the basic purpose of the journal Endocrinology & Diabetes Clinical and Experimental

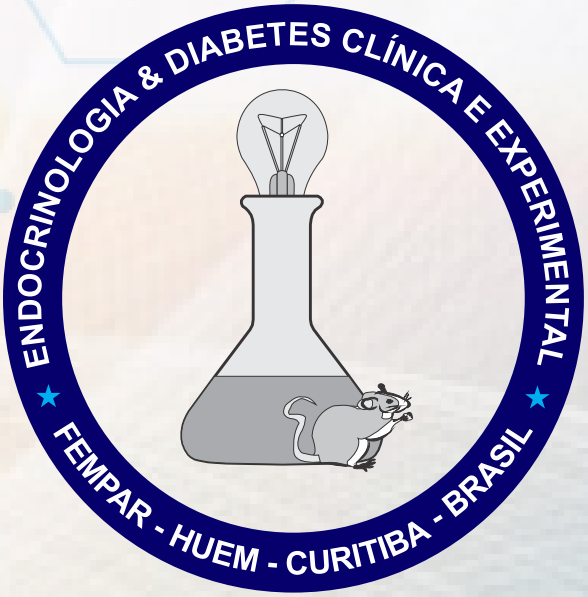

ENDOCRINOLOGIA & DIABETES CLÍNICA E EXPERIMENTAL